Genetic abnormalities in Hereford cattle: the detection of vertical fiber hide defect and identification of quantitative trait loci associated with ocular squamous cell carcinoma

by

Katherine Ward Upshaw

B.S., University of Florida, 2018

A THESIS

submitted in partial fulfillment of the requirements for the degree

MASTER OF SCIENCE

Department of Animal Sciences and Industry
College of Agriculture

KANSAS STATE UNIVERSITY
Manhattan, Kansas

2021

Approved by:

Major Professor
Dr. Megan Rolf

Copyright

Abstract

Genetic abnormalities often exist in opposition to an individual's quality or length of life. Revealing prevalence and inheritance factors underlying these abnormalities is crucial for further understanding and management of these conditions. Vertical fiber hide defect is a genetic disorder that reduces collagen fiber interlacing and causes hides to tear during tanning, which increases cost and waste during leather good production. Hide biopsies were collected from 22 Hereford cattle, dyed with Masson's trichrome stain, and histologically examined to ascertain if the condition could be detected in a modern herd of cattle. Although no samples expressed abnormal fiber orientation, the proposed novel histology approach was effective. Future research should incorporate additional samples from different herds and ancestry to help elucidate modern VFHD prevalence. Bovine ocular squamous cell carcinoma is the most common oncological neoplasm affecting cattle. It presents as ocular tumors, which can eventually metastasize into internal organs and contribute to carcass condemnation or reductions in lifetime productivity. The etiology of ocular squamous cell carcinoma is multifactorial, however prior literature suggests that it is genetically influenced. This experiment aimed to identify genomic regions associated with its expression. A total of 14 cases, 28 individual controls, and 10 control pools of 50 animals each was genotyped using an Illumina® BovineHD BeadChip and MANOVA-based association approaches revealed suggestively significant regions on chromosomes 6, 13, and 15 and one statistically significant region on chromosome 13. The expression of BOSCC appears to follow a polygenic mode of inheritance in which the small effects of many loci predispose cattle to developing the disease, however future research involving a greater number of samples is warranted. Both conditions pose substantial consequences for cattle producers and these experiments should aid in the prevention, detection, and control of these genetic abnormalities.

Table of Contents

List of Figures

List of Tables

Acknowledgements

Assembling this thesis has been an emotional and immensely cathartic experience. However, the culmination of my master's research work is not only a reflection of my academic journey, but also the people who have supported me along the way. I am infinitely grateful for all the encouragement, guidance, and genuine relationships I've experienced while at K-State.

Firstly, I would like to express my appreciation for the members of my committee, Dr. Megan Rolf, Dr. Jennifer Bormann, and Dr. Robert Weaber. Megan is an inspiring mentor who I thank for her encouragement, constructive criticisms, and compassion. I thank Jenny for the many conversations, teaching skills, and life wisdoms she has imparted on me. And I thank Bob for his invaluable assistance during the field work portion of my research.

I would also like to thank Dr. John Keele, Dr. Tara McDaneld, and Dr. David Grieger for mentoring me as I learned lab techniques and bioinformatics. I especially thank Dr. G for his infectious positivity, words of (sometimes questionable) advice, providing opportunities to teach, and of course incorporating *Far Side* comics and exclamations of "Newman!" in my daily life. Further thanks belong to my peers, especially Andrew Lakamp, Tamra Kott, William Shaffer, Jonathan Little, and Sabrina Walsh, for their unwavering support and authentic friendships. Drew and Will deserve additional accolades for their expertise in statistical analyses and helping generate R scripts that actually run.

Lastly, my deepest appreciation belongs to my father for his motivation and unwavering support, even amid panicked 2am phone calls and seemingly insurmountable obstacles. He has stood by my side for every incredible accomplishment and crushing defeat I've experienced in life and I simply would not have reached this milestone without his steadfast guidance, enthusiasm for my success, and loving devotion. Thank you.

Chapter 1 - Vertical Fiber Hide Defect Literature Review

Introduction

Vertical fiber hide defect (VFHD) is a disorder affecting the collagen structure of Hereford and Hereford-cross cattle (Amos 1958, Cundiff et al. 1988). Normal hide collagen is interwoven at an angle of 50-60°, but the vertical orientation associated with VFHD causes collagen fiber bundles to have higher angles of weave and reduced fiber interlacing, which can cause affected hides to fall apart (Cundiff et al., 1987). Figure 1.1 contrasts orientation of collagen fibers in hides of cattle affected by VFHD compared to those that are unaffected. The abnormality has a detrimental effect on the leather industry and its occurrence can have long-lasting economic impacts (Cundiff et al., 1988). The leatherworking industry collects hides that originate from a variety of beef cattle breeds, like Hereford, and sends them to tanneries.

Currently, the only way to confirm the presence of VFHD is through histological examination of the hide, which is not cost-effective due to the high level of skill and lengthy amount of time involved for accurate diagnoses (Cundiff et al., 1987). Unfortunately, this makes identifying the condition before the hide falls apart incredibly difficult. At this point, tanneries have already invested both time and money in the tanning of these affected hides. Cundiff et al. (1988) estimated economic losses to American leathermakers in excess of $10 million in 1973.

According to the Bureau of Labor Statistics consumer price index inflation calculator (2019), $10 million in 1973 is equivalent to the buying power of $59.5 million today. Beyond the borders of the United States, Duivestein et al. (2000) reported that VFHD cost the Australian leather industry $2-5 million per year. Clearly, VFHD is an issue of significance in the global leather industry.

Background

Vertical fiber hide defect was first noted in Australian tanneries. Affected hides were identified by the distinctly vertical orientation of collagen fibers centralized to the hindquarter (Amos 1958). Affected fibers can comprise up to 75% of the entire hide, extending as far as the belly and shoulder areas (Cundiff et al., 1988; Tancous, 1966). Hides with the abnormality are considerably less durable than hides with the normal horizontal fiber weave and have a predisposition to cracking and breaking, as illustrated in Figure 1.2. Furthermore, it was demonstrated in Cundiff et al. (1987) that leather affected by VFHD has only half the tensile strength of normal hides. Amos (1958) noted that the vertical fiber condition had only been observed in Hereford hides and was the first paper to hypothesize that VFHD might be under genetic control.

Everett et al. (1971) presented the first concrete data that VFHD is a hereditary condition when the authors reported higher rates of VFHD in some sire lines, but not all. More recently, Cundiff et al. (1987) offered compelling evidence that VFHD is controlled by an autosomal recessive mutation present uniquely in Hereford and Hereford-crosses, but this has not been confirmed and both the genomic position and causal variant are unknown.

This condition has been studied intermittently since its identification in 1958, but without further data on its current prevalence, it is unknown if VFHD is proliferating within the population and causing associated financial losses. Additional research is necessary to better understand VFHD and its prevalence, etiology, diagnosis, and prevention.

History and Incidence of VFHD

Historical Background

Vertical fiber hide defect has been primarily reported in cattle of Hereford descent since its discovery in the mid-twentieth century. Amos (1958) reported that the condition had been uniquely observed in Herefords, but also acknowledged that a significant number of hides from many breeds would have to be tested to confirm the condition's potentially breed-specific nature.

Tancous (1966) focused on the strength of leather from 24 Hereford hides and 9 Angus hides. Leathers were tested for tensile strength, slot tear strength, and Mullen grain crack strength. If at least two of the tests had a failure rate greater than 30%, the leather was considered weak. Historically, it was assumed that all weak leather was a result of VFHD. Given that 11 Hereford hides and one Angus hide produced weak leather in this study, these animals were presumed to have VFHD. This is the only reported incidence of VFHD in the Angus breed, but Tancous (1966) focused on the strength of the leather rather than the orientation of the fibers, which proved to be an important distinction in future studies.

Further research indicated that weak leather is not always caused by VFHD and the abnormality cannot be identified by sight alone. Histological examination is the only way to definitively diagnose VFHD (Tancous et al. 1967a). Although Angus and Holstein hides were found to produce weak leather, only Hereford hides resulted in pulpy leather, a term used in tanneries for VFHD-affected hides (Tancous et al. 1967a). A total of 1,718 side leathers from 884 hides underwent strength tests and histological examination of the corium fibers underneath the epidermis, where the orientation of collagen fibers can be detected in Tancous et al. (1967a). The study demonstrated that 94% of the weak leather and 100% of the VFHD-affected leather were made from Hereford hides.

The Importance of Breed

Hannigan et al. (1973) conducted a study on the occurrence of VFHD in 14 sets of twin Hereford and 15 sets of twin Holstein heifers. Twins are often essential for genetic research studies, as identical twins share the same DNA sequence as each other. Thus, if a certain phenotype is expressed in one twin and not the other, an external factor may play more of a role in the expression of that characteristic than the genetic sequence itself. Conversely, when a trait is under primarily genetic control, identical twins will likely have a similar phenotype, while fraternal twins may differ significantly. In Hannigan et al. (1973), the twin animals selected for the study were a mix of both identical and fraternal pairs. For each breed used in the experiment, 10 pairs of identical twins were chosen. It was discovered that half of the Herefords presented with VFHD, but none of the Holsteins were diagnosed with the condition. Given that Herefords were the only ones diagnosed with VFHD, this evidence supports the hypothesis that VFHD is a breed-specific disorder. Additionally, the abnormality, or lack thereof, was consistent within all identical twin pairs, but its expression was varied in fraternal pairs, thereby providing evidence of a genetic etiology for VFHD. A decade later, Peters and Bavinton (1983) looked at the prevalence of VFHD by examining hide samples from 652 Herefords and 57 Jerseys. This study found that 148 Herefords (22.7%) and zero Jerseys had VFHD, providing additional evidence for a breed-specific inheritance mechanism. Like the literature that preceded it, Hannigan et al. (1983) also concluded that VFHD appears to be isolated to the Hereford breed after discovering VFHD in 15.3% of 465 Hereford and 0% of 139 Angus hides.

However, two published studies have detected VFHD in cattle of mixed lineage. Everett and Hannigan (1978) analyzed 76 Hereford-Holstein cross calves and identified one calf affected with VFHD. Presuming this condition is autosomal recessive, the calf must have inherited two

VFHD-associated alleles, one from each parent, at the relevant locus. Previous literature has consistently identified VFHD in the Hereford breed, but the origin of the VFHD allele in the Holstein parent of this crossbred calf is perplexing. It is possible that the allele responsible for the condition is not exclusively present in the Hereford breed, but this is unlikely given the results of other VFHD literature. In this case, the VFHD allele is more likely to either be present in a certain Holstein breed line, or the Holstein parent of the affected calf must have Hereford ancestors that passed on the allele. In another study, Cundiff et al. (1988), looked at the prevalence of VFHD in Pinzgauer, Red Poll, Brown Swiss, Charolais, Gelbvieh, Simmental, and Limousin breeds and discovered a single Simmental heifer with VFHD. Upon closer inspection, the authors found that the heifer's sire and dam were each 1/16 Hereford. This is not entirely surprising because many breed associations, including that for Simmental cattle, have allowances for animals with small fractions of other breeds in their distant lineages to still be considered purebred. Even though this result does not offer conclusive evidence of VFHD being a breed-specific disorder, it supports the inferences made by previous literature that VFHD most likely arises from the affected animal's Hereford progenitors.

It should additionally be noted that the structure of the United States beef industry in the 1960s and 1970s when much of this data was collected may have played a role in VFHD susceptibility. Many continental breeds, such as Charolais, Simmental, and Limousin, were imported to the United States during this time in an effort to increase growth rates in offspring when mated to British breeds, like Hereford and Angus (Greiner, 2009). Due to import regulations in the 1960s and 1970s, Continental cattle were often graded up from Herefords and Angus, which would have provided a low level of potential VFHD influence in these populations.

Geographical Pervasiveness

Vertical fiber hide defect has been observed in a variety of countries. While most research on VFHD has been concentrated in Australia and the United States, Everett et al. (1967) presented two leather samples sourced from South America with VFHD, which demonstrates that the condition is likely a matter of global concern.

In the United States, Tancous (1966) estimated that there was a 5-15% rate of VFHD occurrence in Hereford hides in tanneries, depending on the hide lot. Approximately 20 years later, Hannigan et al. (1983) found a similar incidence rate in a sample of 465 Hereford hides in which 62 were affected. Everett and Hannigan (1978) extrapolated from previously published data that VFHD was present in 13% of over 3,400 Hereford hides and 0.8% of 1,500 Angus- and Holstein-cross hides, presumably as a result of previous Hereford lineage.

The incidence of VFHD in Australia has been highly varied. As one of the first papers published on VFHD, Amos (1958) roughly estimated that 0.5% of all hides entering Australian tanneries were affected by VFHD. Years later, Cundiff et al. (1988) estimated that VFHD affects 22.9% of Australian Herefords and only 13.3% of American Herefords, which supports the results obtained in Everett and Hannigan (1978). It is currently unknown why there is such a large difference between the incidence of VFHD in Australian and American Hereford populations, but the disparity may be a result of different lineages or different frequencies of those bloodlines found in the United States and Australia. Duivestein et al. (2000) offered the most recent insight into VFHD prevalence; the abnormality was detected in 28% of the study's 102 Australian Hereford samples. A larger study is warranted, but this data may suggest that the prevalence of VFHD has increased, at least in Australian herds.

Clinical Diagnosis

Sample Collection

Researchers in early VFHD studies would often cut hide samples by hand, but a more efficient method was presented in 1970: a biopsy gun. Schied et al. (1970) explained that hand cutting samples can be extremely time-consuming and painful on a living animal. A biopsy gun could overcome these problems because of its point-and-shoot simplicity and efficiency when collecting samples from a large herd of animals. The biopsy gun was initially developed to be used on mink and sheep, but quickly became popular with swine and bovine researchers. Hannigan et al. (1973) was one of the first VFHD studies to use a biopsy gun and ultimately concluded that the biopsying procedure was not only vastly more efficient than hand-cut sections, but it also made it possible to collect samples from living animals with minimal invasiveness, which would be helpful for selection programs in breeding stock to eliminate the incidence of the condition. Thus, biopsy guns, as shown in Figure 1.3, became increasingly common in VFHD research after the early 1970s.

Identification by Strength Testing

When VFHD was first reported in cattle populations, it was identified by distinctly weak hide strength. Therefore, in order to diagnose the abnormality, early studies tested hides with various strength tests in addition to viewing biopsy samples under a microscope.

Early literature on VFHD relied primarily on hide strength phenotypes, assessed via leather strength tests, to detect the disorder. Amos (1958) identified VFHD-affected hides by the hide's low grain strength; soft, flat feel; and fine breakage. Tancous et al. (1967a) explained that the level of tensile strength in the hide is often indicative of vertical collagen fiber orientation, particularly in the rump area of the animal. Samples were cut 17.8 cm diagonally down from the

tail head, toward the hook bones and thurl of the animal, on both sides of the hide and subsequently tested for tensile strength, slit tear, and Mullen grain crack strength. Vertical fiber hide defect was associated with test results below 9307.9 kPa tensile strength, 2240.8 kPa slit tear, and 95.25 kg Mullen grain crack strength. As in Amos (1958), Tancous et al. (1967a) examined hide cross sections to evaluate the relationship between this weak leather and fiber orientation. Unsurprisingly, this work revealed that most of the weak leathers were a result of vertical fiber architecture. Figure 1.4 provides evidence of this point; as angle of fiber weave increases, hide strength decreases.

Another common leather test used in VFHD diagnostics is a ball-burst test, such as the one conducted in Everett et al. (1971). For this test, a value indicative of the hide's strength was calculated as follows: $\frac{Grain\ Load\ (lbs.)+Burst\ Load(lbs.)}{Thickness\ (in.)} \times \frac{Grain\ Distortion\ (in.)}{Burst\ Distortion\ (in.)}$. According to these values, ball-burst test results were divided into four arbitrarily assigned levels. Grade 1 represented VFHD hides, Grade 2 denoted the intermediate phenotype, and Grades 3 and 4 were indicative of strong leather.

In the early 1970s, microscopic examination become the more common method of diagnosing VFHD. Bitcover et al. (1974) sought to define the relationship between strength-tested hides and microscopically evaluated hides by measuring hide strength in relation to VFHD occurrence. The affected hides used in this study were ascertained by microscopic assessment. This paper reported data from tensile strength tests, slit tear resistance tests, ball-burst tests, grain crack tests, and needle penetration resistance tests on 53 total hides. In all cases, affected hides performed worse than phenotypically normal hides, showing a clear relationship between hide strength and fiber orientation.

Identification by Histological Examination

Leather strength tests are not necessarily the best methods of diagnosis given that processing errors in tanneries can confound VFHD results, weak leather is not always caused by vertically oriented collagen fibers, and once VFHD is detected, it is often too late in the tanning process to track the origin of the hide and provide potentially valuable data to the producer (Tancous et al., 1967a).

Vertical fiber hide defect was first identified in leather samples of low strength and durability. Thus, many researchers used strength tests to diagnose the condition. However, this method of diagnosis was flawed because weak leather is not always a result of VFHD and can be caused by processing errors, machinery malfunctions, or some other external variable. Departing from traditional strength tests, researchers adopted histological diagnostic methods to identify VFHD. In Hannigan et al. (1973), samples collected from living animals were sliced into cross sections and stained with hematoxylin and eosin. The stain color-coded various structural aspects of the sample to alleviate the difficulty involved in assessing fiber orientation. For example, eosin stains collagen structures pink, which helps to differentiate collagen fibers from other tissues in the sample.

Dufty et al. (1981), Dufty et al. (1983), and Cundiff et al. (1988) all fixed hide samples in 10% formalin for up to 3 days at which point they were examined under a stereomicroscope for fiber orientation. In the case that the fiber orientation of a sample was not clearly identifiable under the microscope, both studies followed in the footsteps of Hannigan et al. (1973) by staining these sections with hematoxylin and eosin for a color-coded, detailed view of the fiber orientation.

Histological staining and microscopic evaluation are excellent methods for evaluating hides for VFHD. Leather strength tests are not necessarily the best methods of diagnosis given that processing errors in tanneries can confound VFHD results, weak leather is not always caused by vertically oriented collagen fibers, and once VFHD is detected, it is often too late in the tanning process to track the origin of the hide and provide potentially valuable data to the producer (Tancous et al., 1967a).

Histological Classification Schemes

When gathering data on VFHD, researchers typically sort animals into one of three categories: normal, affected, or intermediate. Everett et al. (1971) and Hannigan et al. (1973) were two of the first studies to follow this method of classification, in which a normal designation was indicative of interwoven collagen fibers at the standard horizontal angle of weave; an affected, or vertical, designation denoted vertical fiber orientation and loose weave; and the intermediate description pertained to fibers of inconsistent weave. These three classifications are depicted in Figure 1.5. When histologically examining samples, normal fibers should align at an angle of 50-60°, and anything closer to 90° suggested abnormal structure and could be qualitatively classified as either vertical or intermediate (Cundiff et al., 1988).

Bitcover et al. (1974) noted that the intermediate expression of VFHD was not well understood but did appear to be its own distinct phenotype. In the study, 68 bull and steer hides were analyzed and in total, 15 hides were labeled as having VFHD (22%), but 23 more were found to have intermediately woven fibers (34%). Everett and Hannigan (1978) sorted Holstein and Hereford hides by the three types of histological classifications and discovered that although none had completely vertical collagen fibers, one of the animals had an intermediate fiber weave.

This implies that the intermediate phenotype may be more common than the extreme vertical orientation in affected animals.

Classifying fiber orientation with three categories became popular in successive studies. Dufty et al. (1981) assigned hide biopsy samples to one of the three collagen fiber orientation categories: vertical, intermediate, or normal. The intermediate structure was more prevalent than the vertical fiber architecture. Out of a total of 119 cattle, 21.8% were diagnosed with VFHD and 26.9% were classified as having intermediate collagen fiber orientation. More recently, Cundiff et al. (1988) considered the vertical and intermediate phenotypes to be varying levels of expression of the same genotype.

Duivestein et al. (2000) explained that because observations are typically qualitatively classified as one of the three phenotypes, it can be difficult to properly assess the fiber orientation of samples and the accuracy of reproducibility is nearly impossible to determine. Most VFHD research involves scientists estimating the proportion of vertical to horizontal collagen fibers, which can get complicated without strict quantitative methods of assessment. Normal fiber orientation is described as having an angle of 50-60°, with anything closer to 90° suggestive of abnormal structure. After training, multiple people should, for the most part, be able to identify whether a hide sample exhibits a normal or abnormal phenotype, but the problematic part of this three-category hide classification system is that individual researchers may have different perceptions of how to divide abnormal samples into either vertical or intermediate classes.

Duivestein and colleagues discovered that because many of the abnormal samples seemed to fall between classifications, it was very difficult to accurately label fiber orientation. In an effort to mitigate this issue, Duivestein et al. (2000) developed a five-category

classification scheme to replace the traditional three-category system. In this five-category model, samples were assigned as normal, normal-intermediate, intermediate, vertical-intermediate, or vertical. This system was responsible for significantly greater phenotypic correlations between the condition and various assessment factors, such as hide tensile strength and hide tear strength, signifying the value of implementing a five-, or potentially more, category classification scheme.

Identification by Quantitative Measures

Microscopic evaluation is not necessarily ideal as it is often associated with human error due to its subjective nature. Everett et al. (1967) sought to establish a quantitative method of diagnosing the condition to help mitigate the effects of human error. In this paper, objective measurements were collected by comparing the light transmission through photographs of polarized light views between normal and affected hide samples. As Amos (1958) was the first to note, phenotypically normal hides have fibers arranged in a mostly horizontal orientation, whereas affected hide fibers aligned mostly vertically. To determine a quantitative measurement of the fiber orientation, samples were cut against the vertical fibers and viewed against polarized light. In this positioning, horizontal collagen fibers show up very brightly, but vertical fibers were much darker, often appearing black. Figure 1.6 contrasts the light and dark regions of polarized photographs of an affected hide sample (left) and a phenotypically normal sample (right).

The researchers subsequently developed negatives of these images, so that the intensity of light transmittance would represent the prevalence of vertical fibers. Overall, strong hide samples had an average light transmission of 51.8%. Conversely, weak hides transmitted 60.9% of light, indicating that weak hides have significantly more vertically-oriented collagen fibers. To

further demonstrate this point, the photographs were edited with a first-order red compensator filter to show the fibers in color. The left side of Figure 1.7 depicts the polarized photographs of a VFHD-affected hide (above) and a normal one (below). In juxtaposition, the right side of Figure 1.7 shows the same hides with a colored filter applied.

The most recent development in VFHD diagnostic investigations was the introduction of small-angle light scattering (SALS) techniques to analyze fiber orientation. Kronick and Buechler (1986) used SALS to examine the fiber orientation in calfskin used for shoe production. When SALS is used on a sample, it produces a circle of white light against a dark background that becomes oblong when fibers are abnormally aligned. A standard alignment of 45° would produce a round circle, whereas a condition like VFHD that increases the angle of this weave would yield an oval outline of light, stretching vertically with the structure of the fibers. This is depicted in Figure 1.8, in which *a* represents the SALS result for a sample with VFHD and sample *b* illustrates the SALS technique on a normally woven hide.

Intrigued by this preliminary data on SALS and fiber orientation, Kronick went on to publish additional data focusing on quantifying VFHD by way of SALS. Kronick and Sacks (1991) obtained SALS measurements on histological samples collected nearly a decade earlier in Hannigan et al. (1983). The samples were collected from live purebred Herefords, fixed in 10% formalin, sliced into cross-sections, stained with hematoxylin and eosin, and classified into one of three phenotypes: normal, intermediate, or vertical fiber weave. The degree of fiber orientation was calculated with the following equation:

$$\langle \cos^2 \Phi \rangle = \frac{\int_0^{\frac{\pi}{2}} I(\Phi) \sin \Phi \cos^2 \Phi \, d\Phi}{\int_0^{\frac{\pi}{2}} I(\Phi) \sin \Phi \, d\Phi \mathrm{b}}$$

in which *I(ϕ)* was the intensity of the scattered light and $\cos^2\phi$ indicated the degree of orientation. As this equation can quickly become cumbersome, the results of $\cos^2\phi$ can be reformatted as an orientation index (*OI*), calculated as

$$OI = \frac{1}{2}[(3\langle\cos^2\Phi\rangle - 1)] \cdot 100\%$$

Higher OI values corresponded to fibers aligned more vertically. Negative OI values, which are associated with horizontal fiber weave, were found consistently in the lower reticular dermis, whereas normal, intermediate, and vertical fibers were all found in the upper reticular dermis. This supports the conclusions made by Peters and Bavinton (1983) that VFHD is only found in the upper reticular dermis. Although the fibers in phenotypically normal hides have a significantly lower OI than intermediate or vertical phenotypes, the degree of OI between intermediate and vertical fiber orientations was indistinguishable, as demonstrated in Figure 1.9. This provides evidence that the intermediate phenotype is much more related to extreme cases of VFHD than normal hides.

There are many variables in a hide sample that may confound the diagnosis of VFHD, including stray hair or thick fiber bundles. Qualitative diagnosis is the most common method of identifying VFHD, but quantitative measurements are believed to increase accuracy and predictability of diagnosis. However, further work is necessary to determine if the advantage of quantitative measurements outweighs the augmented labor, equipment, and cost involved in polarized light photography or the SALS technique.

Etiology

Environmental Factors

Age is often a consideration in disease etiology, and VFHD is no exception. Researchers initially believed that VFHD only occurred in animals older than one year until Hannigan et al. (1983) published compelling evidence of VFHD in four- and seven-month-old calves. The study tested cattle ranging from four months to nine years of age to evaluate the effect of age on VFHD. Hannigan et al. (1983) was the first to conclude that VFHD can affect cattle younger than one year, even though older animals express the condition more frequently than younger ones. Out of 201 four- and seven-month-old calves, 17 were considered to have VFHD via microscopic evaluation. A total of 169 yearlings and 95 animals two years of age or older were included in the study, of which VFHD affected 22 and 23 cattle, respectively. The distribution of animals in each age group is summarized in Table 1.1 and shown in Figure 1.10. The percentage of affected cattle in each age group has a tendency to increase as age increases. Previous literature suggested that VFHD was not apparent until the affected animal was one year or older, so Hannigan et al. (1983) reevaluated the four- and seven-month-old calves at 11- to 14-months old. The researchers found that the 17 calves initially diagnosed with VFHD remained consistent with the abnormal phenotype as yearlings, as expected. However, VFHD was detected in an additional five yearlings that were initially evaluated as phenotypically normal calves. Despite these results and the varied age distribution, the effects of age were not found to be statistically significant.

Studies have tested hides from steers, bulls, heifers, and cows to evaluate the effect of sex on presence of the abnormality. Everett et al. (1971) examined 130 hides from steers with known Hereford lineage and determined that approximately 18% were affected by VFHD. A few years

later, Hannigan et al. (1973) presented data on fiber orientation in Hereford heifers. Seven pairs of heifer twins expressed the disorder out of a total of 14 pairs. Bitcover et al. (1974) was the first to identify VFHD in bull hides, which confirmed that even if VFHD is influenced by sex, it is not restricted by such. The paper concluded that 16% of bull hides and 30% of steer hides were affected by the condition. These hides were collected from an inbred line of Hereford cattle to ensure that the differences in VFHD expression among sampled animals were primarily influenced by sex rather than genetic lineage. Based on this data, there appears to be some effect of sex on incidence of VFHD, but no further discussion of these results was provided. Further research is warranted.

Moreover, although Hannigan et al. (1983) failed to conclusively determine the effects of age on VFHD, the study did find that the effects of sex were statistically significant. The study evaluated 182 males and 283 females to conclude that females were more predisposed to VFHD (17.7%) than males (6.6%). Given the stark contrast of VFHD expression between bulls and steers presented in Bitcover et al. (1974), disclosing the proportion of bulls and steers used in Hannigan et al. (1983) would be critical to discern between bulls and steers. Unfortunately, this paper did not explicitly disclose that information. Although more females than males were affected by VFHD in Hannigan et al. (1983), sex may not be entirely responsible for the expression of VFHD. The large difference in incidence between the sexes could be explained by unequal genetic lineage representation across the sexes. Additionally, testosterone levels may play a role in collagen development, as bulls have been found to produce more collagen than steers (Cross et al., 1985), which may help explain some of the differences found previously in VFHD incidence amongst bull and steer hides.

In contrast to the conclusions made by these studies, a later paper by Dufty et al. (1983), noted that the abnormality was not influenced by sex ($P > 0.10$). Out of 120 total male cattle, for which the proportion of bulls and steers was not divulged, 33 (27.5%) were identified with VFHD. The study then found 50 cases of VFHD in a total sample of 161 females (31%). Given that this study conflicts with the results published in Hannigan et al. (1983), further work is clearly necessary to determine the true effect of sex on incidence of VFHD.

Hide weight and diet were also thought to play a role in the development of VFHD. Tancous (1966) concluded that heavy Hereford hides were more affected by VFHD than lighter hides. In the mid-1900s, the leather industry frequently called heavier hides plump and lighter hides spready and these terms are found repeatedly in VFHD literature when discussing the effects of hide characteristics on incidence of VFHD. The disorder occurred in 67% of hides between 31.75 and 45.36 kg, but only affected 20% of hides between 18.14 and 31.75 kg Unfortunately, Tancous (1966) did not provide further discussion on factors, such as greater growth rates, sires with greater growth rates, or increased age that may explain the difference in VFHD expression between the hide weight categories. The following year, Tancous et al. (1967a) classified plump hides as anything heavier than 9.38 kPa and found that 92% of 800 hides with VFHD came from plump hides, demonstrating a relationship between hide weight and the disorder, although it is still unclear if this is a direct relationship between hide weight and VFHD or indirect relationship between hide weight and an intermediate factor like increased age or growth rate and VFHD expression. Tancous et al. (1967b) provided further information on the role of hide weight by publishing data on an additional 1600 hides. This study found that almost all VFHD-affected hides were from plump Hereford hides, whereas Angus and spready Hereford

hides produced almost entirely strong leather. Furthermore, Duivestein et al. (2000) found a moderately strong phenotypic correlation of 0.43 between hide weight and occurrence of VFHD.

Ornes et al. (1964) hypothesized that at least part of this trend may be attributed to producers putting increased selection pressure on fatter animals to increase intramuscular fat, enhance meat quality, and improve tenderness. Tancous (1966) suggested that this increased prevalence of the abnormality was a result of greater consumer demand for beef and increased fat content associated with cattle raised longer before slaughter. Tancous et al. (1967b) suggested that in breeders' efforts to improve beef tenderness, they may have produced fragile VFHD-affected hides at the same time.

Expanding on the evidence that VFHD affects predominantly heavy hides, Thorstensen (1969) proposed that high-energy diets commonly used in feedlot operations may contribute to the incidence of VFHD. In subsequent years, however, data published in Hannigan et al. (1973) refuted this hypothesis. In this study, low- and high-energy diets were assigned randomly to 28 Hereford and 30 Holstein twin heifers. Biopsy results showed that 13 Hereford heifers were diagnosed with VFHD, 69% of which were fed a low-energy diet. Although more affected animals were fed low-energy diets, identical twins had matching fiber orientations despite some animals being fed different diets than their twins. These results indicated that there is not a direct correlation between diet and the condition.

The influence of season on incidence of VFHD was also considered. Tancous et al. (1966) determined that 44% of the fall and winter hides and 12.5% of the spring and summer hides were associated with VFHD. However, further research revealed no significant relationship between seasonality and frequency of the disorder (Tancous et al. 1967a, Tancous et al. 1967b).

The tanning process itself has been proposed as one cause of VFHD. One characteristic of VFHD hides is the increased risk of splitting or breaking as a result of the poorly interwoven collagen fibers of the corium (Amos 1958). When the first formal data on VFHD was published, Amos (1958) found that several stages of the leather-making process, including mechanical actions in dyeing and fat-liquoring, setting, paste-drying, staking, and lasting further weakened the fibers and greatly increased the chance of hide damage. However, in tanneries with functional machinery and skilled workers, both affected and unaffected hides were found, which suggests that VFHD is a disorder present in the hide prior to processing. Ornes et al. (1964) was one of the first to address the impact of the leather making process on VFHD occurrence. Affected hides were often discovered in lots of normal hides, indicating that variation in hide strength was more likely a result of individual hide differences than the leather-making process itself. Although many commercial operations were still skeptical that improper curing or tanning was responsible for VFHD, Tancous (1966) traced the abnormality back to fresh hides, prior to any processing. It was quickly established that VFHD was not a result of processing errors, but rather an inherent characteristic of the hides themselves.

Several other environmental variables were considered in the search for the ultimate cause of VFHD, particularly those related to the affected animals themselves. In Dufty et al. (1983), VFHD was diagnosed in 83 of the study's 362 cattle, but the presence of VFHD was not influenced by the animal's birth year and season, gestation period, birth weight, dam age, dam parity, or dam weight. The only statistically significant factor influencing the presence or absence of VFHD was parental lineage, providing additional evidence for genetic control of the condition.

Genetic Factors

Previous studies have determined that VFHD has a higher rate of occurrence in Hereford and Hereford-cross cattle (Amos 1958, Tancous 1966, Tancous et al. 1967a, Hannigan et al. 1973, Everett & Hannigan, 1978; Peters & Bavinton, 1983; Hannigan et al., 1983; Cundiff et al., 1988). Although some papers have proposed a genetic cause of this condition, Everett et al. (1967) refuted that suggestion. They asserted that genetic relationships would need to be evaluated in all VFHD-affected crossbred cattle, a task that the authors considered "extremely difficult and unlikely" to provide conclusive support of genetic etiology. Instead, Everett et al. (1967) suggested that localized environmental factors play a major role in the development of VFHD, but many other studies have determined that genetics is the primary regulator of VFHD.

Vertical fiber hide defect is assumed to be mostly, if not entirely, under genetic control (Everett et al. 1971, Cundiff et al. 1988). Amos (1958) drew attention to the breed-specific nature of the disorder and speculated that it may be due to a mutation found only in certain Hereford pedigrees. Everett et al. (1971) assessed the quality of 130 steer hides from 15 registered bulls, hypothesizing that VFHD is the result of genetic predisposition. Hides affected with VFHD primarily came from four bulls and several sires did not produce any affected offspring. This variation demonstrates that the abnormality is present in certain lineages, but not all, which is consistent with genetic regulation. Unfortunately, the results published in Everett et al. (1971) were not conclusive due to the small sample size available; however, this study provided the foundation for further genetics research on VFHD. Hannigan et al. (1973) offered the next cogent evidence of the disorder's genetic origin in the form of Holstein and Hereford heifer twins. Not only did this study determine that all incidences of VFHD came from Hereford heifers, but it also established that identical twins always had matching fiber orientations,

whereas fraternal twins did not. Bitcover et al. (1974) tested cattle from inbred lines of four foundational Hereford sires. Sires A and B had the most frequent rate of VFHD in their progeny, at 30% and 35%, respectively. Sires C and D still produced affected progeny, but at a much lower rate of incidence. This variation was most likely a result of genetic differences. Bitcover et al. (1974) acknowledged that mating animals within this inbred line together means that the results may not be entirely conclusive but this data may indicate that there could be more than one mutation responsible for the VFHD phenotype. Alternatively, sires A and B may have been homozygous for the condition, while sires C and D could have been heterozygous carriers, thereby reducing the probability that sires C and D would pass on a VFHD-affiliated allele to an offspring.

The next obvious step was to crossbreed cattle with known genealogies to determine the abnormality's mode of inheritance. Everett and Hannigan (1978) used the twin heifers from Hannigan et al. (1973) to analyze the effects of breeding VFHD-affected cattle. The Hereford heifers were bred to four Holstein bulls. Conversely, the Holstein heifers were bred to four Hereford bulls. None of the Holstein bull progeny expressed the disorder, but one of the Hereford bull progeny did. This may be consistent with an autosomal dominant mechanism of inheritance with incomplete penetrance or possibly genomic imprinting in which VFHD expression depends on the allele provided by a single parent. In the latter case, only one copy of the VFHD allele would be necessary to express the phenotype as a result of differential methylation processes in the development of maternal and paternal gametes. However, the researchers did not discuss the implication of their work on mode of inheritance, but rather on providing additional evidence that VFHD is primarily under genetic control.

More recently, Dufty et al. (1983) analyzed the presence of VFHD in 362 Hereford cattle and grouped these cattle by sire. The cattle were born, raised, and grazed on the same pastures in the same farm to mitigate any environmental effects. As mentioned previously, Dufty et al. (1983) reported the overall prevalence of VFHD to be 22.9%. Intriguingly, of the 24 sire groups, only 12 had affected animals. There was a significant difference in VFHD expression among sire groups ($X^2 = 62.56$; $P<0.001$), which also demonstrates that VFHD is a trait under primarily genetic control. The second phase of this study involved mating phenotypically normal animals with other phenotypically normal animals and animals with VFHD. The study used six normal bulls, 101 normal females, and 26 VFHD-affected females. The objective of this phase was to identify the mode of inheritance of VFHD by comparing theoretically expected ratios to those realized through the performed matings. Several possibilities were considered, such as autosomal or sex-linked and recessive, dominant, or co-dominant mechanisms, which are summarized below. In this study, 26 VFHD-affected females were mated to six normal bulls that had previously produced VFHD-affected progeny. From this mating, 41 offspring were produced, of which 22 (53.7%) had VFHD. Based on these results, the researchers hypothesized that the condition is inherited via an autosomal recessive mechanism. To confirm this hypothesis, Dufty et al. (1983) compared the observed progeny ratios to what would be expected under this mode of inheritance. For the mating of carrier bulls to VFHD cows, 50% of the progeny should be phenotypically normal and 50% of the progeny should have VFHD. The observed ratio did not differ significantly ($X_2 = 0.22; P > 0.6$) from this hypothetical ratio, which helps support the hypothesis, however additional research would need to be conducted to confirm this conclusion.

Cundiff et al. (1987) examined the inheritance mechanism of VFHD in a herd of 465 Hereford cattle, including 44 dam-offspring pairs, from Hannigan et al. (1983). In this study,

three distinct phenotypes were found: vertical fiber orientation, horizontal fiber orientation, and an intermediary between the two, thereby revealing the possibility of additive inheritance. Under an additive mode of inheritance, VFHD-affected, intermediate, and normal phenotypes would be associated with *VV, Vv, and vv* genotypes, respectively, at one locus. However, Cundiff et al. (1987) showed that *vv* dams produced *VV* offspring and *VV* dams produced *vv* offspring, invalidating the additive pattern of inheritance. It was accordingly presumed that if VFHD is controlled by an allele at a single locus, the VFHD and intermediate phenotypes are not two distinct genotypes, but more likely different levels of expression of the same genotype. Following this thought pattern, the intermediate phenotype could be a result of a modifier at another locus or possibly variable expressivity of alleles at a single locus. Although Dufty et al. (1983) concluded that VFHD is not controlled by autosomal dominance, Cundiff et al. (1987) left no stone unturned. In the case of autosomal dominance, it is possible that the VFHD and intermediate phenotypes could be associated with *VV* and *Vv* genotypes respectively, while normal phenotypes would be a result of the *vv* genotype. The incidence of VFHD in the offspring-dam pairs was consistent with this mode of inheritance, but of the study's 465 progeny by 65 sires, 62 progeny (13.3%) and 31 sires (47.7%) were diagnosed with VFHD. It was expected that the frequency of VFHD in sires would be less than that in offspring, but because this was not the case ($X^2 = 44.2$; $P<0.005$), Cundiff et al. (1987) ultimately determined that the condition is not a result of autosomal dominance inheritance, but is more likely the product of an autosomal recessive mechanism.

To further demonstrate this point, Cundiff et al. (1987) provided evidence of autosomal recessive inheritance by mating affected animals together. In this part of the study, an affected Hereford bull was mated to affected Hereford cows as well as to phenotypically normal Angus

cows. When the bull was mated to affected cows, all 5 offspring were found to have vertical fiber orientation. This is consistent with mating a *vv* genotype to another *vv*, in which case we would expect all offspring to be *vv*. Furthermore, in the mating of the VFHD-affected bull to normal cows, all 12 offspring expressed the normal phenotype. Given that the normal cows were Angus, in which there is minimal to no prevalence of VFHD, this is presumably a *vv* · *VV* cross, which would result in all *Vv* offspring with normal phenotypes, as demonstrated. Despite the small sample size of this study, Cundiff et al. (1987) provided evidence that VFHD is controlled by an autosomal recessive mode of inheritance.

The wide range of VFHD phenotypic expression offers a cogent argument for an increased range of classification categories, which was addressed by Duivestein et al. (2000). Research on VFHD suggests that it is an abnormality of genetic origin, with the prevailing belief that it manifests itself in an autosomal recessive inheritance pattern. The intermediate phenotype is considered to be a lesser degree of VFHD expression, which alludes to the possibility of polygenic inheritance. In other words, VFHD may not be simply determined by recessive alleles at one locus, as previously believed, but rather the combined action of several genes concurrently. If VFHD follows polygenic inheritance, a classification scheme with greater specificity, such as the 5-category scheme proposed by Duivestein et al. (2000), may offer an increased chance of pinpointing the individual effects of associated genes.

Heritability Estimates

Initial research into the VFHD condition focused on recording the incidence of the disorder, but once it was suggested that VFHD may be under genetic control, research shifted to better understanding the heritability of the trait. The first paper to propose a heritability value was Hannigan et al. (1973), which analyzed data from 130 hides to estimate a heritability of

30%. Little information on the method of calculation or analysis was provided. A decade later, Hannigan et al. (1983) estimated heritability for VFHD to be very high. This study analyzed the hides from 182 Hereford males and 283 Hereford females for the presence of the condition. Vertical fiber hide defect heritability was based on sire records of the 465 Herefords in a mixed model analysis and estimated to be 0.88 (SE ± 0.25) for females and 0.81 (SE ± 0.31) for males. Cundiff et al. (1988) later estimated the heritability of VFHD as 84%. No further heritability estimates have been published. Further, the exact mode of VFHD inheritance is unknown. Thus, if the trait was simply inherited, estimating heritability for that trait would not yield meaningful results. Heritability is calculated as the proportion of additive variance of total phenotypic variance. A simply inherited trait would have dominance action and not additive, thereby resulting in a heritability of zero.

Health Implications

Reproductive Performance

While examining the breed-specific nature of VFHD, Everett and Hannigan (1978) discovered an unfortunate consequence of the abnormality on cow fertility. Phenotypically normal Herefords and Holsteins had live calf crop rates of 90% and 86%, respectively. Only Herefords were found to have VFHD, of which those of intermediate phenotype had a live calf crop of 70% and those with excessive vertical fiber orientation had a live crop of only 53%. Unfortunately, this study was not large enough to make definitive conclusions on the effect of VFHD on fecundity, but it prompted further research into the effect of VFHD on other economically relevant traits.

Dufty et al. (1981) also examined reproductive performance in affected animals. A total of 119 Hereford cattle was observed for calving difficulty. Although the number of cows experiencing dystocia was significantly different between initial and successive parturitions, Dufty et al. (1981) discovered that calving difficulty had no significant effect among cattle with normal, intermediate, or vertical fiber orientations. The incidence of calving problems in phenotypically normal animals was found to be 11%, but cattle with intermediate weave and VFHD-affected cows experienced issues during parturition at 14.3% and 9.4%, respectively. In terms of fertility, 91 heifers were also examined for conception rates and estrous cycle lengths, and there were minimal differences among the 3 fiber classifications for either trait. The results in Dufty et al. (1981) suggest a contrast to those presented in Everett and Hannigan (1978), making it difficult to accurately assess the true association between hide fiber orientation and reproductive performance.

Hannigan et al. (1983) contributed to this debate by confirming that pregnancy rates, birth rates, live calf crops, and calf crop weaning rates were not significantly impacted by the presence or absence of the VFHD condition in 465 Hereford animals. For example, affected cattle had pregnancy rates of 94%, while normal cows had an average pregnancy rate of 93%. Furthermore, it was rationalized that because VFHD was more frequently found in older animals in the herd, it must not negatively influence reproductive performance, as animals with poor reproductive performance should have been culled from the herd.

Treatment and Prevention

There is no known treatment for VFHD-affected animals and no research has been completed in this area primarily due to the difficulty of diagnosis. However, several methods of prevention have been proposed since the disorder was recognized in 1958.

Amos (1958) acknowledged that identifying VFHD by sight alone is nearly, if not entirely, impossible, but histologically analyzing every hide entering the tannery is not feasible due to the high cost and technical skills involved. Strength testing leather samples for VFHD is another impractical approach for producers. Firstly, the leather of current breeding stock cannot be tested for VFHD as leather is made once the hide has been removed during carcass processing and by this point, the animal would no longer be used for breeding. Secondly, cutting leather samples and conducting strength tests is expensive and time-consuming, which deceases any potential profits from the hides.

Several papers have suggested selection-based approaches to prevent the incidence of VFHD in cattle herds. Peters and Dufty (1985) examined the impact of three different selection programs on VFHD prevalence via simulation. In the first program, all VFHD-affected animals were removed from the herd. Affected cattle were considered homozygous, while phenotypically normal cattle could either be carriers or homozygous. There was a substantial reduction in disorder occurrence when all affected animals were removed from the herd. However, VFHD could rarely be eliminated from the population, because the recessive VFHD allele persisted in carrier animals and continued to show up in the progeny produced by heterozygous parents.

In the next system, only affected sires were removed from the herd, which showed a similar pattern as the first method, but was slightly less efficient. There was a sharp initial decrease in the prevalence of VFHD that leveled out over time.

The final selection program only used bulls homozygous for the normal phenotype in disassortative mating decisions. This was the most complex management system and required bulls to be mated to VFHD-affected or known carrier cows. Homozygous normal bulls could be identified by the production of all normal offspring and could then be used in the selection program. Like the previous programs, initial VFHD presence decreases, but when at least 50% of dams were replaced each generation, this program was found to be the most efficient of the three. In the first generation of this mating program, all progeny would be phenotypically normal with at least one normal allele. Some female progeny will be carriers, but when mated to homozygous normal bulls, the resulting progeny will also be phenotypically normal. However, when fewer than 50% of the dams were replaced, the first selection system was found to be the most efficient in reducing the incidence of VFHD (Peters and Dufty, 1985). Even though there are not many other means by which to reduce VFHD incidence currently, these systems may not be practical for producers as they involve hide evaluations to assess individual animal phenotypes and a substantial investment of time.

Cundiff et al. (1987) proposed that crossbreeding programs would be the best method of reducing VFHD incidence because the condition appears to be breed-specific. Hannigan et al. (1983) found that 13.3% of tested Herefords expressed VFHD, while 0% of Angus did. Simulated rotational crossing of Hereford and Angus cattle would reduce the incidence rate to around 4%. Adding another unaffected breed would reduce the incidence even further, to about 2%. In Cundiff et al. (1987), it was estimated that nearly 70% of beef cattle produced in the United States are crossbred, so the benefits of this type of selection program would be widespread. Currently, crossbred cattle are thought to compose between one- and two-thirds of the United States beef industry (Ishmael, 2020; USDA-APHIS, 2009). A survey given by the

United States Department of Agriculture and Animal and Plant Health Inspection Service (2009) revealed that 65% of producers raise mostly crossbred cattle. An additional survey conducted by BEEF Magazine (Ishmael, 2020) found that as of 2019, approximately 40% of U.S. producers described their herds as crossbred. With so many crossbred cattle involved in the beef industry, implementing crossbreeding management programs would not only be feasible, but advantageous for producers as well.

However, selecting non-VFHD-affected animals to crossbreed may prove to be as challenging as sorting leathers at the tannery without the availability of a genomic test. There are many other considerations that must go into mating decisions and reducing the occurrence of VFHD may simply not be worth the risk of inbreeding or labor involved in classifying the abnormality. Culling decisions should not be made lightly, and some VFHD-affected bulls may provide alternative benefits, such as in traits associated with economic importance.

With such high estimates of heritability for VFHD (Hannigan et al.,1973; Hannigan et al., 1983; Cundiff et al., 1988), assuming that VFHD is a polygenic trait, genomic selection against the VFHD phenotype would be especially successful in reducing incidence of the disorder and subsequently alleviating associated financial losses to the leather industry. Until genomic tests are developed to diagnose VFHD, selective breeding to reduce the abnormality is likely not worth the extra effort and expense when compared to other, more financially significant traits. There is no premium or discount, and therefore no incentive, for producers to select against the condition. Thus, it is imperative for future VFHD research to focus on identifying the current prevalence of the condition and its causal mutation(s) in the hopes of eventually developing a genomic test to aid producers in eliminating VFHD without sacrificing genetic potential of other traits.

Current Advancements in Research

Recent research on VFHD is minimal, with the most recent data on the condition published in the beginning of the 21st century. Duivestein et al. (2000) took samples from 102 hides visually identified to be of Hereford descent. Sections were cut from each sample either by hand or microtome. Hand-cut sections were excised by a standard surgical scalpel and examined under a magnifying glass (10X). Microtome sections were cut into 60-micron slices with a Leitz 1512 microtome and subsequently stained with haematoxylin and eosin and examined under a microscope (30X). The main goal of the study was to determine if VFHD could be consistently identified by both methods. Duivestein et al. (2000) ultimately concluded that the hand-cut sections were as beneficial in identifying VFHD as the laborious microtome sections. However, hand-cut sections were found to have increased variability between sections cut from the same hide, most likely as a result of the varying degrees of thickness per slice, especially as compared to the consistent and uniformly thin microtome slices.

More recently, Sizeland et al. (2013) measured collagen fiber orientation in seven mammalian species to broadly examine the relationship between collagen strength and fiber orientation. The mammals included in the study were sheep, possum, cattle, goat, water buffalo, deer, and horse. Skin samples were collected from each animal, processed into leather, and tested for tear strength. Sizeland et al. (2013) found that the tear strength of leather depended largely on the orientation of the collagen fibers as fiber orientation has a very strong correlation with tear strength in all species. It was noted that the strongest leathers had fibers that were parallel to the plane of the hide. However, when fibers are perpendicular to this plane, the leather is highly susceptible to tearing. Sizeland et al. (2013) explained that this is indicative of VFHD, but

unfortunately, no VFHD-affected samples of any species were included in the study for further discussion. Ultimately, collagen was concluded as being crucial for the structural composition of leather and skin and any disorder or disease that affects collagen can have devastating effects on the health of an animal (Sizeland et al., 2013).

Most literature regarding VFHD was published in the mid-20th century and since then, few studies have followed the disorder into modern-day cattle populations. The more recent articles on VFHD focus primarily on collagen orientation and strength in leather processing without providing any new data on the condition. It is unknown if VFHD has continued to increase in frequency or has been eradicated from the population, so the lack of novel publications on the abnormality offers a compelling argument for its further study. Despite limited recent research on VFHD, there are many other collagen abnormalities in other species described in the literature that may help elucidate the underlying mechanisms of VFHD. The tear strength of cattle hide is very similar to that of goat and sheep, indicating that research on collagen mutations of other species may hold clues to the etiology of VFHD (Sizeland et al., 2013).

Related Disorders in Other Species

Dermatosparaxis is a genetic connective tissue disorder that commonly affects sheep and cattle and is often characterized by easily torn skin and joint hypermotility (Holbrook et al., 1980). The skin is so fragile that the abnormality is easily detected at parturition, or soon after, and affected animals tend to have limited life spans as a result of accompanying lesions and septicemia (Hanset and Lapiere, 1974). Simar and Betz (1971) used electron microscopy to view

dermatosparaxis skin samples from calves and discovered that the normally horizontal collagen fiber orientation was compromised, and fibers tended to orient more vertically than expected. Dermatosparaxis is attributed to malfunctioning procollagen precursors that assist in assembling collagen fibers. This mutation prevents normal collagen fibers from forming, thereby reducing the skin's tensile strength and has been traced to a disintegrin and metalloproteinase with the thrombospondin type 1 motif 2 (ADAMTS2) gene in Dorper sheep (Zhou et al., 2011), which may prove to be a useful candidate gene for VFHD.

The condition is not limited to sheep and cattle exclusively. Holbrook et al. (1980) found dermatosparaxis in a Himalayan cat and upon further histological evaluation, it was discovered that the collagen fibers were oriented perpendicular to the skin surface, like the orientation of fibers in VFHD-afflicted cattle. In a control cat without dermatosparaxis, the collagen fibers were parallel to the skin surface. Dermatosparaxis is analogous to Ehlers-Danlos syndrome type VIIC in humans (Holbrook et al., 1980).

Ehlers-Danlos syndrome type VIIC arises as a result of mutations in the genes in charge of producing normal collagen precursors, which are in turn responsible for producing normal collagen fibers (Nusgens et al., 1992). Nusgens et al. (1992) conducted a case study on a two-year old girl affected by Ehlers-Danlos syndrome type VIIC. She had delicate skin that easily tore and frequently bruised. Severe wounds could not be treated surgically due to the skin's fragility and associated inability to suture it. The researchers noted that the child's skin was comparable to that of calves affected by dermatosparaxis.

Dermatosparaxis is also similar to a connective tissue disorder in horses, hereditary equine regional dermal asthenia (HERDA). This is a genetic disorder that primarily affects Quarter Horses and is characterized by extremely fragile skin that sloughs off the animal upon

minimal physical trauma (Grady et al., 2009). Tryon et al. (2007) used homozygosity mapping of 68 HERDA-affected horses and found that 64 of these animals had a common haplotype on *Equus caballus* chromosome 1 (ECA1). A missense mutation in cyclophilin B (PPIB), a chaperone protein responsible for proper collagen protein folding, was uniquely identified in horses with HERDA and was proposed as a likely causal candidate mutation. Both HERDA and VFHD appear to be localized to similarly specific areas on affected animals. VFHD is found most often on the rumps of cattle, between the hook and pin bones, while HERDA is typically exhibited along the dorsal skin surface of affected horses (Grady et al., 2009).

In addition to collagen disorders in cattle and other species, small biochemical processes may provide clues toward the development of VFHD. Decorin is one of four main small leucine-rich proteoglycans (SLRPs) involved in collagen fiber formation and tissue regulation (Grady et al., 2009). Danielson et al. (1997) interrupted, or knocked-out, the decorin gene in mice and discovered that the resulting knockout mice had easily torn skin with lower tensile strength. Figure 1.11 depicts images of three mice from the study, from left to right: wild-type, heterozygote, and homozygous knockout. The animals with both of their decorin loci disrupted had loosely arranged collagen fibers, just like those of VFHD-affected animals. Further biochemical study of VFHD may also prove helpful in diagnosing and selecting against VFHD in the future. However, biochemical studies often involve the use of protein assays, which are considerably more difficult to do than genomic testing, especially in the cattle industry. Thus, these types of studies may prove useful in obtaining more information about the disorder and the components, like decorin, potentially involved in its expression but would not be practical for industry implementation.

Collagen disorders that affect skin strength are incredibly important to understand for a variety of applications. Collagen-based materials are often used medically, including processed pericardium for heart valve repairs, or industrially, such as in shoes and upholstery (Sizeland et al., 2013). The soft leather and splitting associated with VFHD produces unsatisfactory leather for shoe factories and can cause significant financial loss (Amos, 1958). Additional studies on VFHD may provide clues to improving industrial applications of collagen.

Conclusion

Vertical fiber hide defect is an enigmatic disorder affecting collagen fiber orientation and the corresponding hide strength of Hereford and Hereford-cross cattle. Although it is widely believed to be a genetic abnormality, no causal mutation has been discovered and VFHD may have minor environmental influences. There are no recent publications that discuss the current frequency of VFHD in cattle herds and thus it is unknown if producers have inadvertently increased its prevalence or whether it has been eradicated from the population. Despite the lack of current research, VFHD has significant implications for the beef and leather industries and recognizing similar collagen gene mutations in cattle and other species may aid researchers in elucidating the inheritance mechanisms of this disorder. Vertical fiber hide defect demands further study to better understand the current frequency of the condition and the associated allele in the population.

Figure 1.1. A comparison of normal fiber orientation (left) and vertical fiber orientation (right).

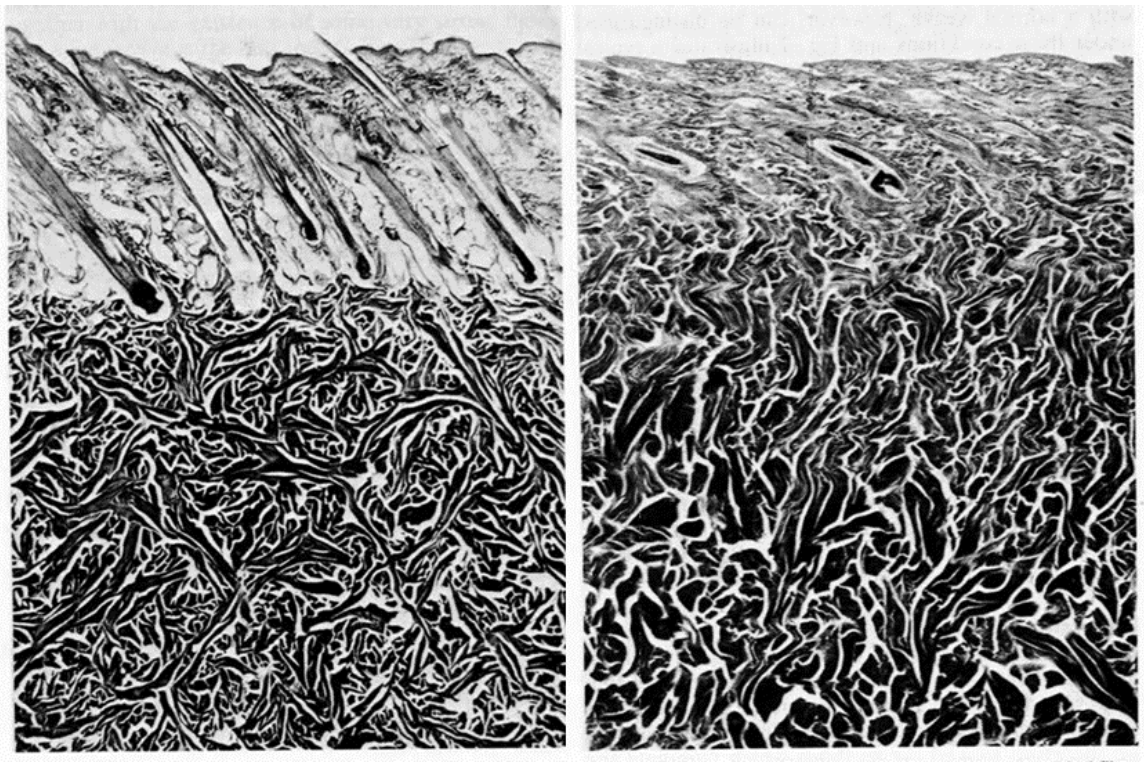

Reprinted from Peters, D. E. and J. H. Bavinton. 1983. The characterization of vertical fiber and high weave structures of Hereford cattle hides. Journal of the Society of Leather Technologists and Chemists 67: 67.

Figure 1.2. Phenotypic differences in hide collagen structure.

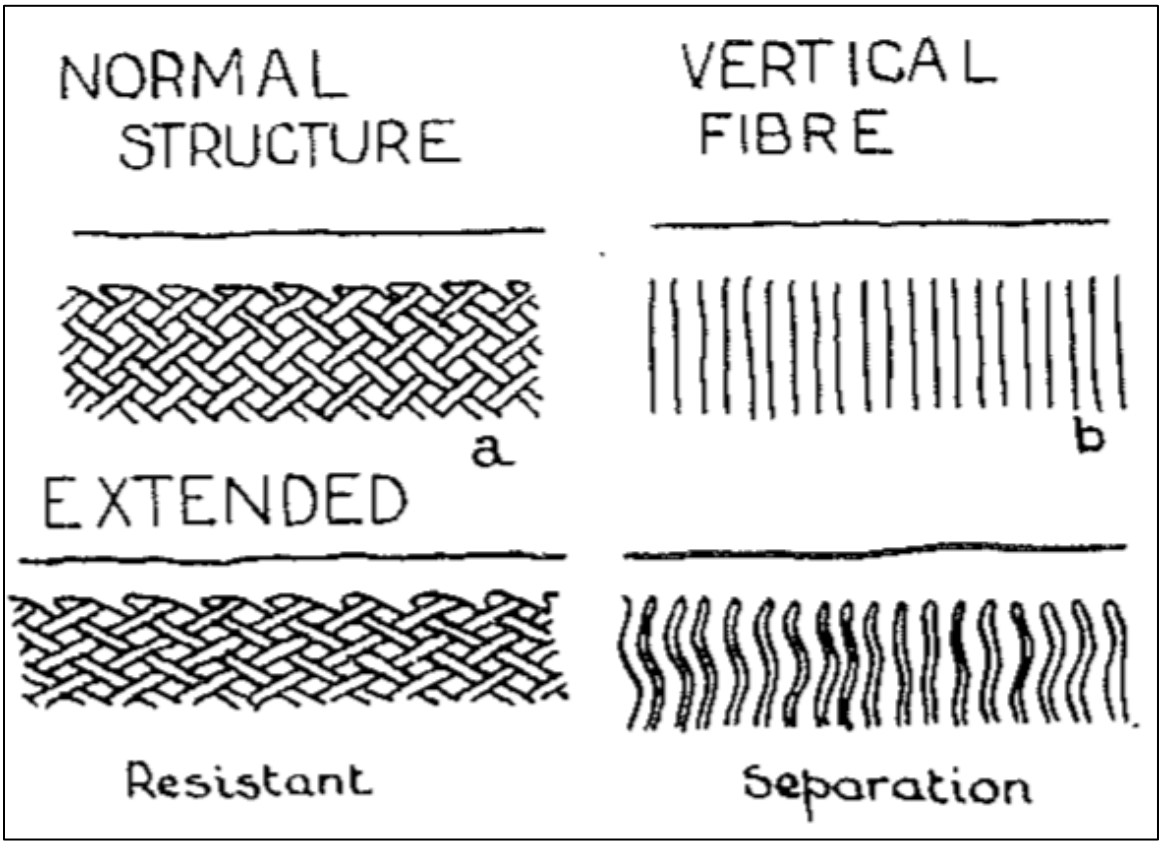

Reprinted from Amos, G. L. 1958. Vertical fibre in relation to the properties of chrome side leather. Journal of the Society of Leather Trades' Chemists 42:87 (Diagram 1).

Figure 1.3. Photograph of biopsy gun and components.

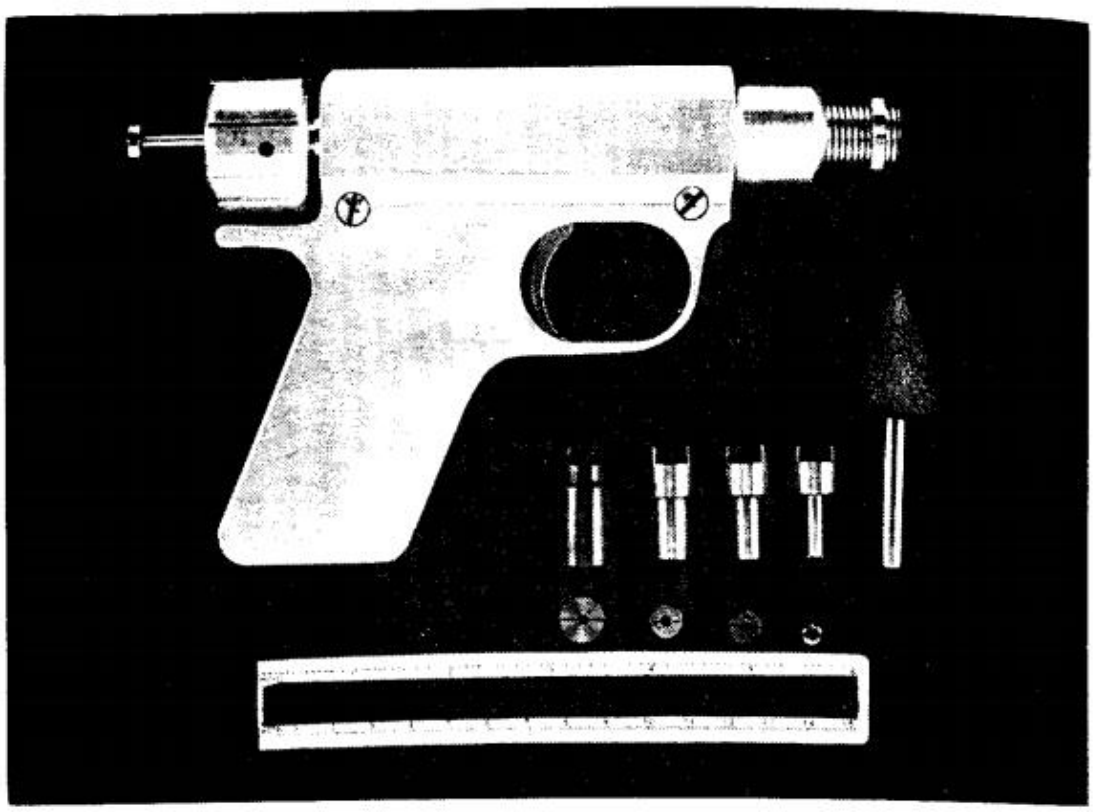

Reprinted from Schied, R. J., E. H. Dolnick, and C. E. Terrill. 1970. A quick method for taking biopsy samples of the skin. Journal of Animal Science 30(5):771-773.

Figure 1.4. The relationship between grain crack strength and fiber orientation.

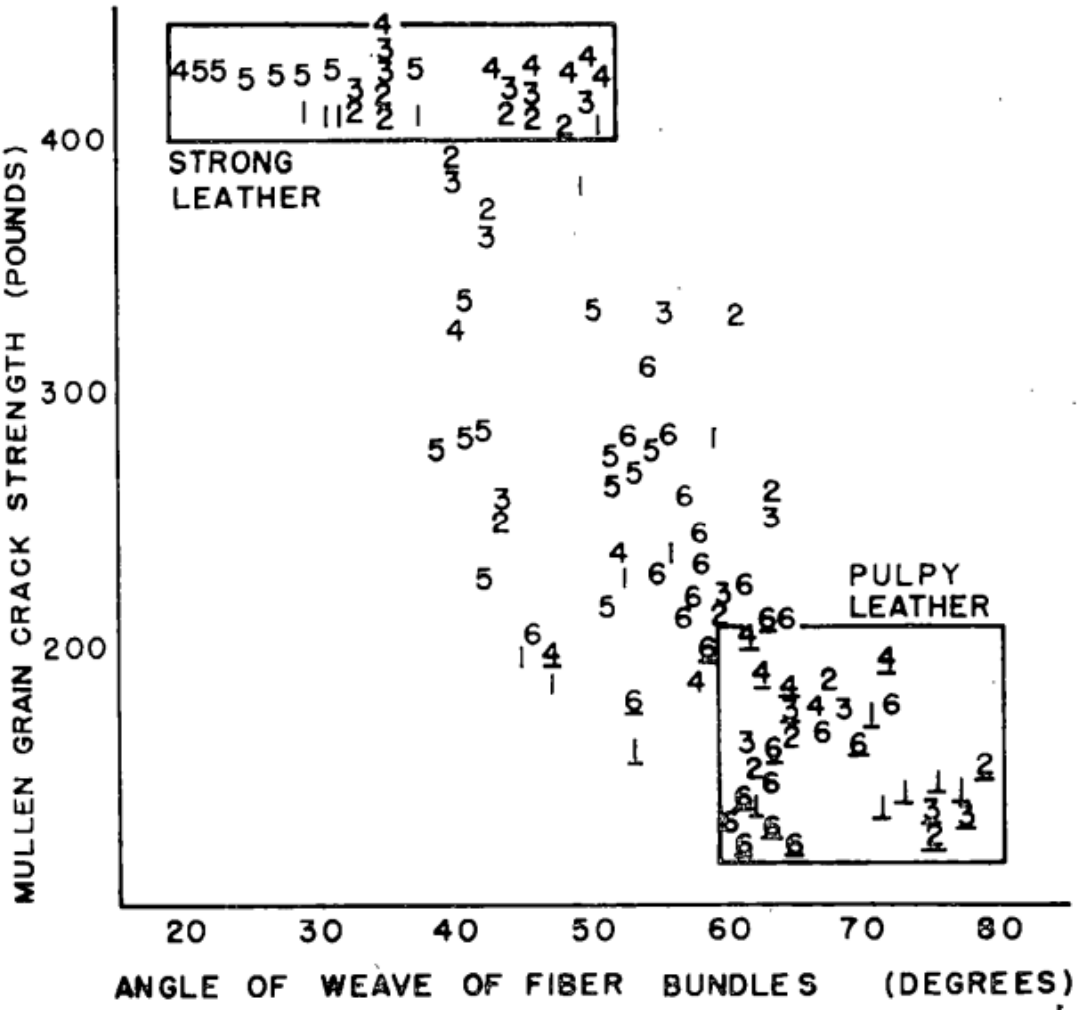

Reprinted from Tancous, J. J., W. Schmitt, and W. Windus. 1967a. The incidence and predictability of weakness and pulpiness in side upper leather. Journal of the American Leather Chemists Association 62:4-24.

Figure 1.5. Stained cross-sections of normal fiber structure (left), intermediate fiber structure (center), and vertical fiber structure (right).

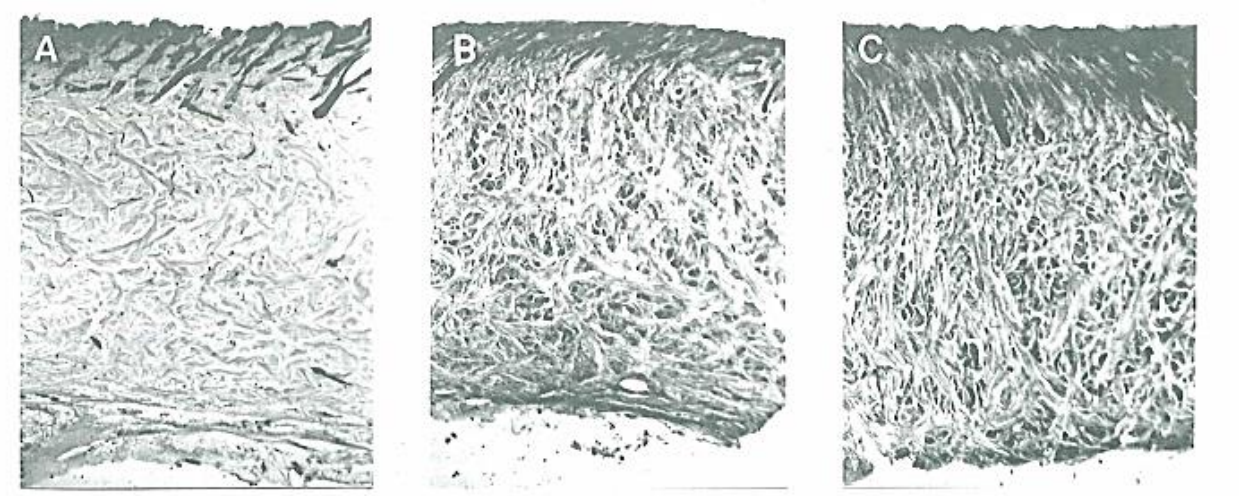

Reprinted from Duivestein, J., W. Pitchford, & C. Bottema. 2000. Detection of vertical fiber hide defect (VFHD) in Hereford cattle hides by biopsy. Journal of the American Leather Chemists Association 95(3):92-101.

Figure 1.6. Vertical fiber structure (left) and normal fiber structure (right) under polarized light.

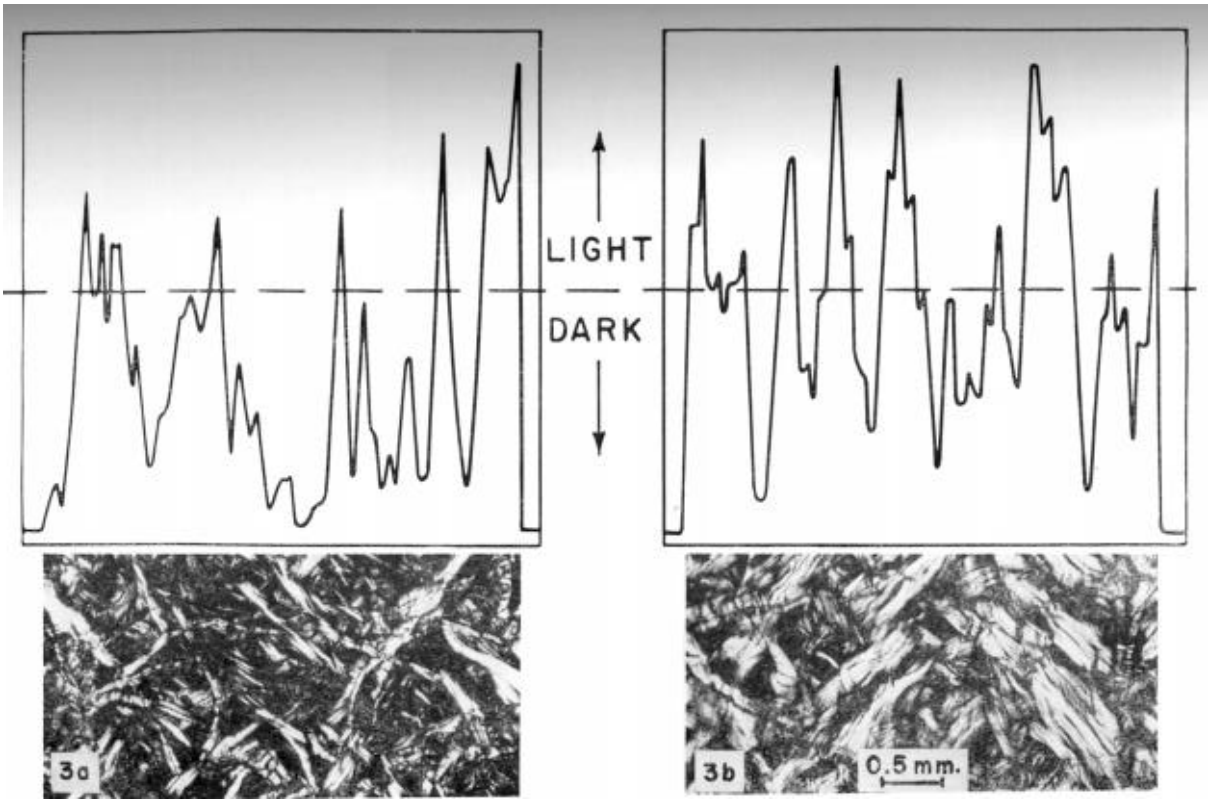

Reprinted from Everett, A. L., H. J. Willard, and W. Windus. 1967. Microscopic study of leather defects: II. Inherent vertical fiber structure in side leather. Journal of the American Leather Chemists Association 62:25-44.

Figure 1.7. A juxtaposition of vertical fiber orientation (top) and normal fiber orientation (bottom) before (left) and after (right) applying a red compensator filter.

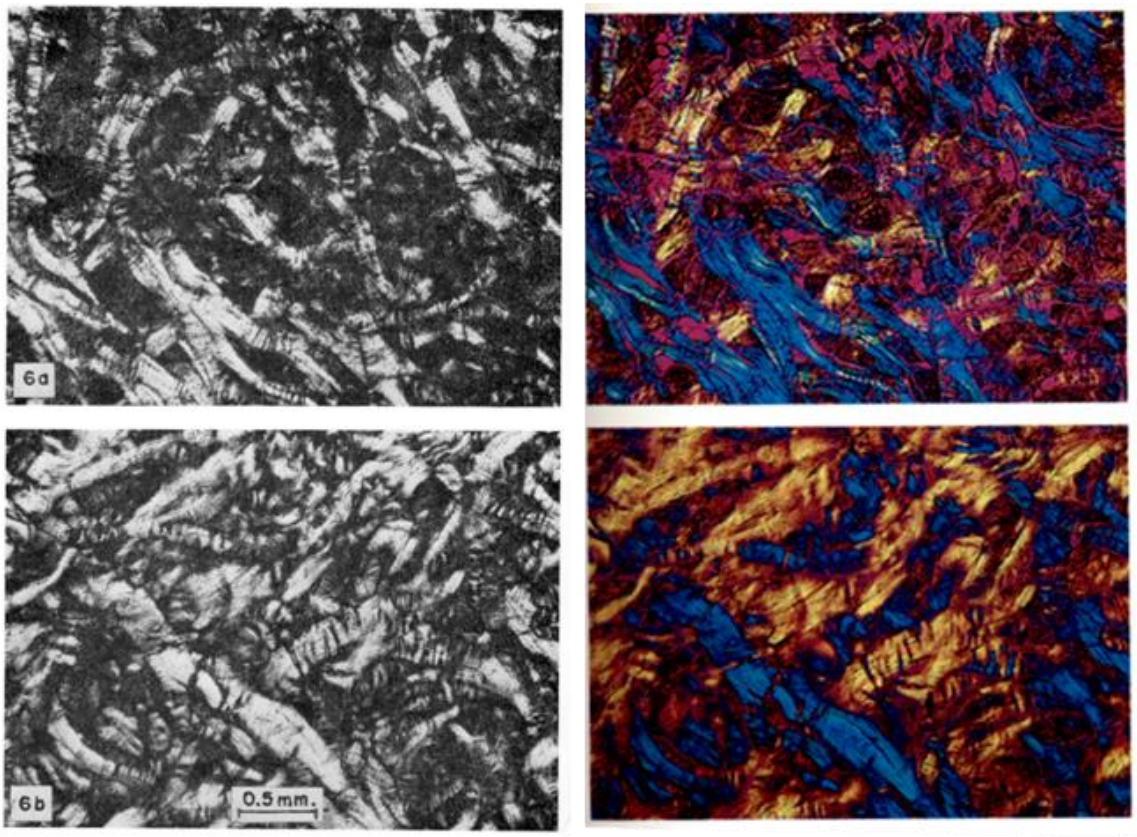

Reprinted from Everett, A. L., H. J. Willard, and W. Windus. 1967. Microscopic study of leather defects: II. Inherent vertical fiber structure in side leather. Journal of the American Leather Chemists Association 62:25-44.

Figure 1.8. SALS patterns of a VFHD hide sample (left) and a normal hide sample (right).

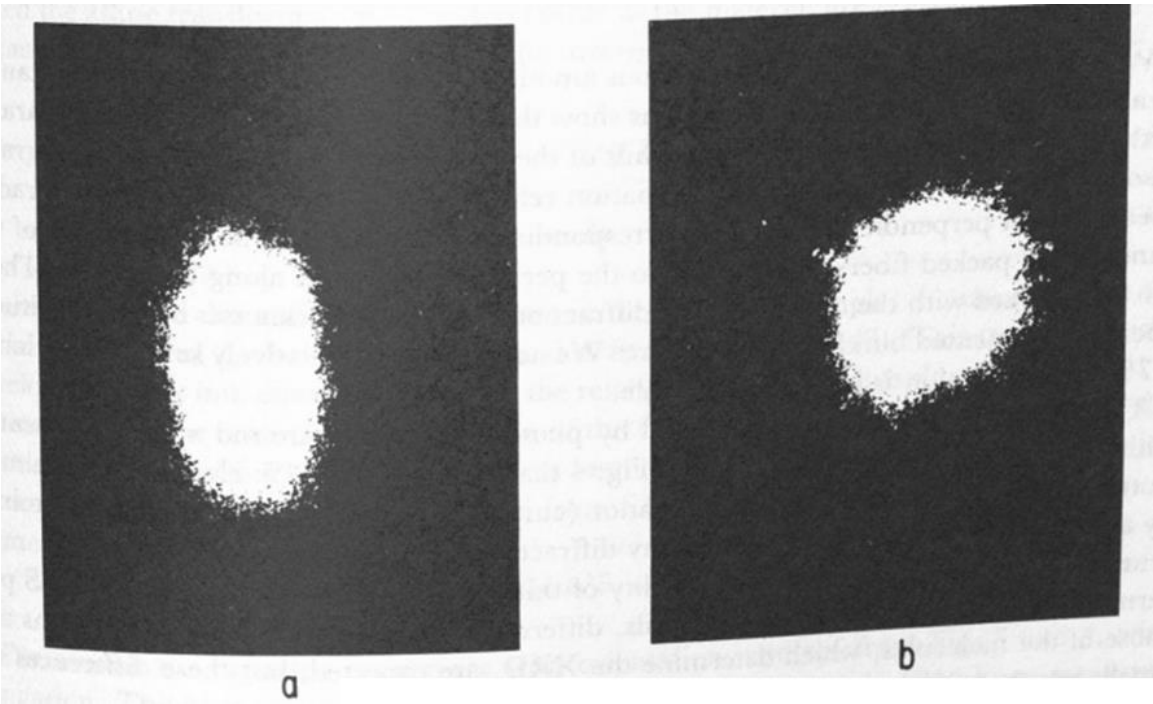

Reprinted from Kronick, P. L. and P. R. Buechler. 1986. Fiber orientation in calfskin by laser light or x-ray diffraction and quantitative relation to mechanical properties. Journal of the American Leather Chemists Association 81(7):221-230.

Figure 1.9. Orientation index values for the three-classification system.

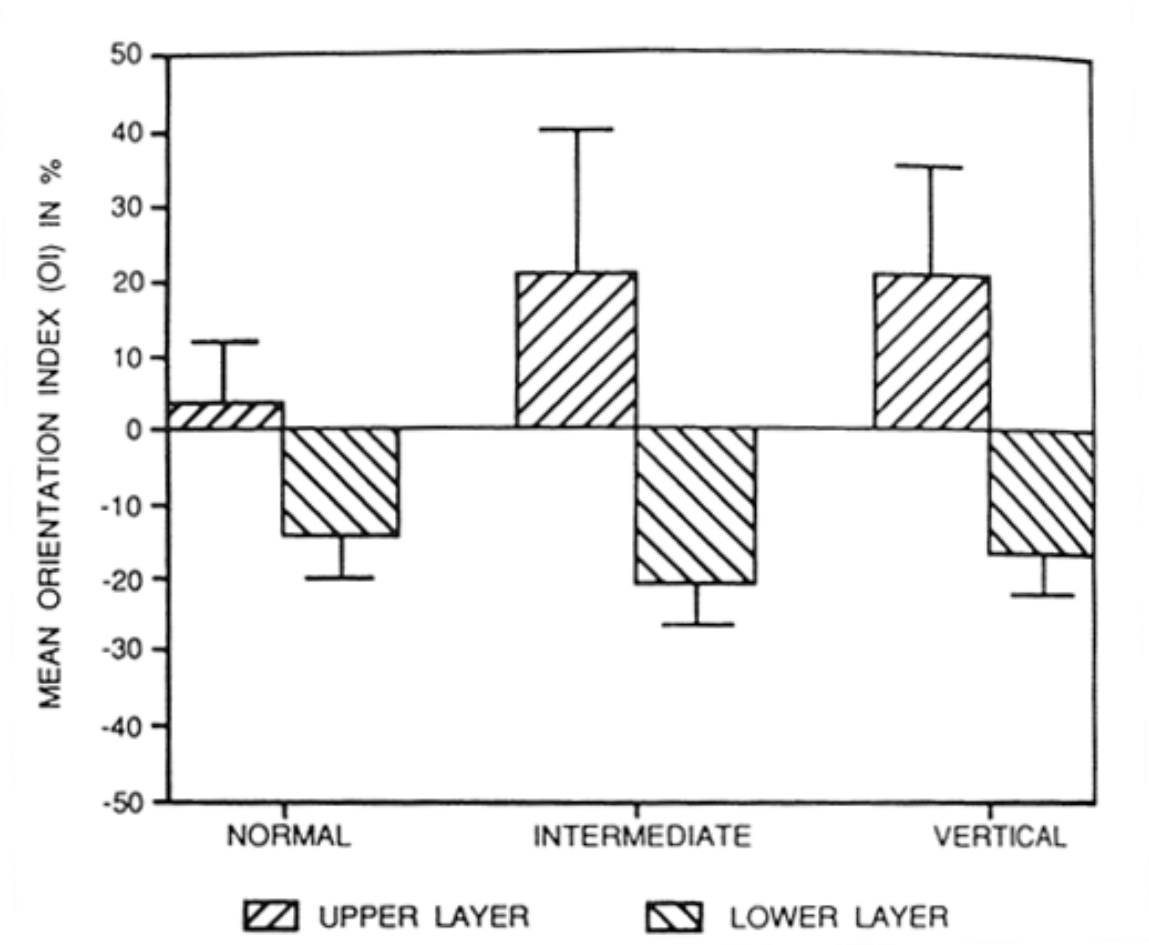

Reprinted from Kronick, P. L., & M. S. Sacks. 1991. Quantification of vertical-fiber hide defect in cattle hide by small-angle light scattering. Journal of Connective Tissue Research 27(1):1-13.

Table 1.1. Age distribution of affected cattle prior to resampling of younger animals.

Age Group	Affected Cattle	Unaffected Cattle	Total Cattle
4 months	7	94	101
7 months	10	90	100
1 year	11	59	70
1.5 years	11	88	99
2 years	6	18	24
3 years	6	17	23
4 years	5	17	23
5+ years	6	19	25

Adapted from Hannigan, M. V., A. L. Everett, M. P. Dahms, & P. R. Buechler. 1983. Vertical fiber hide defect: a biopsy study of Hereford and Angus cattle of known genealogy. Journal of the American Leather Chemists Association 78(7):178-187.

Figure 1.10. The effect of cattle age on the incidence of VFHD.

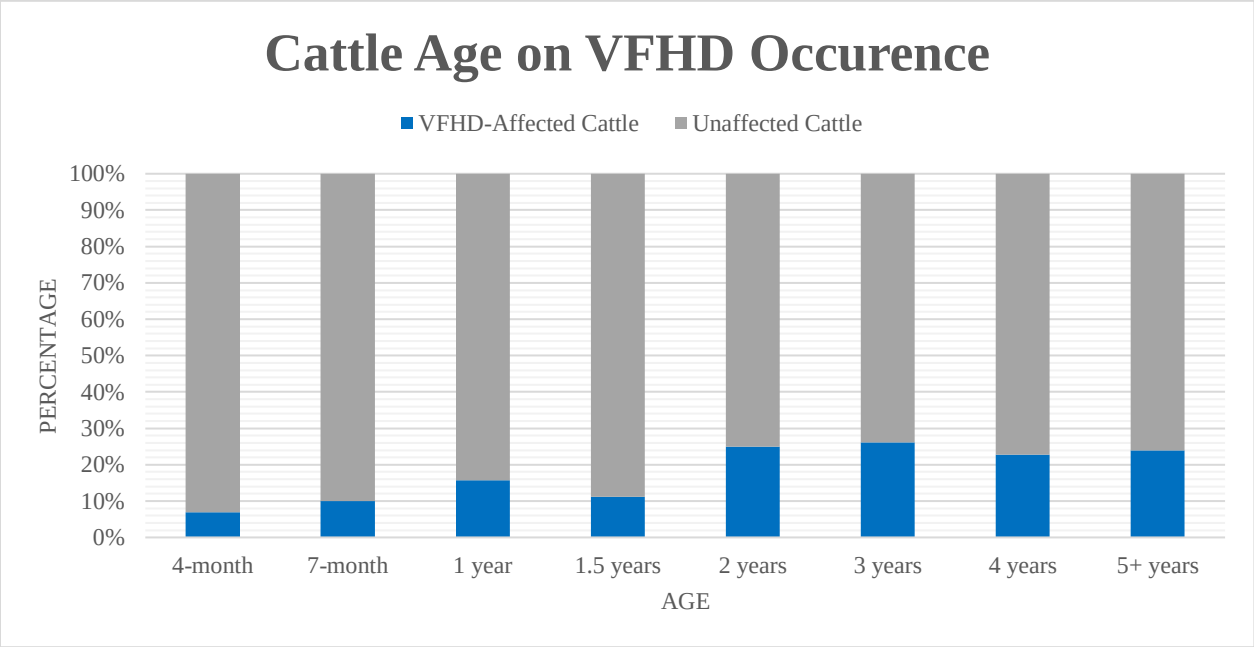

Adapted from Hannigan, M. V., A. L. Everett, M. P. Dahms, & P. R. Buechler. 1983. Vertical fiber hide defect: a biopsy study of Hereford and Angus cattle of known genealogy. Journal of the American Leather Chemists Association 78(7):178-187.

Figure 1.11. Skin fragility of wild-type (left), heterozygous (center), and homozygous knockout (right) mice at the decorin locus.

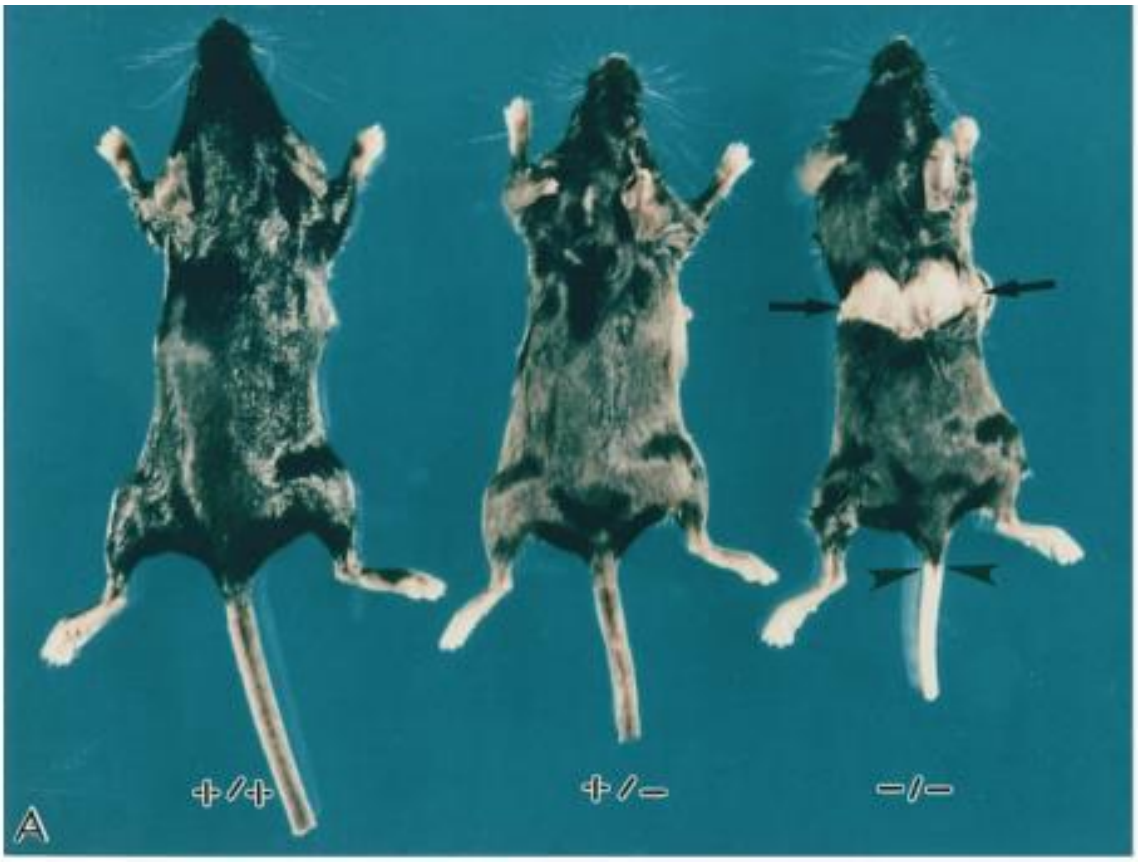

Reprinted from Danielson, K. G., Baribault, H., Holmes, D. F., Graham, H., Kadler, K. E., & Iozzo, R. V. 1997. Targeted disruption of decorin leads to abnormal collagen fibril morphology and skin fragility. Journal of Cell Biology 136: 729-743.

Chapter 2 - Detection of vertical fiber hide defect in beef cattle

K. W. Upshaw[1], M. D. MacNeil[2], A. J. Tarpoff[1], J. M. Gonzalez[3], J. M. Bormann[1], R. L. Weaber[1], and M. M. Rolf[1]

[1]Department of Animal Sciences and Industry, Kansas State University, Manhattan, KS

[2]Delta G, Miles City, MT

[3]Department of Animal and Dairy Science, University of Georgia, Athens, GA

Abstract

Vertical fiber hide defect (VFHD) is a genetic disorder that affects the collagen structure of cattle hides by reducing fiber interlacing and causing hides to tear during tanning. Thus, it results in increased cost and waste during leather good production. Literature from the 1970s reports that VFHD affects 13% of Hereford cattle in the US, however contemporary data is scarce. The primary purpose of this study was to ascertain if VFHD could be detected in a modern herd of purebred Hereford cattle.

Hide biopsies collected from 22 Hereford cattle at the Kansas State University Purebred Unit were dyed with Masson's trichrome stain and microscopically examined to assess collagen fiber architecture. The disorder would be recognized in its vertical or intermediate form when collagen fibers were interwoven between 60-90°.

Of the samples examined, none had abnormal fiber orientation. Thus, VFHD was not detected in this herd. However, this was a small university-owned herd and only contained germplasm from 12 purebred Hereford foundation sires. Due to limited pedigree diversity and sample size, a larger number of samples would need to be tested to determine that the condition does not currently exist in Hereford cattle or to obtain a more contemporary estimate for VFHD presence or frequency. Additional samples from different herds and ancestry may help elucidate modern VFHD prevalence.

VFHD has significant implications for the beef and leather industries and current prevalence estimates will determine whether the identification of markers or causal mutations for genomic testing may be required for practical identification and control of this condition.

Key Words: vertical fiber hide defect, Hereford cattle, leather industry, beef industry, collagen fiber orientation

Introduction

Collagen provides the skin with an interesting combination of rigidity and flexibility, which is important for the production of leather and leather-made goods. Hide collagen disorders can negatively impact leather quality, which can be detrimental for livestock producers because leather is one of the most important by-products of the meat industry (Naffa et al., 2019). Vertical fiber hide defect (VFHD) is one such abnormality that affects the collagen structure of cattle hide (Amos, 1958; Tancous, 1966). The disorder was first identified in the mid-1900s and has a higher rate of occurrence in Hereford and Hereford-cross cattle than in other breeds (Amos, 1958; Tancous, 1966; Tancous et al., 1967a; Tancous et al., 1967b; Hannigan et al., 1973; Everett and Hannigan, 1978; Hannigan et al., 1983; Cundiff et al., 1988).

Hides with VFHD are considerably less durable than hides with normal fiber weave. One of the most important factors involved in hide durability is the alignment of collagen fibers (Sizeland et al., 2013). Hides affected with VFHD are comprised of collagen fibers that are nearly perpendicular to the plane of the hide, as opposed to a more parallel orientation. Vertically oriented collagen fibers reduce normal collagen fiber interlacing, which can cause affected hides to fall apart during tanning (Amos, 1958; Tancous, 1966; Tancous et al., 1967a; Tancous et al., 1967b). Leather produced from VFHD hides has only half the tensile strength and a greater predisposition to cracking and breaking than leather obtained from normal hides (Amos, 1958; Bitcover et al., 1974).

Histological evaluation is currently the only method of diagnosing VFHD. However, histological examination is not practical for the beef or leather industries due to the high level of skill and lengthy amount of time involved for accurate diagnoses (Cundiff et al., 1987). Unfortunately, this makes identifying the condition before the hide falls apart incredibly difficult.

At this point, tanneries have already invested both time and money in the tanning of these affected hides.

Several studies have provided evidence that VFHD is under primarily genetic control. The abnormality has been detected at significantly different frequencies within different sire lines (Everett et al., 1971; Bitcover et al., 1974; Dufty et al., 1983). Moreover, monozygotic identical twin heifers have been found to have matching fiber structures, whereas the fiber structure between sets of dizygotic twins does not always match (Hannigan et al., 1973). Previous studies have provided evidence that VFHD most likely follows an autosomal recessive mode of inheritance, but this has yet to be confirmed and both the genomic position and causal variant are unknown (Dufty et al., 1983; Cundiff et al., 1987).

Previous estimates of VFHD prevalence in the United States suggest that it affects approximately 13% of American Hereford cattle populations (Everett and Hannigan, 1978; Cundiff et al., 1987). The most recent estimate of VFHD occurrence was obtained in Australia, where the abnormality was detected in 28% of the 102 Herefords sampled (Duivestein et al., 2000). There are no publications that discuss the current frequency of VFHD and thus it is unknown if producers have inadvertently increased its prevalence or whether it has been eradicated from the population. If it were detected, genomic tests could be developed to allow for easier management of the condition. The primary purpose of this exploratory study was to ascertain if VFHD can be detected in a modern herd of purebred Hereford cattle. A secondary objective was to present a modified approach to staining VFHD samples.

Materials and Methods

All procedures involving animals were performed in compliance with Kansas State University Institutional Animal Care and Use Committee (IACUC) protocol number 4066.

Sample Collection

Hide biopsies were collected from 22 live Hereford cattle housed at the Kansas State University Purebred Beef Unit in Manhattan, Kansas. The group of cattle used in this study was comprised of 11 cows, eight heifers, and three bulls. The cattle ranged in age from one to nine years. The age and sex distributions of these cattle are provided in Figure 2.1.

Prior to the biopsy procedure, cattle were restrained in a squeeze chute to minimize animal movement and stress. Two biopsies were taken from the left side of each animal 2-3 cm apart on the upper rear quadrant of the hide. Hair covering the biopsy sites, approximately 25 cm in front of the tail and 25 cm down from the backbone, was clipped with a #40 blade on commercial clippers. The biopsy sites were sanitized with Betadine® Surgical Scrub (7.5% povidone-iodine) and 70% isopropyl alcohol. Once the area was clean, 1-3 cc of lidocaine hydrochloride with 1% epinephrine was administered subcutaneously per site, followed by a 5-minute waiting period and gentle poke with an 8-gauge needle to ensure desensitization.

Biopsies were collected using 8 mm Miltex® Disposable Biopsy Punches. One biopsy was obtained for histological examination and the other was retained for future genetic analyses. The biopsy intended for histological analysis was embedded immediately in Tissue Tek® optimum cutting temperature tissue freezing medium and frozen in liquid nitrogen cooled isopentane. The second biopsy was collected in a cryotube and flash frozen in liquid nitrogen. Both biopsies were stored at -80°C until subsequent analyses.

Direct pressure was applied to the biopsy sites after collection to facilitate hemostasis, followed by the application of a 5:1 dilute Betadine® solution. Sites were closed with a size 0 Prolene® polypropylene absorbable suture and covered in a thin coating of AluShield aerosol bandage. Cattle were checked once per day over the following seven days to ensure adequate healing of biopsy sites.

Of the 22 total animals sampled, 18 were purebred Herefords out of 12 known sires, three of which are related as grandsire, sire, and son. The nine remaining known sires were unrelated within a four-generation pedigree. The four non-registered cattle sampled for the study were commercial cows of Hereford ancestry with incomplete pedigree records. Known familial relationships for each animal were generated in Pedigraph version 2.4 (Garbe and Da, 2008) and are shown in Figure 2.2. The numbers used to identify animals in Figure 2.2 replaced breed registration numbers in an effort to maintain producer confidentiality.

Histology

Each biopsy sample was sliced in the plane of the hair follicle into a minimum of six cryosections 30-60 microns thick with a Microm HM 550 Cryostat (Thermo Fisher Scientific Inc.; Waltham, Massachusetts, USA). Individual cryosections were subsequently mounted on positively charged glass microscope slides for histological examination.

A Nikon SMZ745T microscope (Nikon Inc.; Melville, New York, USA), fitted with a Samsung SM-G973U 12MP wide-angle lens camera (Samsung Electronics Co., Ltd.; Suwon, South Korea), was used to obtain images of cryosections at a 20-fold magnification. Fiber direction was categorized as normal, intermediate, or vertical, according to the classification parameters defined in Hannigan et al. (1983). An example of each classification is shown in Figure 2.3. Briefly, normal fiber orientation is represented by fiber bundles that are tightly

woven at an angle of 50-60°, whereas vertical fiber orientation is indicated by collagen fibers that are loosely woven at an angle of approximately 90°. Intermediate samples have loosely woven fibers interlaced at an angle of 60-90°.

Samples were chilled overnight at -20°C prior to staining with a Masson's trichrome staining kit (PolySciences, Inc.; Warrington, Pennsylvania, USA). The first step of the staining process was hydrating slides in deionized water for two minutes. Samples were then incubated in a preheated 60°C Bouin's fluid solution for 60 minutes, followed by a 10-minute cooling period at room temperature. Picric acid was removed from the samples by rinsing slides in tap water for five minutes. Slides were then cleansed in deionized water and stained with Weigert's Hematoxylin, which is a solution comprised of equal parts Weigert's Solution A and Weigert's Solution B, for 10 minutes. Slides were washed in tap water for five minutes and rinsed in deionized water, followed by incubation in Biebrich scarlet-acid fuchsin stain for 10 minutes and another rinse in deionized water. Samples were subjected to a phosphotungstic and phosphomolybdic acid solution for 10-15 minutes, immediately stained with aniline blue solution for five minutes, and subsequently rinsed in deionized water. Slides were then sequentially immersed in 1% acetic acid, deionized water, 95% ethanol alcohol, 100% ethanol alcohol, and xylenes for one minute each. Samples were then coverslipped for microscopic evaluation and photographed before and after staining to confirm fiber orientation.

Results and Discussion

Detection of VFHD

When examining each sample under the microscope, most collagen fibers appeared tightly woven at low angles of weave. Some variation between and within samples was present,

as shown in Figure 2.4. Despite this variation, all samples remained within normal parameters. Slight variation within samples was anticipated. Normal samples often have a small proportion of fibers that are woven at angles approaching 90°; however, the sample is considered normal if more than half of its fibers are observed at the normal angle of weave (Hannigan et al., 1983). Likewise, had the sample been primarily comprised of fibers intertwined at angles around 90°, it would be classified as vertical regardless of the presence of a few horizontal fibers. In this dataset, the highest proportion of vertical fibers was approximately 15% in one animal. The remaining samples were comprised of 10-15%, 5-10%, and 5% vertical fibers, affecting four, seven, and 10 animals, respectively. However, these proportions do not meet the classification parameters to designate a sample as vertical. The variation observed in these samples remained within expected limits.

The images in Figure 2.4 are representative of the entire herd and have been presented on a gradient to demonstrate an increasing angle of weave. Figure 2.4A contains the fewest number of vertical fibers, which compose approximately 5% of total collagen fibers in the sample and increases to about 7% in 2.4B, 10% in 2.4C, and 15% in 2.4D.

The colors in each sample aid in identifying fiber alignment by corresponding to different tissue types. Specifically, blue represents collagen, red indicates muscle or keratin, and yellow denotes lipid tissue. The upper layers of hide are primarily comprised of hair shafts, hair follicles, and sebaceous glands, beneath which collagen fibers can be found. Muscle exists below the layer of collagen fibers, but these tissues are often too deep to be included in the biopsy.

There was no evidence of VFHD in any hide samples examined. Previous estimates of VFHD prevalence indicate that the abnormality affects 5-15% of Herefords in the United States (Tancous, 1966; Hannigan et al., 1983; Everett & Hannigan, 1978; Cundiff et al., 1988).

Assuming VFHD still affects 5-15% of American Herefords, only 1-3 cases would have been expected in a study of this sample size. Though not finding any VFHD cases in a sample this small is not entirely unexpected, it does provide some evidence that the condition has likely not increased in frequency to a very high degree in the Hereford population, at least within the families represented in this study.

Population Structure

The cattle evaluated in this study were selectively bred, which greatly influences various aspects of herd structure, such as age, sex, and allele frequency. This study was constrained by sample size and thus its results should not be extrapolated to the entire Hereford cattle population. However, understanding the underlying population structure of these animals is important for the interpretation of results obtained in this experiment and may assist researchers who may work to identify this condition in a larger population.

Age

Figure 2.1 reveals a relatively wide age distribution among sampled animals, ranging from one to nine years at the time of biopsy. However, age biases within the dataset are apparent. Yearling was the most populous age group, representing over one-third of the entire population sampled. The next most frequent age was nine years with four individuals falling under this category. Conversely, several age groups, including five- and six-year-olds, were not represented. Previous literature reports that VFHD can affect cattle as young as four to seven months of age (Hannigan et al., 1983), which provides evidence that the skewed proportion of yearling animals in this study should not have hindered detection of VFHD. However, older animals tend to express VFHD more frequently than younger animals, thereby providing a possible explanation for the lack of VFHD cases noted in this herd. Nonetheless, previous

research has not found the effect of age to be statistically significant, so it is unlikely that age effects were the major determinant in not detecting VFHD in the sampled animals. Further work on VFHD detection should not only incorporate more cattle, but also a more comprehensive representation of each age group to better gauge potential age effects.

Sex

The sex distribution of sampled animals is also depicted in Figure 2.1. Over 86% of the herd was comprised of cows and heifers. Only three males, all bulls, were biopsied for the study. Although VFHD can affect cattle of any sex, steers seem to express the abnormality nearly twice as frequently as bulls (Bitcover et al., 1974), thereby providing a cogent argument to sample steers in future experiments. Interestingly, both cows and heifers have been shown to express VFHD at a statistically higher rate than their male counterparts (Hannigan et al., 1983). Given a higher likelihood of cows and heifers expressing VFHD, this dataset provided a good opportunity to detect VFHD, provided it was present in the population.

Genetic Variation

Previous literature has presented strong evidence that VFHD is primarily under genetic control. Nonrandom mating practices, such as those employed by the Kansas State University Purebred Beef Unit, have a substantial impact on allele frequencies and may have inadvertently played a crucial role in the inheritance of VFHD alleles, or lack thereof, in this herd.

The mode of inheritance of VFHD remains unknown, however data from experimental matings suggests that the condition most likely follows a simple autosomal recessive mode of inheritance (Dufty et al., 1983; Cundiff et al., 1987). Provided this is correct, given that our population did not exhibit intense inbreeding and high levels of relationship among animals, it is

possible that the recessive allele responsible for VFHD expression could exist at low levels in this herd, but was not expressed because no animals were homozygous.

Given that no sampled animal expressed VFHD, it is assumed that the herd is comprised of cattle that are either heterozygous or homozygous normal at the VFHD locus. Given previous evidence that only certain lineages possess the VFHD allele, heterozygous animals likely descend from related progenitors and the presence of recessive alleles would be amplified by inbreeding affected or heterozygous individuals. We were not able to ascertain which pedigree lineages were originally noted to be affected by VFHD from either the literature or personal contacts to the authors of the original studies, so we were unable to specifically include descendants of these lines in an effort to detect the conditions in a contemporary population.

Remarkably, there was no evidence of inbreeding in the animals evaluated in this study, as supported by the pedigree in Figure 2.2. Coefficients of inbreeding and relatedness were calculated based on all available pedigree information to construct the additive genetic relationship matrix shown in Figure 2.5. Off-diagonal values in Figure 2.5 represent the relatedness of an animal on the x-axis to a corresponding animal on the y-axis. A coefficient of zero indicates that the two animals are not related within the confines of the known pedigree structure, whereas higher values represent increasing levels of relationship. Inbreeding can be detected by examining the diagonal elements (each animal's relationship with itself), where any animal with a diagonal element greater than one would be considered inbred. No values greater than one were identified in the additive genetic relationship matrix, confirming that these animals are not inbred to 4 generations. Consanguinity between animals is also represented by color, ranging from white to dark purple. Darker shades are indicative of relationship coefficients

approaching one, whereas lighter shades correspond with pairs of animals that are distantly or unrelated.

Complex intergenerational relationships exist within this pedigree, as revealed in Figure 2.5. For example, cattle 11 and 13 in this study are paternal half-siblings. The coefficient of relatedness for half-siblings is 0.25, however the coefficient of relatedness between 11 and 13 is 0.33, implying that these animals are more genetically related than typical half-siblings. According to Figure 2.2, the dams of 11 and 13 are paternal half-siblings to each other, thereby making 11 and 13 half-siblings and half-cousins. There are many such cases of complex kinship in this herd but interestingly, no inbred lines are present when accounting for 4 generations of pedigree.

Although related animals did not mate with each other to produce the cattle sampled for this experiment, it is still possible that inbreeding occurred further back in the pedigree or that the VFHD allele is present in multiple distinct lines of cattle. However, even if more than one carrier exists in the pedigree and those animals were mated to each other, the chance of observing an affected offspring is only 25%. The statistical probability of observing VFHD in a non-inbred herd of 22 animals with varying ancestry is very small, which helps rationalize why no cases were identified. Future research on VFHD detection would likely benefit from designing an experiment in which several groups of Hereford cows are bred to a single bull per group. If the cows were related to the male, it would increase the probability of detecting VFHD in the population of calves that resulted from those matings. Alternatively, daughters could be bred back to the same bull to increase the probability of detecting VFHD if the allele exists in the bull. If all animals are homozygous for the normal allele, then performing a similar experiment with different cattle from different bloodlines may eventually expose VFHD. Another

alternative would be sampling widely in large populations of Hereford cattle, with the hope that size of the population would increase the frequency of detection of the condition provided that it still exists in the population.

Sires have substantial influence on herd allele frequencies because they produce more progeny per year than dams. If a bull is affected by an autosomal recessive condition, like VFHD, he would pass the recessive allele to each calf he sires, which could be up to thousands or millions of calves over a lifetime as an artificial insemination (AI) sire. Conversely, an affected cow can only pass the recessive allele to one calf per year, with twinning or embryo transfer as a rare exception. Genetic abnormalities can spread much more rapidly throughout a population when the sire possesses an affected allele than if the dam possesses it. As such, it is crucial to consider sire lines when evaluating genetic conditions like VFHD.

Animals evaluated in this study can be traced back to 12 direct sires and 10 foundation sires, as shown in Figure 2.6. Genetic diversity increases as the number of sires increases because each sire contributes unique genetic material to the herd. Unfortunately, the cattle in this herd only contained germplasm from a small fraction of the diversity in the Hereford breed. The lack of VFHD in this study does not rule out the presence of VFHD in the breed, however additional samples from different herds and ancestry should be pursued to determine which genetic lines still carry the VFHD allele, or if it has been eradicated from the Hereford population.

Histology Technique

Despite the lack of VFHD cases detected, the histology techniques presented in this study would be useful to implement in future experiments of this nature. Evaluating fiber direction in previous VFHD studies entailed sending biopsies to the Eastern Regional Research Laboratory in

Philadelphia, Pennsylvania for assessment. The current experiment was performed in-house, which substantially decreased research expenses while maintaining sample quality. However, this required training to properly operate the freezing microtome, stain samples, and gauge fiber orientation in order to prepare, analyze, and classify samples for evaluation. Several common mistakes made during this process are demonstrated in Figure 2.7. Figure 2.7A depicts a partially sliced cryosection. This can occur for a multitude of reasons, such as if the sample is not chilled enough, the slice is too thin, or the slicing angle is offset. In Figure 2.7B, the staining process was not performed well, as evidenced by the lack of stain in the upper right corner and dark fibers that have been overly saturated with aniline blue dye. An example of a torn sample is shown in Figure 2.7C. Tears are very common and can occur during the slicing process when a section folds over on itself, is cut too fast, or is sliced at an inappropriate thickness. Tears can also be introduced in the staining process if the sample was not adequately heat-fixed or if staining steps were performed improperly.

Unfortunately, many histology errors are not identified until after devoting a significant amount of time, energy, and resources toward the project. Facilitating adequate training prior to sample preparation as well as evaluating samples before and after staining can help alleviate these issues. Training is crucial to ensure that results are consistently accurate and evaluating samples before and after staining helps assess and mitigate technical errors, such as sample tearing or overaccumulation of dye. To demonstrate this point, pairs of stained and unstained cross-sections are juxtaposed in Figure 2.8. Different tissue types are not as easy to identify, but unstained samples often contain fewer tears and provide a supplemental perspective of fiber orientation.

Furthermore, technical mistakes encountered during sample preparation present a serious risk of depleting biopsies. Thus, obtaining at least two biopsy samples per animal is recommended for future experiments following this methodology, provided that animals cannot easily be sampled again at a later time. Retaining a duplicate hide sample reduces the likelihood of exhausting all samples from an individual animal and affords researchers the opportunity to replicate cryosections as needed.

Previous VFHD literature typically employed the use of eosin and hematoxylin for staining, but Masson's trichrome was selected for this experiment because the use of three dyes provides enhanced tissue differentiation over two-stain procedures and is especially well suited for identifying collagen. Although Masson's trichrome stain facilitates visual identification of different tissue types, it is not required to evaluate fiber orientation, as demonstrated by Figure 2.9. Excluding the staining process decreases research costs and eliminates technical errors introduced during staining at the expense of tissue differentiation by color. At minimum, retaining an extra unstained cryosection per biopsy affords researchers the opportunity to confirm fiber alignment or restart the staining process if needed. In this study, samples were examined both before and after staining to verify results.

Conclusion

None of the animals evaluated in this experiment expressed VFHD, however there was marginal variation in weave angle observed between and within samples. The abnormality was reported to affect 5-15% of American Herefords in the mid-to-late 1900s, which suggests that only 1-3 cases of VFHD would be expected in this study if VFHD frequency has remained the same. More animals need to be sampled to obtain a broader estimate of VFHD frequency in the larger Hereford population, and inclusion of more samples in aged cows may assist in this effort.

These results support conclusions made in previous literature that selection decisions made to reduce the prevalence of VFHD are not urgent, and emphasis should be placed on other traits of economic importance at this time.

The histology protocols followed in this study were effective for evaluating fiber orientation. Hide samples were sliced, stained, and assessed by a single trained technician to maintain consistency of results. Samples were evaluated for VFHD before and after staining to ensure the novel staining process used did not damage the samples and to also provide additional confirmation of fiber alignment. Based on the results of this study, these methods are recommended for use in future collagen fiber research.

Figure 2.1. Age and sex distribution of sampled cattle.

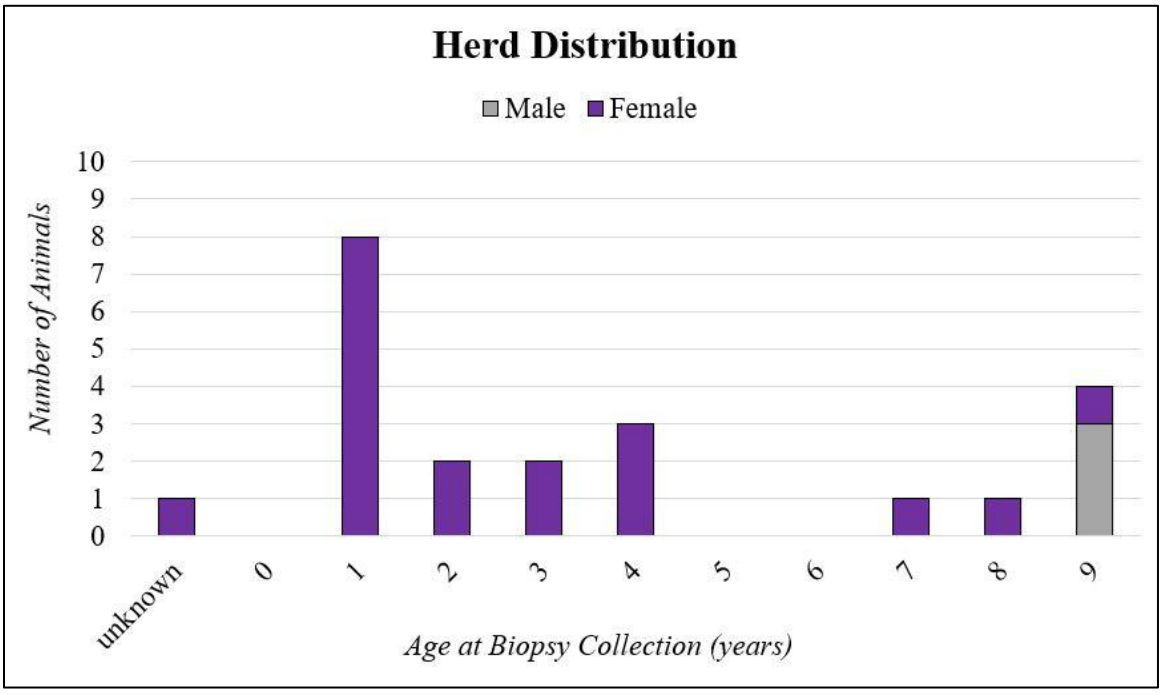

Figure 2.2. Pedigree of sampled cattle organized hierarchically from top to bottom by generation. Two sampled animals without any pedigree information were removed for this figure. Rectangular nodes indicate male animals and circular nodes represent female animals. Blue shading denotes an animal that has been sampled for hide fiber evaluation. Edges represent parent-offspring relationships and each edge color represents a distinct parent in a generation as there are not enough colors for all family lines to be unique. Animals that share edges of the same color descend from a common sire or dam.

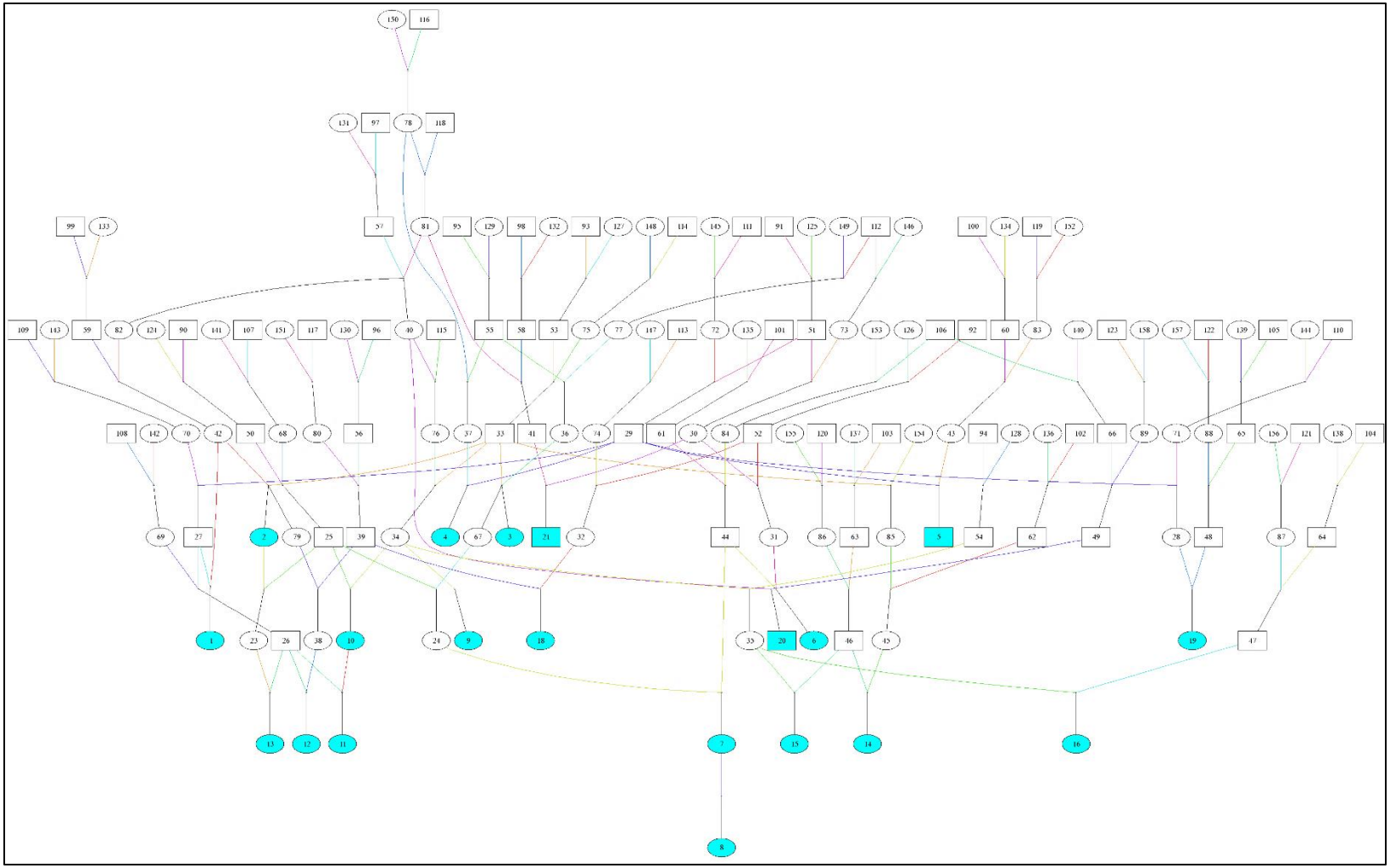

Figure 2.3. An example of normal (A), intermediate (B), and vertical (C) fiber orientation.

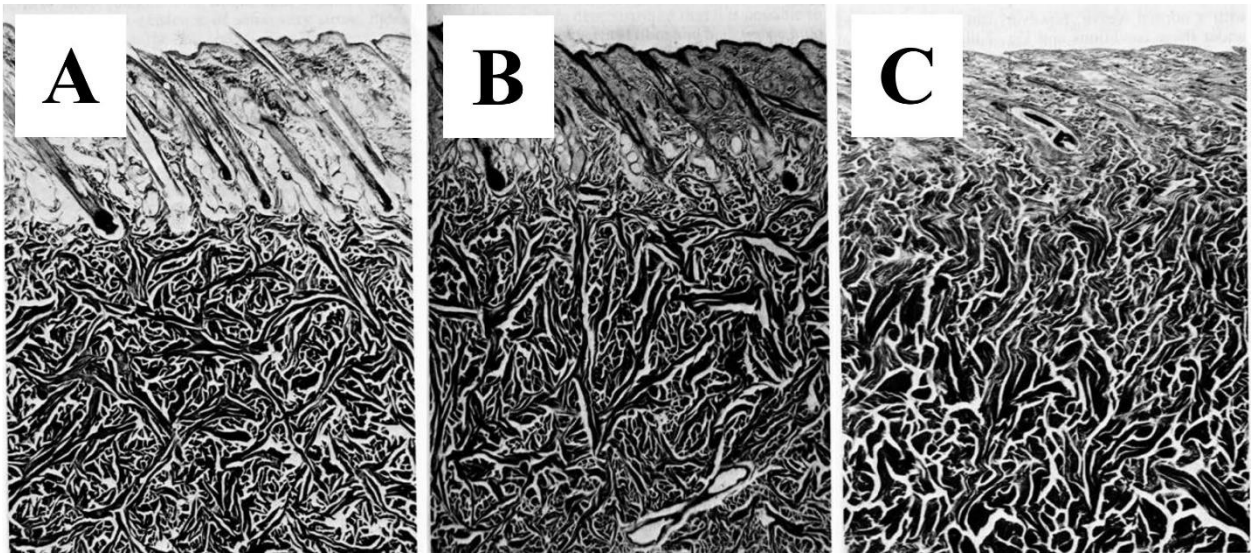

Adapted from The characterization of vertical fiber and high weave structures of Hereford cattle hides by D. E. Peters and J. H. Bavinton. 1983. Journal of the Society of Leather Technologists and Chemists 67:67.

Figure 2.4. Biopsy cross-sections illustrating fiber orientation variation among sampled cattle, from samples with the least (A) to most (D) vertical fibers.

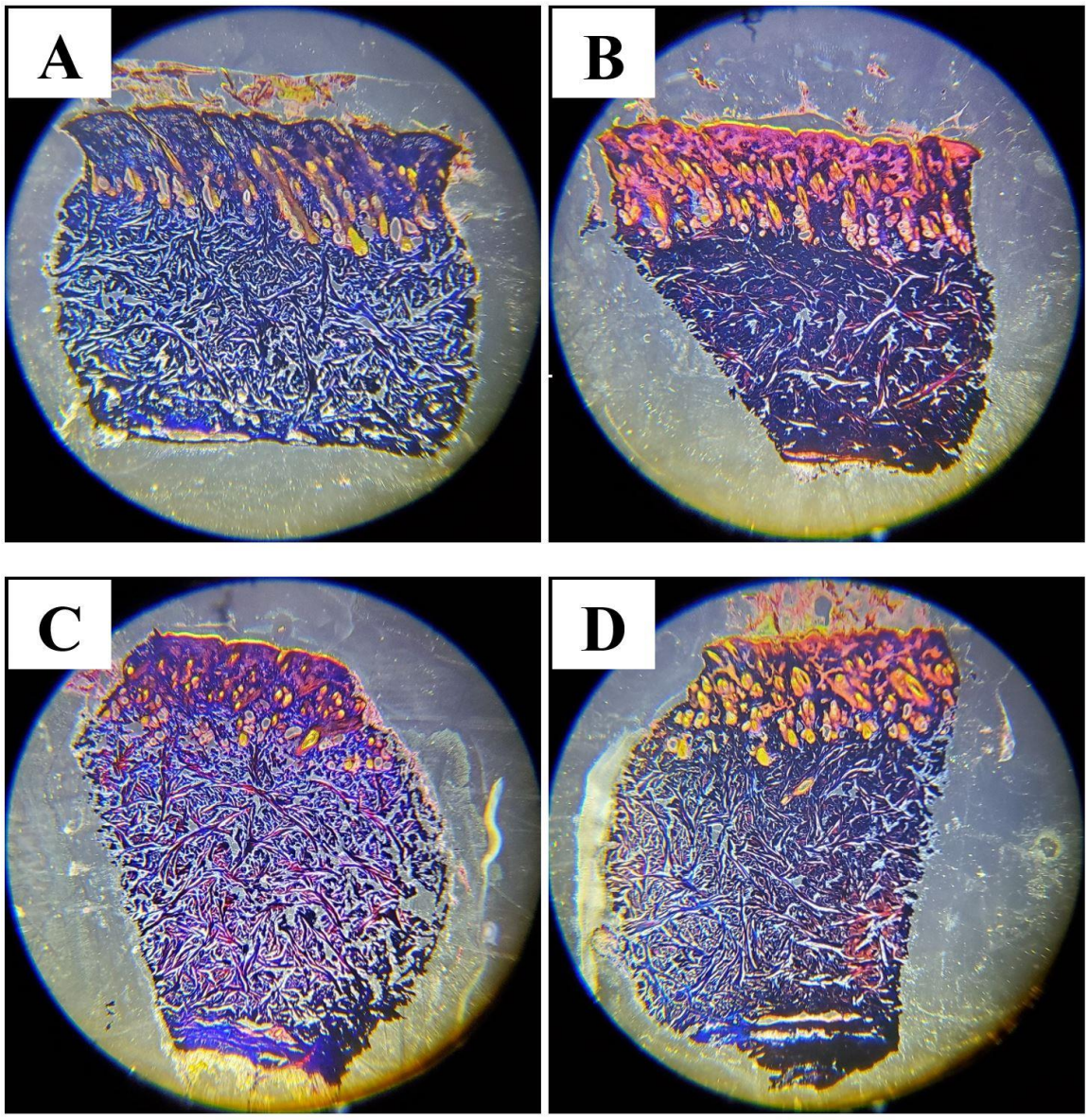

Figure 2.5. A symmetric pedigree-based additive genetic relationship matrix. Consanguinity between each pair of animals is indicated by relationship coefficients on the off diagonal. Values along the diagonal represent an individual's relationship to itself. Various shades of purple correspond with degree of relationship, ranging from white (no relation) to dark purple (identical).

Animal ID

Animal ID	1	2	3	4	5	6	7	8	9	10	11	12	13	14	15	16	17	18	19	20	21	22
1	1.0000	0.2500	0.0000	0.1406	0.1250	0.0156	0.0000	0.0000	0.0156	0.0156	0.1328	0.1875	0.1875	0.0000	0.0078	0.0078	0.0000	0.0000	0.0625	0.0625	0.0625	0.0000
2	0.2500	1.0000	0.2500	0.0156	0.0000	0.0000	0.0625	0.0313	0.1406	0.1406	0.0703	0.1250	0.2500	0.0625	0.0703	0.0703	0.0000	0.0000	0.0000	0.0625	0.0313	0.0000
3	0.0000	0.2500	1.0000	0.0625	0.0000	0.0078	0.1250	0.0625	0.1250	0.1250	0.0625	0.0625	0.0625	0.0625	0.0625	0.0625	0.0000	0.0000	0.0000	0.0000	0.0156	0.0000
4	0.1406	0.0156	0.0625	1.0000	0.2500	0.0313	0.0156	0.0078	0.0078	0.0078	0.0664	0.0664	0.0664	0.0000	0.0039	0.0039	0.0000	0.0000	0.1250	0.0313	0.0938	0.0000
5	0.1250	0.0000	0.0000	0.2500	1.0000	0.0313	0.0000	0.0000	0.0000	0.0000	0.0625	0.0625	0.0625	0.0000	0.0000	0.0000	0.0000	0.0000	0.1250	0.0000	0.0625	0.0000
6	0.0156	0.0000	0.0078	0.0313	0.0313	1.0000	0.2520	0.1260	0.0000	0.0000	0.0078	0.0078	0.0078	0.0000	0.0000	0.0000	0.0000	0.0625	0.0156	0.0156	0.1250	0.0000
7	0.0000	0.0625	0.1250	0.0156	0.0000	0.2520	1.0000	0.5000	0.0313	0.1563	0.0781	0.0156	0.0781	0.0156	0.0156	0.0156	0.0000	0.0000	0.0000	0.0156	0.0039	0.0000
8	0.0000	0.0313	0.0625	0.0078	0.0000	0.1260	0.5000	1.0000	0.0156	0.0781	0.0391	0.0078	0.0391	0.0078	0.0078	0.0078	0.0000	0.0000	0.0000	0.0078	0.0020	0.0000
9	0.0156	0.1406	0.1250	0.0078	0.0000	0.0000	0.0313	0.0156	1.0000	0.2500	0.1250	0.0352	0.0352	0.0313	0.1250	0.1250	0.0000	0.0000	0.0000	0.0625	0.0156	0.0000
10	0.0156	0.1406	0.1250	0.0078	0.0000	0.0000	0.1563	0.0781	0.2500	1.0000	0.5000	0.0352	0.1602	0.0313	0.1250	0.1250	0.0000	0.0000	0.0000	0.0625	0.0156	0.0000
11	0.1328	0.0703	0.0625	0.0664	0.0625	0.0078	0.0781	0.0391	0.1250	0.5000	1.0000	0.2676	0.3301	0.0156	0.0625	0.0625	0.0000	0.0000	0.0313	0.0313	0.0234	0.0000
12	0.1875	0.1250	0.0625	0.0664	0.0625	0.0078	0.0156	0.0078	0.0352	0.0352	0.2676	1.0000	0.2813	0.0156	0.0176	0.0176	0.0000	0.1250	0.0313	0.0156	0.0234	0.0000
13	0.1875	0.2500	0.0625	0.0664	0.0625	0.0078	0.0781	0.0391	0.0352	0.1602	0.3301	0.2813	1.0000	0.0156	0.0176	0.0176	0.0000	0.0000	0.0313	0.0156	0.0234	0.0000
14	0.0000	0.0625	0.0625	0.0000	0.0000	0.0000	0.0156	0.0078	0.0313	0.0313	0.0156	0.0156	0.0156	1.0000	0.2656	0.0156	0.0000	0.0000	0.0000	0.0000	0.0000	0.0000
15	0.0078	0.0703	0.0625	0.0039	0.0000	0.0000	0.0156	0.0078	0.1250	0.1250	0.0625	0.0176	0.0176	0.2656	1.0000	0.2500	0.0000	0.0000	0.0000	0.0313	0.0078	0.0000
16	0.0078	0.0703	0.0625	0.0039	0.0000	0.0000	0.0156	0.0078	0.1250	0.1250	0.0625	0.0176	0.0176	0.0156	0.2500	1.0000	0.0000	0.0000	0.0000	0.0313	0.0078	0.0000
17	0.0000	0.0000	0.0000	0.0000	0.0000	0.0000	0.0000	0.0000	0.0000	0.0000	0.0000	0.0000	0.0000	0.0000	0.0000	0.0000	1.0000	0.0000	0.0000	0.0000	0.0000	0.0000
18	0.0000	0.0000	0.0000	0.0000	0.0000	0.0625	0.0000	0.0000	0.0000	0.0000	0.0000	0.1250	0.0000	0.0000	0.0000	0.0000	0.0000	1.0000	0.0000	0.0000	0.0000	0.0000
19	0.0625	0.0000	0.0000	0.1250	0.1250	0.0156	0.0000	0.0000	0.0000	0.0000	0.0313	0.0313	0.0313	0.0000	0.0000	0.0000	0.0000	0.0000	1.0000	0.0000	0.0313	0.0000
20	0.0625	0.0625	0.0000	0.0313	0.0000	0.0156	0.0156	0.0078	0.0625	0.0625	0.0313	0.0156	0.0156	0.0000	0.0313	0.0313	0.0000	0.0000	0.0000	1.0000	0.0625	0.0000
21	0.0625	0.0313	0.0156	0.0938	0.0625	0.1250	0.0039	0.0020	0.0156	0.0156	0.0234	0.0234	0.0234	0.0000	0.0078	0.0078	0.0000	0.0000	0.0313	0.0625	1.0000	0.0000
22	0.0000	0.0000	0.0000	0.0000	0.0000	0.0000	0.0000	0.0000	0.0000	0.0000	0.0000	0.0000	0.0000	0.0000	0.0000	0.0000	0.0000	0.0000	0.0000	0.0000	0.0000	1.0000

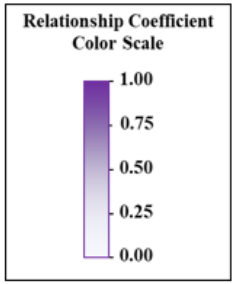

Figure 2.6. Pedigree of sampled cattle traced to paternal root nodes. Rectangular nodes represent males and circular nodes represent females. Blue nodes denote animals that have been sampled for this study. Tree edges connect sires to progeny and each edge color corresponds to a unique sire line.

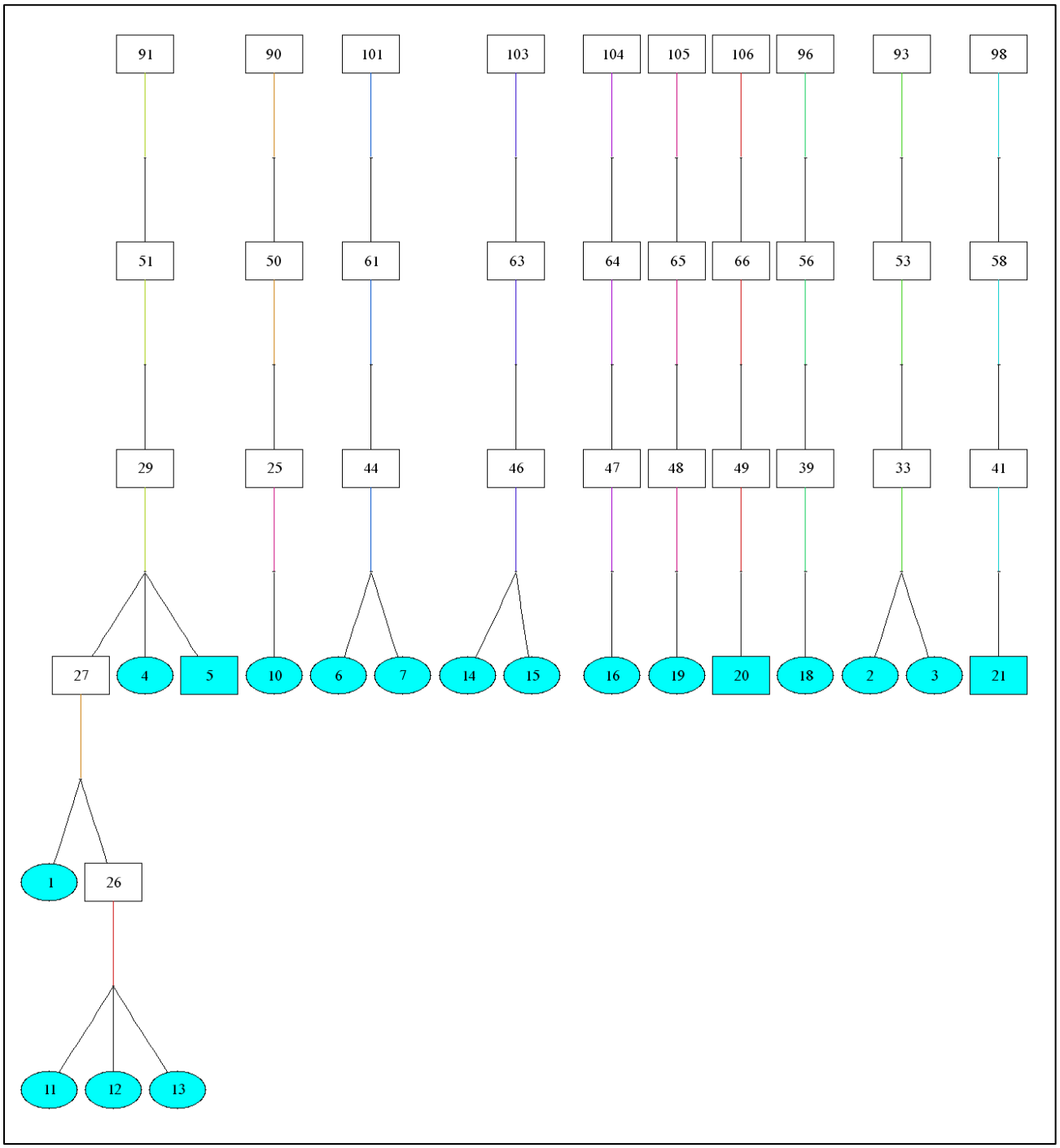

Figure 2.7. Mistakes commonly encountered when preparing biopsy samples for microscopic evaluation include incomplete cryosections (A), improper staining (B), and excessive tears (C).

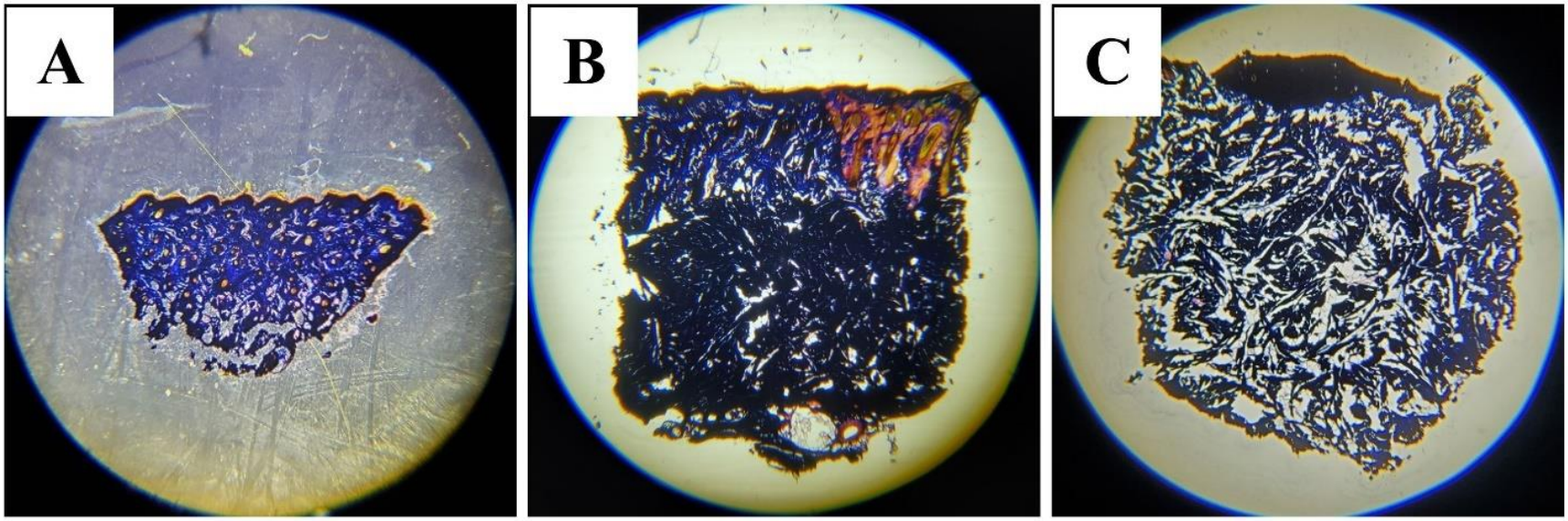

Figure 2.8. Pairs of unstained (left) and stained (right) cross-sections. Each pair of cross-sections was obtained from a single hide sample before and after staining.

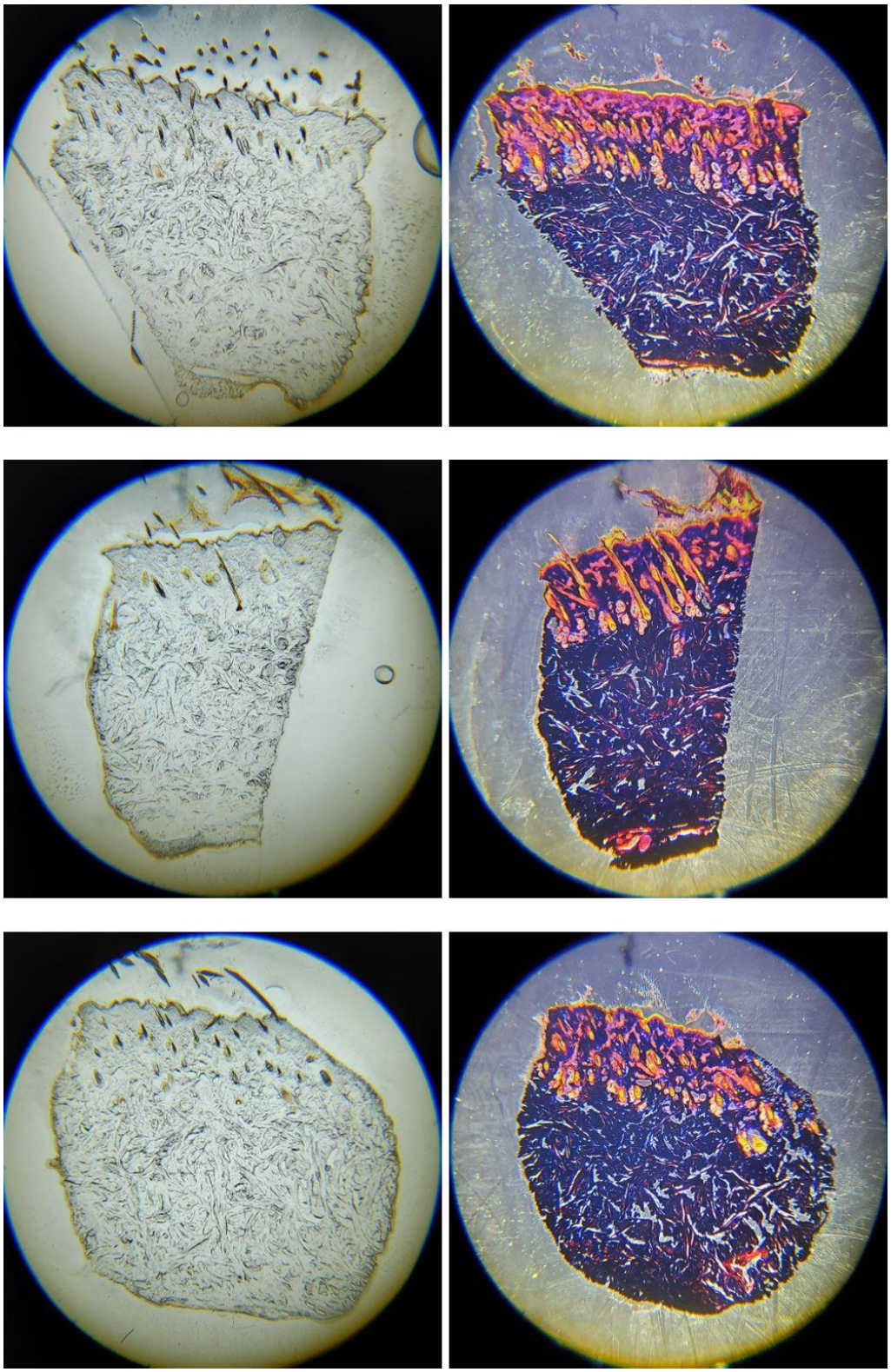

Figure 2.9. Cross-sections of unstained samples organized by least (A) to most (D) vertical fibers.

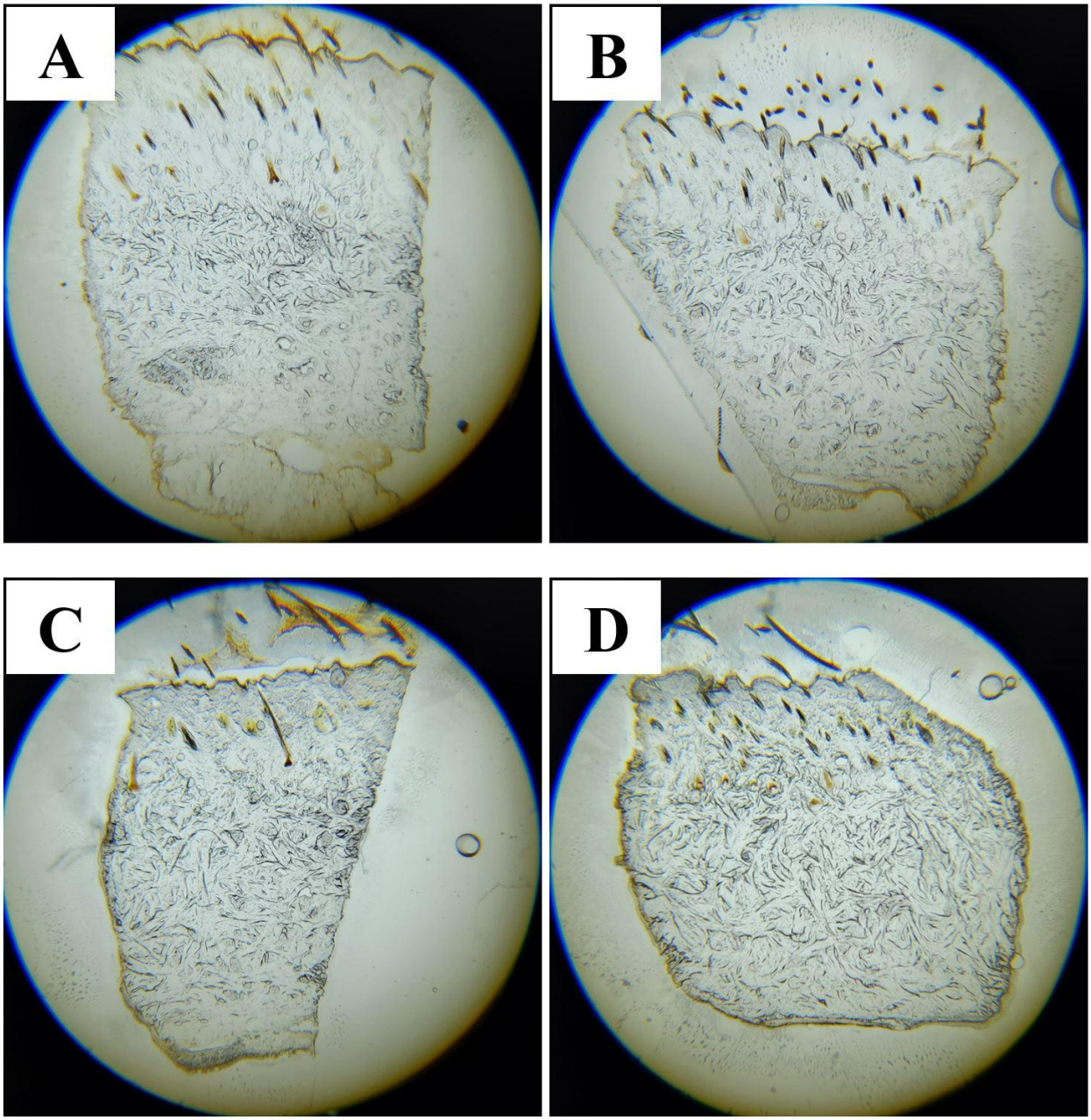

Chapter 3 - Identification of quantitative trait loci associated with bovine ocular squamous cell carcinoma

K. W. Upshaw[1], J. W. Keele[2], T. G. McDaneld[2], L. A. Kuehn[2], J. M. Bormann[1], R. L. Weaber[1], and M. M. Rolf[1]

[1]Department of Animal Sciences and Industry, Kansas State University, Manhattan, Kansas

[2]Genetics, Breeding, and Animal Health Research Unit, United States Meat Animal Research Center, Clay Center, Nebraska

Acknowledgements: We would like to recognize and thank Dr. Bob Schnabel at the University of Missouri for his contribution of a SNP map aligned to the ARS-UCD1.2 bovine genome assembly.

Abstract

Bovine ocular squamous cell carcinoma (BOSCC) is the most common oncological neoplasm affecting cattle. Cattle with BOSCC have tumors that appear on the eyeballs, eyelids, or caruncles and affect animal health by metastasizing further behind the orbital socket or into internal organs. The etiology of BOSCC is multifactorial; however, existing literature suggests that it is influenced by genetic factors. Heritability estimates for cancer eye are low to moderate, and heritability estimates for traits that contribute to BOSCC predisposition are high. The primary goal of this study was to identify genomic regions associated with BOSCC expression.

DNA was extracted from over 500 Hereford cattle located in south central Kansas. Fourteen cases of cancer eye were detected in the population with the remaining cattle classified as controls. A BovineHD BeadChip was used to obtain genotypes for 14 individual cases, 28 individual controls, and 10 control pools of 50 animals each. Genome-wide association tests of cases and individual controls revealed one significant QTL on chromosome 13 (α = 0.05) and suggestively significant (α = 1) QTL on chromosomes 6, 7, 13, 15, 20, and 21. Results differed among a standard case/control association test (n = 42), MANOVA of haplotype analysis (n = 42), and MANOVA of theta approach (n = 52), likely due to different types of data input.

The expression of BOSCC appears to have polygenic inheritance where the small effects of many loci predispose cattle to developing the disease. Association testing indicates that a locus on chromosome 13 has the greatest influence on disease expression, however the exact position and corresponding causal mutation(s) remain unknown. Future studies to identify causal variants are warranted to aid in the prevention, detection, and control of BOSCC.

Key Words: bovine ocular squamous cell carcinoma, cancer eye, pooled genotyping, Hereford cattle, genome wide association study

Introduction

Bovine ocular squamous cell carcinoma (BOSCC) is a type of skin cancer that affects tissues of the eyeball, eyelids, or caruncles of cattle (Blackwell et al., 1956; Gardiner et al., 1972). Lesions associated with BOSCC typically present as raised white to pink plaques or wart-like papillomas (Russell et al., 1956). When one of these tumors becomes malignant, it often ulcerates and becomes vulnerable to infection. The cancer can invade tissues behind the eye or continue to proliferate, eventually metastasizing into the lymph nodes or internal organs of the affected individual (Russell et al., 1956; Gardiner et al., 1972).

Financial losses of up to $20 million annually are associated with cancer eye in the United States, primarily from condemnation at slaughter and reduced productive lifespan in affected cattle (Anderson, 1991; Foster, 2014). Cancer eye occurs more frequently in breeds of cattle with white faces, such as Herefords, Holsteins, and Simmentals (Gardiner et al., 1972; Pausch et al., 2012). Several factors that contribute to the development of cancer eye are age, environmental carcinogens, and genetic predisposition (Russell et al., 1956; Gardiner et al., 1972; Russell et al., 1976).

Identifying factors influencing genetic predisposition to cancer eye is crucial to understanding the disorder because several of its causal factors, such as pigmentation, are partially, if not entirely, under genetic control. Heritability estimates for cancer eye are low to moderate, ranging from 0.1 to 0.3 (Russell et al., 1976; Blackwell et al., 1956), but heritability estimates for lid, corneoscleral, and circumocular pigmentation are high, ranging from 0.4 to 0.8 (Anderson, 1991; Gardiner et al., 1972; Pausch et al., 2012). The heritability of pigmentation is high, and producers can mitigate incidence of BOSCC by selecting animals with pigment around the eye; however, pigmentation is only an indicator of increased environmental susceptibility and

not a direct cause of carcinogenesis. Mutated regulatory genes, called oncogenes, overexpress cell growth and result in tumors. A genomic test has not yet been developed to assess individual susceptibility nor dysfunctional oncogene variants related to BOSCC.

Identifying quantitative trait loci (QTL), or regions of the genome, associated with BOSCC can not only help cattle producers manage incidence of the condition but can also elucidate underlying mechanisms of oncogenes in cattle and other species. Analogous lesions have been identified in many species, including humans, horses, sheep, goats, dogs, cats, and mice, among others (Russell et al., 1956; Cook et al., 1984; Dugan et al., 1990; De Vries et al., 1998; Sironi et al., 1999; Hendrix, 2005; Mara et al., 2005; Palamar et al., 2014). Ocular squamous cell carcinomas are usually rare, however OSCC is the most common malignancy in cattle, which offers researchers the opportunity to study squamous cell tumors for applications in the cattle industry and beyond.

The primary purpose of this study was to gain insight into which regions of the genome are associated with the expression of BOSCC. A secondary goal was to provide additional methods of evaluating individual and pooled samples for implementation in future disease studies.

Materials and Methods

All procedures involving animals in this study were deemed exempt from Institutional Animal Care and Use Committee (IACUC) approval by Kansas State University IACUC.

Sample Collection

Hair samples from the tail switch were collected on 557 cows, 3 steers, and 7 bulls, which comprised a complete herd of Herford cattle housed on two pastures located in south

central Kansas. This herd was closed, randomly mated, and experienced minimal selection or management interventions for approximately 65 years at the time of collection. All animals were examined for cancer eye in September 2015 and samples were classified as either cases or controls. Fourteen female cattle were identified as cases, of which 10 animals presented with oncological lesions in the left eye and the remaining four in the right eye. There is no current literature detailing significant differences between left or right eye presentations of the disease.

DNA Extraction

All DNA extractions followed a silica-membrane-based nucleic acid purification protocol and were performed at the United States Meat Animal Research Center (USMARC) in Clay Center, Nebraska. Genomic DNA was extracted from cattle hair using the QIAamp® DNA Mini Kit following a version of the manufacturer's protocol adapted for hair samples (QIAGEN; Santa Clarita, CA).

Hair strands for each animal were cut into as many 1 cm long fragments as possible, including the root bulb, and subsequently mixed with 200 µL buffer AL, pulse-vortexed for 15 seconds, and incubated at 70°C for 10 minutes. After incubation, samples were briefly centrifuged to remove excess buffer from the tube lid. Then, samples were mixed with 200 µL of 100% ethanol, pulse-vortexed for 15 seconds, and briefly centrifuged again. The resulting sample was carefully transferred to a QIAamp Mini spin column in a 2 mL collection tube and centrifuged at 8,000 rpm (6,000 x g) for 1 minute. The used collection tube was discarded, the spin column was placed into a clean 2 mL tube, and 500 µL of buffer AW1 was added. The column was centrifuged at 8,000 rpm (6,000 x g) for an additional minute and the old collection tube was replaced by a clean one before adding 500 µL of buffer AW2 and centrifuging at 14,000 rpm (20,000 x g) for 3 minutes. The QIAamp spin column was transferred to a clean 1.5

mL microcentrifuge tube, the used collection tube was discarded, and 150 µL of buffer AE was added. After the addition of buffer AE, the sample was incubated at room temperature for 1 minute and centrifuged for 1 minute at 8,000 rpm (6,000 x g). This elution step was repeated once more, without discarding the collection tube, to maximize DNA yield before evaluating the eluate for DNA concentration and A260/A280 ratios.

Quality Control

The genetic material from all samples was quantified and evaluated for purity using a DeNovix DS-11 FX Series spectrophotometer (DeNovix Inc.; Wilmington, DE). Samples with poor DNA concentrations (fewer than 10 ng/µL) and insufficient A260/A280 ratios (below 1.5 or above 3.0) were re-extracted. If adequate DNA quality was not obtained by the third extraction, the sample was removed from further analysis. Only one control sample failed to meet quality control standards. The average concentrations and A260/A280 ratios for all selected animals (selection process detailed below) are summarized in Table 3.1.

Individual Selection

The usefulness of a case/control study often relies on an optimal case:control ratio. However, defining the optimal case:control ratio is a complex problem that does not have a universally correct answer. The best case:control ratio primarily depends on evaluating the costs and benefits of acquiring or testing additional samples. Further complexities were introduced as this experiment incorporated genotypes from individual cases and controls as well as pooled control samples. It was essential to carefully consider the allocation of samples into individual and pool groups.

Prior to classifying animals into individual control or pooled control groups, the control population was refined from 553 animals to 541. Due to the small number of males in this herd

and their lack of cancer eye expression, bulls and steers were not included in subsequent analysis, and thus sex was not considered. Two control cows were also removed after being diagnosed with hypotrichosis and pinkeye to avoid potential complications associated with multimorbidity.

For this study, the optimal case:control ratio for individual samples was identified as 1:2 by evaluating the change in standard error of the mean as sample size increased. Standard error of the mean is usually defined as standard deviation of the sample divided by the square root of sample size. However, standard error of the mean of a binomial distribution, which is appropriate for disease studies, is defined as the square root of the likelihood of having a condition, in this case cancer eye (p), multiplied by the likelihood of not having the condition (q) divided by sample size (n), which is represented mathematically as

$$SE = \sqrt{\frac{pq}{n}}$$

The binomial standard error of the mean was calculated for increasing sample sizes and graphed. There was a substantial reduction in standard error initially, but it eventually became a case of diminishing returns. The standard error curve began to flatten around a sample size of 40-50 individuals, implying that somewhere within this range is the maximum benefit-to-cost ratio. Case:control ratios of 1:1, 1:2, 1:3, and 1:4 would require 28, 42, 56, and 70 total individuals, respectively. Thus, using a ratio of 2:1 (all 14 cases and 28 individual controls) yielded the greatest return on investment. Ideally, individual controls would have been age-matched to cases, however age information for these animals was not available. Instead, individual controls (n = 28) were randomly selected from all available controls (n = 541).

Pool Construction

Ten pools of 50 animals each were constructed from the remaining control population (n = 513), thereby excluding a random sample of 13 animals from subsequent analyses. The addition of 500 animals increases statistical power of the study, while the pooled design mitigates costs associated with individual genotyping. A total of 400 ng of DNA from each animal was added to its corresponding pool to ensure equal representation from each animal in the final genotyped sample.

Genotyping

Each case, individual control, and pool was genotyped with the Illumina® Bovine HD 770K single-nucleotide polymorphism (SNP) array (777,962 SNPs; Illumina, Inc., San Diego, CA) by Neogen Corporation (Lincoln, NE). All genotype data for individually genotyped cases and controls was quality-filtered in PLINK version 1.07 (Purcell et al., 2009). The minor allele frequency threshold was set at zero because low minor allele frequency SNPs are a feature of the 770K SNP array and it was assumed that QTLs associated with a disease like cancer eye would be rare in the population. A total of 135,538 monomorphic SNPs were identified and omitted from further analysis. Only 2 SNPs significantly ($p \leq 10^{-8}$) deviated from Hardy-Weinberg Equilibrium and were subsequently removed from the dataset to avoid outlier bias. Additionally, 29,615 SNPs with a SNP call rate < 0.9 were excluded from the study. Lastly, zero animals with individual call rate < 0.9 were removed, leaving a total of 618,656 SNPs and 42 samples available for analysis.

Pooled samples contain more missing or ambiguous values than individual samples as a feature of pool construction. Genomic information obtained from each pooled sample prior to any filtering showed that missing data per pool ranged from 17.96% in Pool 8 to 19.82% in Pool

6. Similarly, the proportion of missing data per SNP in pooled samples ranged from 0% in 428,015 SNPs to 100% in 13,042 SNPs. When the filter criteria mentioned previously for individual samples were applied to pools, all pools were omitted from further analysis, which provides additional evidence that filtering pooled samples is more complicated than for individuals.

Methods of association testing presented in this study included a standard case/control association test (n = 42), window-based analyses of haplotypes from individuals (n = 42), and analysis of allele frequencies from individuals and pools simultaneously ($n_{individuals}$ = 42 and n_{pools} = 10). Samples in the standard case/control association test were filtered according to the parameters discussed previously; however, samples in the window-based analyses would not be subjected to SNP filtering parameters because the filter criteria should not significantly affect haplotyping results nor reflect accurate allele frequencies in pooled samples because genotypes obtained from pools are not directly comparable to those from individual samples. Including pooled samples would require filtering parameters to be set too leniently. Furthermore, limited numbers of genotyped samples ($n_{individuals}$ = 42 and n_{pools} = 10) indicate that the exclusion of a single sample reduces available genomic information by nearly 2%. Although it is possible that unfiltered markers can negatively influence analyses, this possibility was unlikely to transcend the risk of excluding potentially valuable data, given the methodologies used in this study.

Statistical Analysis

Allele Frequencies in Pooled Samples

Bead intensity values can be exploited in DNA pools to reveal the approximate proportion of A or B alleles in a sample comprised of genetic material from multiple animals (Macgregor et al., 2006; Macgregor et al., 2008). Bead fluorescence is not an absolute measure

of pooling allele frequency but serves as a relative estimate of allelotype. Illumina® genomic output files encode bead intensities as X for the streptavidin-green fluorophore and Y for the anti-DNP-red fluorophore. The pooling allele frequency approach selected for this experiment was based on the allelic intensity ratio, theta. Theta (θ) represents the frequency of the B allele at each marker and uses an arctangent transformation to convert bead intensity coordinates to B allele frequencies (Peiffer et al., 2006; Staaf et al., 2008), as follows:

$$\theta = \frac{2}{pi} * \arctan\frac{Y}{X}$$

where θ, Y, and X are as defined above.

Population Stratification

Population stratification was assessed by constructing a Euclidean distance plot and neighbor-joining tree. Euclidean distances were calculated between B allele frequencies per SNP for individuals and theta per SNP for pools using the *dist* function in R (R Core Team, 2021). A Euclidean distance plot charts the shortest distances between datapoints on a multidimensional plane, thereby offering a method to visualize data diversity and relationships among samples. The neighbor-joining tree was generated using the *dendextend* package version 1.15.1 (Galili, 2015) in R (R Core Team, 2021) and uses a cladogram to reveal similarities between sample types based on allelic proportions at each marker.

Association Testing

Three GWAS methodologies were utilized to detect relationships between SNP data and BOSCC: (1) a standard case/control chi-square test for association of cases and individual controls; (2) a distance-based multivariate analysis of variance (MANOVA) among case and individual control fixed-length haplotype blocks; and (3) a distance-based MANOVA among θ of cases, individual controls, and pooled controls within fixed-length genomic windows.

Suggestive (α = 1) and significant (α = 0.05) association thresholds for each method of association are listed in Table 3.2.

Standard Case/Control Association Test

Only cases (n = 14) and individual controls (n = 28) were selected for a standard case/control association test in PLINK (Purcell et al., 2007) because of the computational difficulty involved in using partial genotype calls from genotyped pools. Associations among cases and controls were tested by a chi-squared (X^2) allelic test (df = 1) in PLINK (Purcell et al., 2007). The model for this GWAS follows that of a classical Pearson's chi-squared test, calculated as

$$X^2 = \sum_{i=1}^{n} \frac{(O_i - E_i)^2}{E_i}$$

where i represents a SNP, n represents the total number of SNPs, O_i is the allele frequency of the *i*th SNP for each case, and E_i is the allele frequency of the *i*th SNP for each control. Under the null hypothesis, no significant association exists between allele frequency and phenotype. The alternative hypothesis is that allele frequency and phenotype are significantly associated.

The X^2 test statistic was computed for each SNP that passed quality control filtering and a corresponding p-value was determined based on a chi-square distribution. Each SNP and associated p-value were plotted by position on the ARS-UCD1.2 genome assembly using the *qqman* version 0.1.8 package (Turner, 2018) in R (R Core Team, 2021). Regions on the X and Y chromosomes were included in this analysis and unknown regions were mapped to chromosome 0.

A Bonferroni correction was applied to significance thresholds to control the inherent inflation of type I error in multiple comparison testing. Corrected thresholds were calculated by

dividing the number of false positives deemed acceptable (α) by the number of SNPs tested. Markers were determined significant at a p-value of 8.08×10^{-8} ($\alpha = 0.05$) and suggestive at a p-value of 1.62×10^{-6} ($\alpha = 1$).

A functional analysis of genes within 300 kb of the 25 most significant SNPs was performed to account for the range of LD in cattle (McKay, 2007). Markers that did not reach statistical or suggestive significance were still reviewed due to the stringency of Bonferroni correction and potential for biological meaning regardless of significance thresholds. Relevant QTL regions were evaluated using the Animal QTL Database (Hu et al., 2019) managed by the United States Department of Agriculture National Animal Genome Research Program.

Distance-Based Multivariate Analysis of Variance of Haplotype Blocks

Haplotype interpretation is ambiguous for pooled samples because pools represent average allele frequencies and therefore do not have defined genotypes at each locus from which to produce haplotypes. Thus, only cases and individual controls were used for the association test involving haplotype blocks.

The *hap-ibd* function (Zhou et al., 2020) in Beagle 5.2 version 28Jun21.220 (Browning & Browning, 2007) was used to obtain one maternal and one paternal phased haplotype for each individual animal (84 haplotypes per specified genomic region) and perform a pairwise search for matching sequences therein. The sum of the length of identical segments within a pair of haplotypes was divided by total haplotype length to generate a symmetric 84 x 84 haplotype relatedness matrix (H) for each haplotype block.

Various lengths of concatenated SNPs were selected as haplotype blocks. The goal was to partition the genome into levels of aggregation that ranged in size from whole chromosomes to 20 Mb, 10 Mb, 5 Mb, 2 Mb, and 1 Mb. However, actual haplotype block sizes were determined

by dividing chromosome length by intended block length and rounding to minimize omitted chromosomal regions. Thus, haplotype blocks roughly corresponded to distances of 20 Mb, 10 Mb, 5 Mb, 2 Mb, and 1 Mb. Realized window sizes per chromosome are summarized in Table 3.3. Regions on the X and Y chromosomes, as well as unmapped regions, were not included in this analysis.

Each element in the H matrix represents the probability that any given pair of haplotypes are identical-by-descent (IBD) within a designated haplotype block (Anderson, 2001; Braak et al., 2010). Thus, an H matrix is constructed for every haplotype block and can be conveyed by

$$H = \begin{array}{c} \\ a_1 \\ a_2 \\ a_3 \\ \vdots \\ a_n \end{array} \begin{array}{c} \begin{array}{ccccc} a_1 & a_2 & a_3 & \cdots & a_n \end{array} \\ \begin{bmatrix} 1 & a_1 \cap a_2 & a_1 \cap a_3 & \cdots & a_1 \cap a_n \\ a_2 \cap a_1 & 1 & a_2 \cap a_3 & \cdots & a_2 \cap a_n \\ a_3 \cap a_1 & a_3 \cap a_2 & 1 & \cdots & a_3 \cap a_n \\ \vdots & \vdots & \vdots & \ddots & \cdots \\ a_1 \cap a_n & a_n \cap a_2 & a_n \cap a_3 & \vdots & a_n \cap a_n \end{bmatrix} \end{array}$$

in which a_n is the concatenation of SNPs along a given genomic region for the nth animal and every element of the matrix is the probability that a pair of a_n is IBD. Each diagonal element indicates the probability that a haplotype is IBD with itself and is therefore 1.

Matching genomic sequences from two or more animals are inherently identical-by-state (IBS) but considered IBD when inherited from a common ancestor without recombination. Pedigree information is useful in detecting sequences IBD, however it is not necessary. Instead, the probability of genomic segments IBD can be inferred from observing prolonged regions IBS and estimating effective population size (N_e) of the sample (Kong et al., 2008; Chiang et al., 2016; Zhou et al., 2020).

The *hap-ibd* function (Zhou et al., 2020) used in this study detected genomic sequences IBD by identifying lengthy segments IBS. The length of segments IBD is expected to decrease each generation due to recombination. Thus, short sequences IBS potentially reveal a region IBD

from a distant common ancestor and long sequences IBS imply a more recent common ancestor (Browning and Browning, 2011).

An estimate of N_e helps gauge the number of generations, and thus the number of recombination events, that have occurred between the sequences of interest and that of the common ancestor. As N_e decreases, herd relatedness increases, which consequently increases the probability of genomic sequences being IBD (Browning and Browning, 2020).

An estimate of N_e was determined by

$$N_e = \frac{4MF}{M + F}$$

(Wright, 1931) in which *M* represents the number of active breeding males and F represents the number of active breeding females. In this present study, *M* was defined as the number of bulls (n = 7) and *F* was estimated as 25 actively bred cows for every bull, resulting in a total estimate of 175 females. Bulls are expected to be capable of covering around 15-35 cows in a given breeding season. To account for this, we approximated the value of *F* to be in the middle of this range at 25 cows per bull. The subsequent N_e of 27 was provided as input for the Beagle IBD algorithm (Browning & Browning, 2007).

Within each haplotype block, Euclidean distances between elements of *H* matrices were calculated using the *dist* function in R (R Core Team, 2021) and assembled into one distance matrix (*Y*) for each chromosome. Each *Y* matrix can be calculated as

$$Y = \begin{bmatrix} 0 & d(H_{12}) & d(H_{13}) & \cdots & d(H_{1j}) \\ d(H_{21}) & 0 & d(H_{12}) & \cdots & d(H_{2j}) \\ d(H_{31}) & d(H_{32}) & 0 & \cdots & d(H_{3j}) \\ \vdots & \vdots & \vdots & \ddots & \cdots \\ d(H_{i1}) & d(H_{i2}) & d(H_{i3}) & \vdots & d(H_{ij}) \end{bmatrix}$$

where $d(H_{ij})$ is the Euclidean distance between the value in the *i*th row and *j*th column of *H* matrices in the haplotype block. Euclidean distance is computed as (Legendre and Gallagher, 2001):

$$d(H_{ij}) = \sqrt{\sum_{k=1}^{n} (H_{k_{ij}} - H_{k'_{ij}})^2}$$

where *k* represents a particular haplotype block, *n* is the total number of *H* matrices along a chromosome, *k'* represents each ensuing haplotype block, and *i* and *j* are defined as above. Zeroes appear on the diagonal of the *Y* matrix because no distance exists between a haplotype and itself.

Effects of case and control phenotypes (independent variables) on *Y* matrices (dependent variables) were computed using the *adonis* function in the *vegan* package version 2.5-7 (Oksanen et al., 2020) in R (R Core Team, 2021). The analysis of variance model implemented by *adonis* per haplotype block size is as follows:

$$Y = X\beta + \epsilon$$

(McArdle and Anderson, 2001) where Y is the Euclidean distance matrix of shared haplotype segments, X is a design matrix in which the rows are individual animals and the columns are phenotypes (cases and controls), β is a matrix containing the effects of phenotypes on distances between shared haplotype segments, and ϵ is a matrix of errors.

The null hypothesis is $\beta = 0$, in which no effect exists and was tested with the F statistic presented in McArdle and Anderson (2001). Briefly, the F statistic divides the explained sums of squares of the model by the residual sums of squares of the model (McArdle and Anderson, 2001) and is based on permutations of samples (haplotypes) across phenotypes (case and control) to produce an unbiased statistic (Anderson and Legendre, 1999). For this analysis, 10,000

permutations were used. P-values can then be determined from the distribution of F statistics (Oksanen et al., 2020).

A Bonferroni correction was applied to significance thresholds per haplotype block size to regulate the number of type I errors among multiple comparisons. Corrected thresholds were calculated by dividing α by the number of blocks across the genome.

The QTL within 300 kb of the five most significant regions per haplotype block size were evaluated using the Animal QTL Database (Hu et al., 2019).

Distance-Based Multivariate Analysis of Variance of Theta

The final association test was a distance-based MANOVA between cases and all controls using θ. A symmetric θ relatedness matrix (T) was constructed with each axis consisting of concatenated θ frequencies of a sample (n = 52) at each SNP along a specified region of a chromosome.

The same lengths of genomic windows were employed for this test as for the previous haplotype tests and sizes of blocks are presented in Table 3.3. Regions on the X and Y chromosomes, as well as unmapped regions, were not included in this analysis.

The elements within the θ matrix represent identity-by-state (IBS) by presenting shared proportions of allele frequency for each pair of samples within designated genomic windows. The T matrix for each window is computed as

$$T = \begin{array}{c} \\ a_1 \\ a_2 \\ a_3 \\ \vdots \\ a_n \end{array} \begin{array}{c} \begin{array}{ccccc} a_1 & a_2 & a_3 & \cdots & a_n \end{array} \\ \begin{bmatrix} 1 & a_1 \cap a_2 & a_1 \cap a_3 & \cdots & a_1 \cap a_n \\ a_2 \cap a_1 & 1 & a_2 \cap a_3 & \cdots & a_2 \cap a_n \\ a_3 \cap a_1 & a_3 \cap a_2 & 1 & \cdots & a_3 \cap a_n \\ \vdots & \vdots & \vdots & \ddots & \cdots \\ a_1 \cap a_n & a_n \cap a_2 & a_n \cap a_3 & \vdots & a_n \cap a_n \end{bmatrix} \end{array}$$

where a_n is a vector of θ for the SNPs in a specified genomic window of the *n*th sample and each cell is the intersection ($\cap$) of a pair of a_n. A value along the diagonal represents the comparison of a θ vector to itself, resulting in a proportion of IBS equal to 1.

A separate T matrix is computed for each window (whole chromosome, 20 Mb, 10 Mb, 5 Mb, 2 Mb, and 1 Mb) across the genome, followed by construction of a Euclidean distance matrix of the shared proportions of θ for cases and controls over all windows on a chromosome, which can be represented as

$$Y = \begin{bmatrix} 0 & d(T_{12}) & d(T_{13}) & \cdots & d(T_{1j}) \\ d(T_{21}) & 0 & d(T_{12}) & \cdots & d(T_{2j}) \\ d(T_{31}) & d(T_{32}) & 0 & \cdots & d(T_{3j}) \\ \vdots & \vdots & \vdots & \ddots & \cdots \\ d(T_{i1}) & d(T_{i2}) & d(T_{i3}) & \vdots & d(T_{ij}) \end{bmatrix}$$

where a_n is as defined above and $d(T_{ij})$is the Euclidean distance between the value in the ith row and jth column of each T matrix, which can be calculated as follows (Legendre and Gallagher, 2001):

$$d(T_{ij}) = \sqrt{\sum_{k=1}^{n} (T_{k_{ij}} - T_{k'_{ij}})^2}$$

where *k* represents a given genomic window, *n* is the total number of *T* matrices along a specified chromosome, *k'* represents the following window, and *i* and *j* are defined as above.

Values along the diagonal of the Y matrix portray the degree of dissimilarity, represented by Euclidean distance, between the sequence IBS of each θ vector to itself. Each θ vector is an exact match to itself, thereby resulting in zeroes on the diagonal.

The *adonis* function in R (R Core Team, 2021) was used once again to determine the effects of phenotypes on distances between values in the Y matrix. However, the analysis of variance model per window size is now

$$Y = X\beta + \epsilon$$

(McArdle and Anderson, 2001) where Y is the Euclidean distance matrix of θ, X is a design matrix in which rows are samples and columns are phenotypes (cases and controls), β is a matrix containing the effects of phenotypes on distances between θ, and ϵ is a matrix of errors.

The null hypothesis is that no significant effect exists, represented by $\beta = 0$. Significance is determined by p-values, which are calculated from the F ratio distribution (Oksanen et al., 2020) of the F statistic in McArdle and Anderson (2001). In this test, the F statistic was based on 10,000 permutations of θ on phenotype.

A Bonferroni correction was applied to the p-values for each genome window to constrain the number of type I errors expected. Suggestive ($\alpha = 1$) and significant ($\alpha = 0.05$) association thresholds for each window length correspond to the same thresholds listed in Table 3.3. The QTL within 300 kb of the five most significant regions per haplotype block size were evaluated using the Animal QTL Database (Hu et al., 2019).

Results & Discussion

Population Stratification

Given that pooled samples contain DNA from several animals, the overall allele frequency of a pooled sample regresses toward the mean and should therefore be more closely related to other pools than individual animals. Allele frequencies of individual animals are not biased by averages, which facilitates more extensive variance than those of pools. Pools that

express a wider disparity of allele frequency than individuals can suggest contamination or other errors associated with pool construction.

Figure 3.1 is a Euclidean distance plot in which case, individual control, and pooled control samples are colored red, blue, and black, respectively. Variation appeared as expected; pooled controls aggregated together while individual controls and cases were widely distributed across the plane. This helps confirm that pools were properly constructed as well as diversity of the dataset and suggests disparities between cases and controls, which may ultimately lead to QTL associated with BOSCC.

Figure 3.2 is the neighbor-joining tree depicting similarities among cases, individual controls, and pooled controls based on allele frequencies. Pools form a distinct clade, whereas individual samples vary considerably from other individuals and pools, as anticipated.

Association Testing

Multiple genome-wide association approaches were employed to reveal associations between QTL and BOSCC based on genomic data from cases, individual controls, and pooled controls.

Standard Case/Control Association Test

No significant or suggestive associations were detected in the standard case/control association test (Figure 3.3). However, 20 of the 25 most significant SNPs (Table 3.4) were all found on chromosome 3 and correspond to possible candidate genes related to carcinogenesis and tumor development in cattle and other species.

For example, the most significant SNP (rs136649651) is found about 240 kb upstream of the VANGL planar cell polarity protein 1 gene (*VANGL1*), which contributes to mammalian hair follicle pigmentation (Chen and Chuong, 2012; Cetera et al., 2017) and tumor progression.

Although the effects of bovine *VANGL1* are not well known, its mouse and human orthologs have been studied extensively. This gene has been shown to be significantly upregulated in colorectal tumors (Hee et al., 2004; Lee et al., 2011; Peyravian et al., 2021), breast cancer tissues (Anastas et al., 2012), and esophageal squamous cell carcinomas (Yoon, et al., 2013; Qin et al., 2016).

The next most significant SNP is only 263 kb away from the AP-1 transcription factor subunit gene (*JUN*), which is responsible for transcription-level processes and regulation of cell proliferation in cattle (Gaudet et al., 2011). It is also recognized as a proto-oncogene for its role in intestinal cancer development (Abdolrahman et al., 2005), breast cancer metastasis (Zhang et al., 2007), and liver cancer initiation (Maeda and Karin, 2003) in mice. The third-most significant marker is near another proto-oncogene, notch receptor 2 (*NOTCH2*). Malignant notch signaling pathways have been well researched, with previous literature providing evidence of *NOTCH2* upregulation in mouse liver tumors (Dill et al., 2013) and human esophageal squamous cell carcinomas (Liu et al., 2018; Gan et al., 2021). Furthermore, the bovine variant of *NOTCH2* prevents apoptosis and stimulates cell growth (Li et al., 2021), which are key contributing factors to carcinogenesis.

The next two SNPs listed in Table 3.4 are located 160 kb apart and are both near T-box transcription factor 15 (*TBX15*). This gene is associated with hepatocellular carcinoma proliferation in humans (Morine et al., 2020) and mutations of *TBX15* have been shown to result in craniofacial abnormalities (Lausch et al., 2008) and changes in pigmentation (Candille et al., 2004), however, the role of *TBX15* in bovine carcinogenesis remains unknown. Likewise, the remaining potential candidate genes listed in Table 3.4 are associated with carcinogenesis, primarily squamous cell carcinomas in humans.

The candidate genes discovered in these QTL offer compelling evidence that this study identified results of biological significance, even though no SNPs reached the p-value threshold of statistical significance. Putting the most significant potential candidate genes, *ANGL1*, *JUN*, *NOTCH2*, and *TBX15*, in the context of BOSCC suggests that genes in these QTL regions may directly, or through interaction with other factors, increase cancer susceptibility.

Distance-Based Multivariate Analysis of Variance of Haplotype Blocks

Results of the distance-based MANOVA of haplotype blocks are summarized in Figure 3.4. Haplotype block analysis of whole chromosomes revealed three suggestively significant chromosomes: 6, 20, and 15. Chromosome 15 was the most significant, however literature of potential candidate genes for BOSCC on this chromosome is sparse. The next most significant was chromosome 6, which encodes several genes previously shown to be associated with circumocular pigmentation and incidence of cancer eye in cattle (Pausch et al., 2012). The Wnt signaling pathway inhibitor 2 gene (*DKK2*) is upregulated in human oral squamous cell carcinomas (Kawakita et al., 2014) and colorectal cancers (Hu et al., 2020a). A second candidate gene, lymphoid enhancer binding factor 1 (*LEF1*) is significantly associated with tumor growth and metastasis of carcinomas (Nguyen et al., 2009). The third possible candidate gene on chromosome 6 was speculated to be the KIT proto-oncogene, receptor tyrosine kinase (*KIT*), which controls melanocyte formation involved in pigmentation, proliferation of bovine ovarian cancer (Parrott et al., 2000), and development of human colorectal cancer (Shah and den Brink, 2015). Lastly, a gene called cadherin 12 (*CDH12*) on chromosome 20 is highly associated with carcinomas of the human salivary gland (Wang et al., 2011).

The analysis of 20 Mb long haplotype blocks resulted in suggestively significant regions on chromosomes 6 and 15, consistent with the whole-chromosome results, in addition to a

haplotype block on chromosome 13. Although the suggestively significant region on chromosome 15 was narrowed down from whole chromosome to a single 20 Mb block, no relevant candidate genes were identified, nor were any detected within the suggestive block on chromosome 13. The haplotype block on chromosome 6, however, is within the same region of the genome as *KIT*, which suggests that the significance detected on the whole-chromosome level may have been due to the effect of a mutation in or near *KIT* and not *LEF1* or *DKK2*. This supports existing literature that has identified *KIT* near QTL related to pigmentation and BOSCC susceptibility (Pausch et al., 2012).

When haplotypes were refined to lengths of 10 Mb, three blocks on chromosomes 6, 15, and 13 were suggestively significant. These blocks were all consistent with the regions identified in the 20 Mb block analysis. Interestingly, *KIT* was no longer within the significant window on chromosome 6. Instead, a different potentially related gene was in this region, protein phosphatase with EF-hand domain 2 (*PPEF2*), which inhibits apoptosis and facilitates unregulated cell growth (Kutuzov et al., 2010). The suggestively significant region on chromosome 13 includes the par-3 family cell polarity regulator gene (*PARD3*). This gene is in the same family of cell polarity regulators as the candidate gene detected in the most significant QTL of the standard case/control GWAS, *VANGL1*, and performs similar functions of controlling cell division and cell growth. Finally, the sequence on chromosome 15 revealed the DENN domain containing 2B gene (*DENND2B*), which has been shown to promote skin cancer metastasis in humans (Ioannou et al., 2015).

Only one suggestively significant haplotype block on chromosome 13 was identified in the 5 Mb analysis. This region corresponded to the same potential candidate gene as the 10 Mb analysis, *PARD3*. The 2 Mb analysis revealed the only statistically significant result with this

association method, which also identified a QTL region containing *PARD3*. Another haplotype block on chromosome 13 was found to be suggestively significant and encompassed the coiled-coil domain containing 7 gene (*CCDC7*), which is responsible for the proliferation of several types of human carcinoma (Zhou et al., 2020).

The most refined analysis of 1 Mb blocks revealed three suggestively significant regions on chromosome 13, two of which correspond to the *PARD3* and *CCDC7* genes discussed previously. The third region holds plexin domain containing 2 (*PLXDC2*), a gene that is significantly upregulated in various human carcinoma tissues, including that of colorectal cancer (Hamada et al., 2021), which supports the results of the standard case/control association test performed previously.

Distance-Based Multivariate Analysis of Variance of Theta

Results of the distance-based MANOVA of θ are shown in Figure 3.5. At the whole-chromosome level of aggregation, chromosomes 6, 13, 15, and 21 are suggestively significant. No candidate genes were identified on chromosome 21, however, chromosome 6, 13, and 15 may be signaling the effects of *PPEF2*, *PARD3*, and *DENND2B*, respectively.

Interestingly, only one window on chromosome 13 remained suggestively significant in the 20 Mb analysis. This is the same window that was suggestively significant in the 20 Mb haplotype block discussed in the last section, which encompassed *PARD3*.

Unsurprisingly, the 10 Mb analysis matched the results of the previous MANOVA once the windows were narrowed down to 10 Mb in length for the region containing *PARD3*. Two other regions, one on chromosome 7 and one on chromosome 21, were also deemed suggestively significant at this level of aggregation. Chromosome 7 and chromosome 21 were not identified in

the standard case/control GWAS nor the distance-based MANOVA on haplotype. However, these QTL regions did not harbor any obvious candidate genes.

Once windows were refined to 5 Mb sections of the genome, a region on chromosome 21 remained suggestively significant. However, the reduced window size facilitated the discovery of a potential candidate gene, (*TM2D3*). This gene is associated with signaling pathways involving the notch family of genes (Jakobsdottir et al., 2016), one of which (*NOTCH2*) was identified in the standard case/control association test. The QTL found previously in the haplotype MANOVA on chromosome 13 corresponding to *CCDC7* was suggestively significant as well.

The 2 Mb analysis indicated that the QTL on chromosome 13 encompassing *CCDC7* continued to be suggestively associated, in addition to a region on chromosome 7. The suggestive area on chromosome 7 is a subset of the region found within the 10 Mb window lengths. The solute carrier organic anion transporter family member 4C1 gene (*SLCO4C1*) was identified within this region. Previous literature suggests that *SLCO4C1* upregulates cell growth and is correlated with endometrial cancer development and metastasis in humans (Hu et al., 2020b), but any similar role in the expression of BOSCC is currently unknown. Finally, the 1 Mb window analysis identified one suggestively significant QTL region, near the *SLCO4C1* gene on chromosome 7.

Conclusion

The results from the present study suggest that BOSCC most likely follows a polygenic mode of inheritance. Many of the candidate genes discovered through this experiment have yet to be fully explored in cattle. However, many of the genes identified as putative candidates in this study are related to cancer expression in other species. Future investigation of these cellular

mechanisms may yield future promise in the mitigation of BOSCC in addition to cancers in other species.

Only one statistically significant QTL was identified on chromosome 13, containing *PARD3*. However, chromosomes 6, 13 and 15 were identified over multiple methods of association testing and may contribute substantial biological significance to BOSCC development, susceptibility, or progression. Interestingly, some QTL regions differed between the standard case/control association test, MANOVA of haplotypes, and MANOVA of theta approaches. This is likely a result of different types of data input, but future work should aim to ascertain why these discrepancies exist and if they have any biological impact. Moreover, the exact position and corresponding causal variant(s) for BOSCC remain unknown. Nonetheless, the results from these association tests are promising for ascertaining the genetic mechanisms and relevant QTL underlying BOSCC.

Table 3.1. Average DNA concentrations and absorbance ratios after quality control according to sample type (case, individual control, or pool).

Sample Type	Average DNA Concentration (ng/µL)	Average A260/A280 Ratio
Cases (n = 14 animals)	86.01	2.05
Controls (n = 28 animals)	127.67	2.06
Pools (n = 500 animals)	104.35	2.01
Overall	**106.01**	**2.04**

Table 3.2. Bonferroni-corrected p-value thresholds for suggestive and significant associations for each statistical method.

Association Test	Window Size	Number of Windows	Threshold of Suggestive Significance	Threshold of Statistical Significance
Standard Case/Control	1 SNP	618,656	$p \leq 1.616 \times 10^{-6}$	$p \leq 8.082 \times 10^{-8}$
MANOVA of haplotypes	1 chromosome	30	$p \leq 3.333 \times 10^{-2}$	$p \leq 1.667 \times 10^{-3}$
	20 Mb	101	$p \leq 9.901 \times 10^{-3}$	$p \leq 4.950 \times 10^{-4}$
	10 Mb	232	$p \leq 4.310 \times 10^{-3}$	$p \leq 2.155 \times 10^{-4}$
	5 Mb	493	$p \leq 2.028 \times 10^{-3}$	$p \leq 1.014 \times 10^{-4}$
	2 Mb	1,284	$p \leq 7.788 \times 10^{-4}$	$p \leq 3.894 \times 10^{-5}$
	1 Mb	2,596	$p \leq 3.852 \times 10^{-4}$	$p \leq 1.926 \times 10^{-5}$
MANOVA of theta	1 chromosome	30	$p \leq 3.333 \times 10^{-2}$	$p \leq 1.667 \times 10^{-3}$
	20 Mb	101	$p \leq 9.901 \times 10^{-3}$	$p \leq 4.950 \times 10^{-4}$
	10 Mb	232	$p \leq 4.310 \times 10^{-3}$	$p \leq 2.155 \times 10^{-4}$
	5 Mb	493	$p \leq 2.028 \times 10^{-3}$	$p \leq 1.014 \times 10^{-4}$
	2 Mb	1,284	$p \leq 7.788 \times 10^{-4}$	$p \leq 3.894 \times 10^{-5}$
	1 Mb	2,596	$p \leq 3.852 \times 10^{-4}$	$p \leq 1.926 \times 10^{-5}$

Table 3.3. Actual lengths of each window size. Windows roughly corresponded to intended distances of whole chromosome, 20 Mb, 10 Mb, 5 Mb, 2 Mb, and 1 Mb, but varied slightly due to chromosome length.

Chromosome	Whole-Chromosome Window (Mb)	20 Mb Window Length (Mb)	10 Mb Window Length (Mb)	5 Mb Window Length (Mb)	2 Mb Window Length (Mb)	1 Mb Window Length (Mb)
1	158.528	22.64685	10.56853	5.113805	2.03241	1.003341
2	136.219	22.70309	10.47835	5.239173	2.033112	1.009026
3	120.963	24.19251	10.9966	5.259242	2.050213	1.008021
4	119.836	23.96714	10.89415	5.210247	2.031113	1.007022
5	120.075	24.01493	10.91588	5.220636	2.035163	1.009031
6	117.793	23.55853	10.70842	5.121419	2.030908	1.006775
7	110.664	22.13276	11.06638	5.269705	2.04933	1.006034
8	113.265	22.65301	11.32651	5.148412	2.02259	1.011295
9	104.641	26.16031	11.6268	5.232062	2.051789	1.006166
10	103.277	25.81935	11.47527	5.16387	2.025047	1.012524
11	106.942	26.73558	10.69423	5.347116	2.056583	1.00889
12	87.207	29.06896	10.90086	5.45043	2.028066	1.014033
13	83.457	27.81901	11.92243	5.216064	2.035537	1.017768
14	82.399	27.46624	11.77125	5.493248	2.059968	1.017268
15	85.007	28.33573	10.6259	5.312949	2.02398	1.01199
16	80.980	26.99331	11.56856	5.398661	2.076408	1.012249
17	73.155	24.3851	12.19255	5.225378	2.032091	1.016045
18	65.814	32.90719	10.96906	5.484531	2.056699	1.012529
19	63.432	31.71616	12.68646	5.286026	2.046203	1.023102
20	71.971	23.99049	11.99525	5.536267	2.056328	1.013682
21	69.859	34.92928	11.64309	5.373736	2.054663	1.012443
22	60.712	30.35576	12.14231	5.51923	2.093501	1.011859
23	52.477	26.23847	13.11923	5.830771	2.099077	1.02896
24	62.294	31.14696	12.45878	5.663082	2.076463	1.021211
25	42.321	42.32116	14.10705	6.045879	2.116058	1.032223
26	51.990	25.99517	12.99759	5.776706	2.079614	1.019418
27	45.609	45.60942	11.40236	5.701178	2.073156	1.013542
28	45.935	45.9353	11.48382	5.741912	2.087968	1.020785
29	51.090	25.54518	12.77259	5.676706	2.043614	1.021807
30	139.005	23.16748	10.69269	5.148329	2.014564	1.007282
Averages	**87.564**	**28.284**	**11.607**	**5.407**	**2.052**	**1.014**

Figure 3.1. Euclidean distances calculated between allele frequencies and color-coded by sample type (red for cases, blue for individual controls, and black for pooled controls).

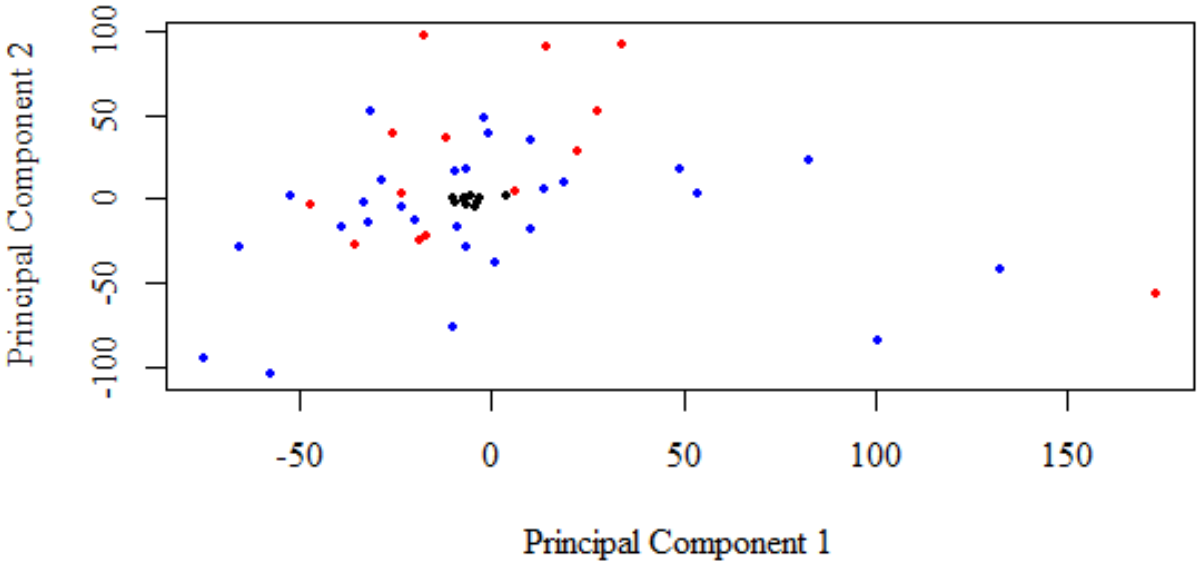

Figure 3.2. A neighbor-joining tree depicting relationships among samples based on allele frequencies. Each sample is colored according to its phenotypic status (red for cases, blue for individual controls, and black for pooled controls).

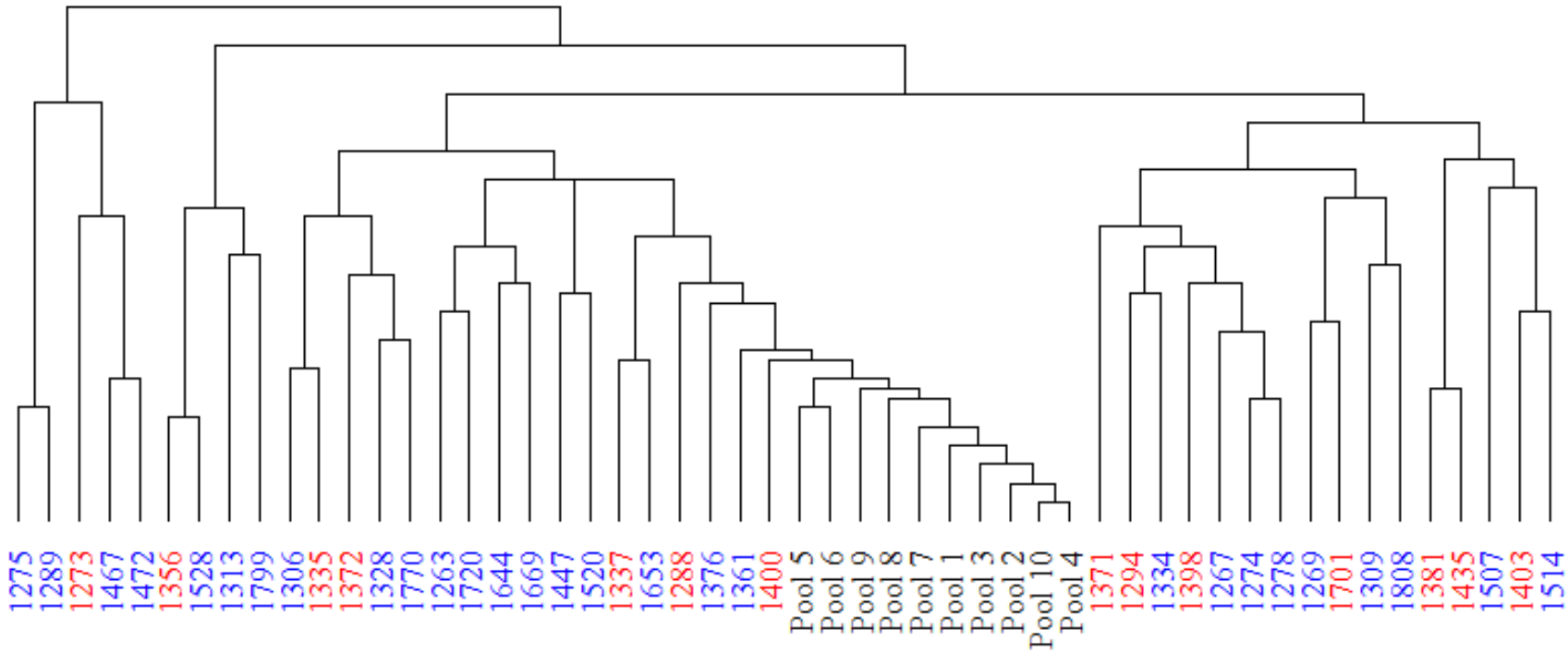

Figure 3.3. A Manhattan plot of a standard case/control association test for cases (n = 14) and individual controls (n = 28). The genome-wide suggestive association threshold (p > 5.791) is indicated by the blue dashed line and the genome-wide significant association threshold (p > 7.092) is represented by the red dashed line.

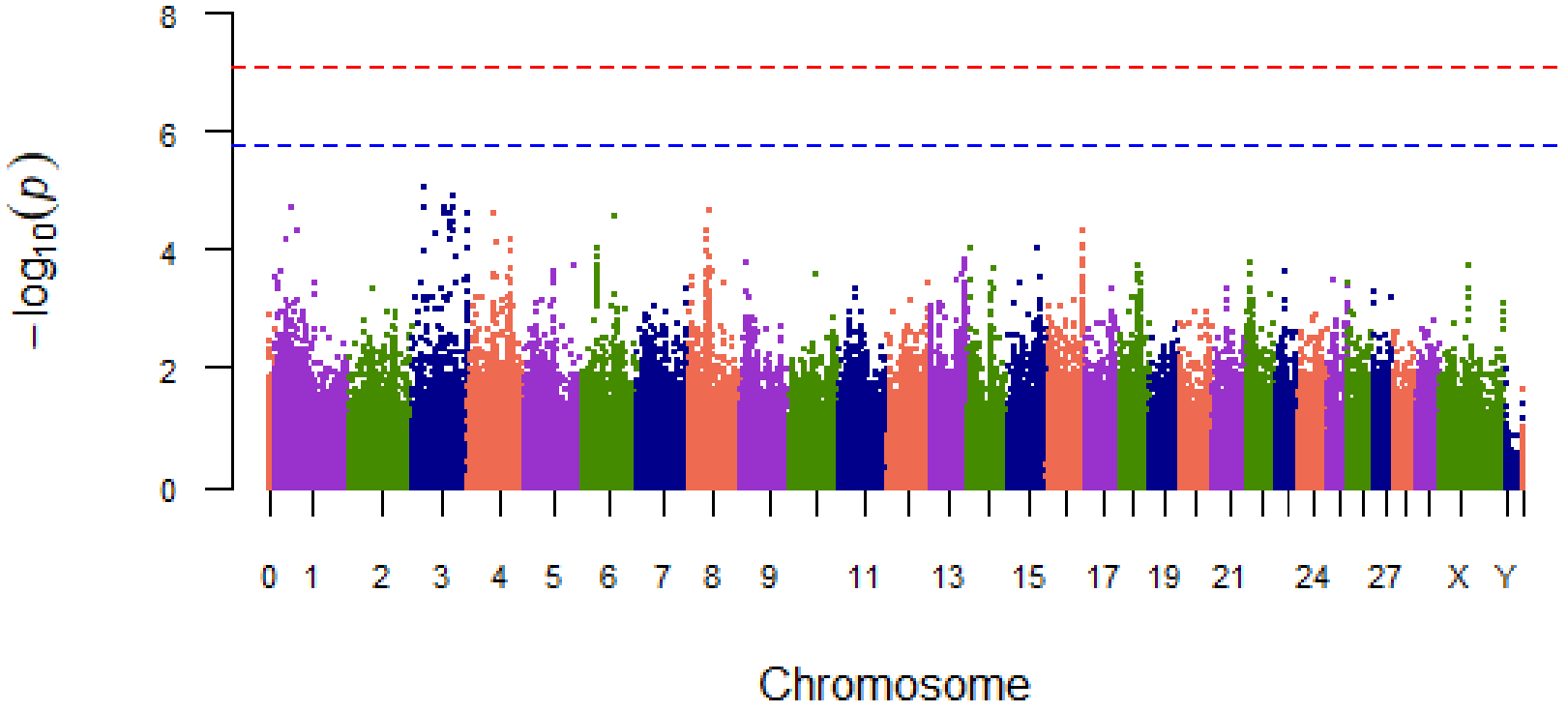

Table 3.4. The 25 most significantly associated SNPs of the standard case/control association test organized in a descending order of significance.

SNP rsID	Chromosome	Location (bp)	*p*	Candidate Gene	Gene Location (bp)
rs136649651	3	27,376,631	0.00000865 [NS]	*VANGL1*	27,617,522 – 27,677,266
rs133389492	3	87,002,696	0.00001240 [NS]	*JUN*	87,265,962 – 87,268,009
rs137808830	3	23,267,644	0.00001997 [NS]	*NOTCH2*	23,196,491 – 23,371,807
rs133946673	3	23,999,128	0.00001997 [NS]	*TBX15*	24,129,612 – 24,255,111
rs135014432	3	24,161,330	0.00001997 [NS]		
rs134138112	3	25,711,280	0.00001997 [NS]	*VTCN1*	26,011,339 – 26,074,137
rs135931826	3	25,980,774	0.00001997 [NS]		
rs136783335	1	40,666,043	0.00001997 [NS]	-	-
rs41594372	3	66,256,094	0.00001997 [NS]	*PTGFR*	66,127,446 – 66,193,794
rs43052973	3	66,229,204	0.00002070 [NS]		
rs136872768	3	84,519,219	0.00002088 [NS]	*NFIA*	84,197,144 – 84,620,790
rs133597234	8	47,550,695	0.00002220 [NS]	-	-
rs132977024	3	70,045,294	0.00002561 [NS]	*TNNI3K*	70,209,854 – 70,556,639
rs134311609	3	70,125,810	0.00002561 [NS]		
rs136232546	3	75,637,926	0.00002561 [NS]	-	-
rs137016426	3	77,095,932	0.00002561 [NS]	*RPE65*	76,832,298 – 76,853,872
rs136436924	3	78,869,181	0.00002561 [NS]	*PDE4B*	78,957,188 – 79,406,811
rs110167383	3	120,208,922	0.00002608 [NS]	*ANO7*	120,406,804 – 120,420,118
rs43394594	4	54,795,638	0.00002608 [NS]	*PPP1R3A*	54,551,935 – 54,592,517
rs43394593	4	54,797,865	0.00002608 [NS]		
rs133389837	6	73,090,381	0.00002725 [NS]	-	-
rs132914262	3	84,585,167	0.00003353 [NS]	*NFIA*	84,197,144 – 84,620,790
rs136554498	3	80,738,471	0.00003375 [NS]	*CACHD1*	80,788,190 – 81,022,953
rs135922619	3	80,545,872	0.00004375 [NS]		
rs43347750	3	81,003,999	0.00004375 [NS]		

[NS] Not suggestively or significantly significant (suggestive association was set at $p < 0.0000016164$ and significant association was set at $p < 0.00000008082$)

Figure 3.4. Dissimilarities among haplotypes from individual animals evaluated for significance across whole chromosome (A), 20 Mb (B), 10 Mb (C), 5 Mb (D), 2 Mb (E), and 1 Mb (F) haplotype blocks. The blue dashed line corresponds to the Bonferroni-corrected suggestive association threshold (α = 1) and the red dashed line is the Bonferroni-corrected significant association threshold (α = 0.05).

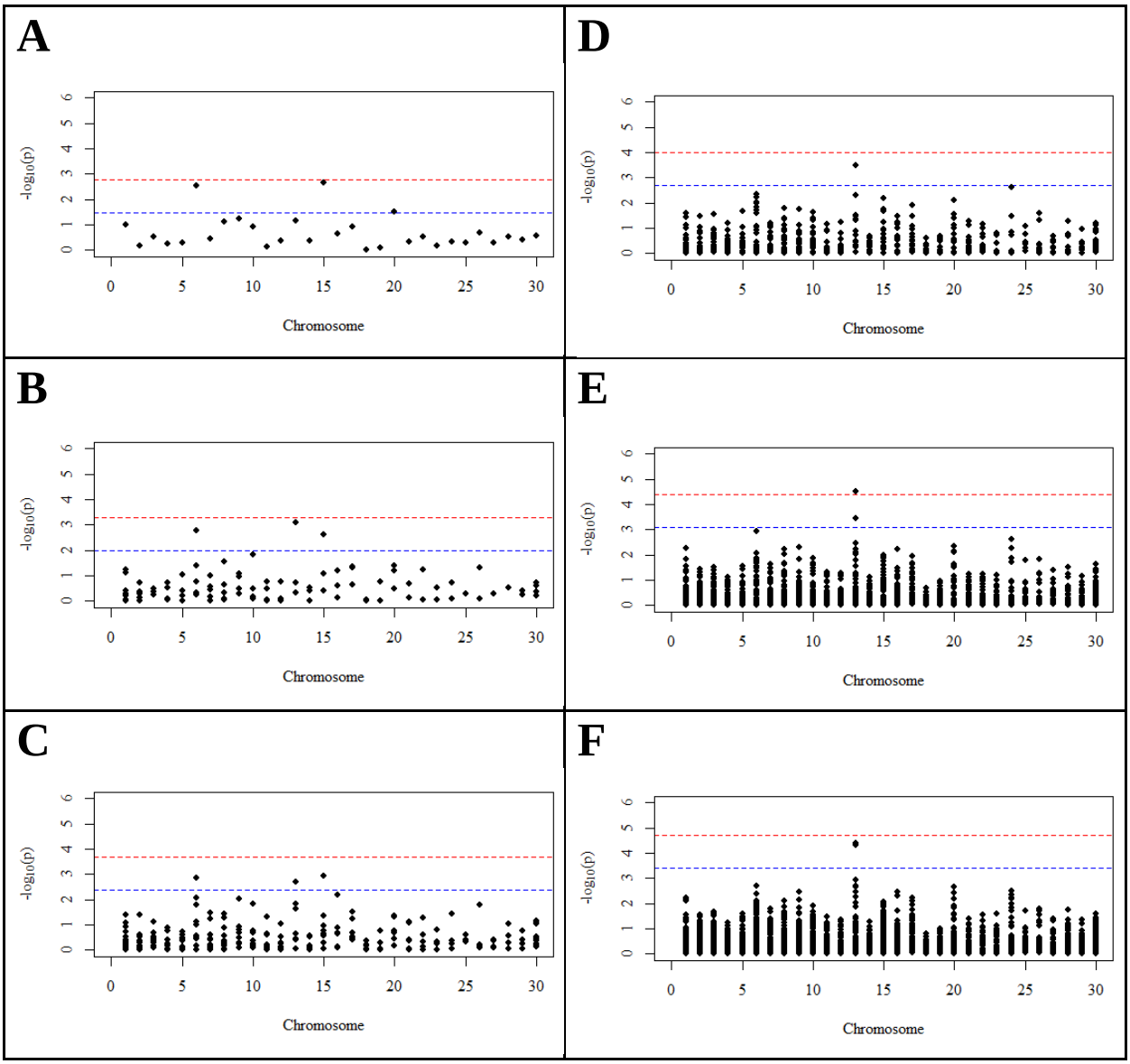

Figure 3.5. Dissimilarities among θ from cases, individual controls, and pooled controls evaluated for significance across whole chromosome (A), 20 Mb (B), 10 Mb (C), 5 Mb (D), 2 Mb (E), and 1 Mb (F) genomic windows. The blue dashed line corresponds to the Bonferroni-corrected suggestive association threshold ($\alpha = 1$) and the red dashed line is the Bonferroni-corrected significant association threshold ($\alpha = 0.05$).

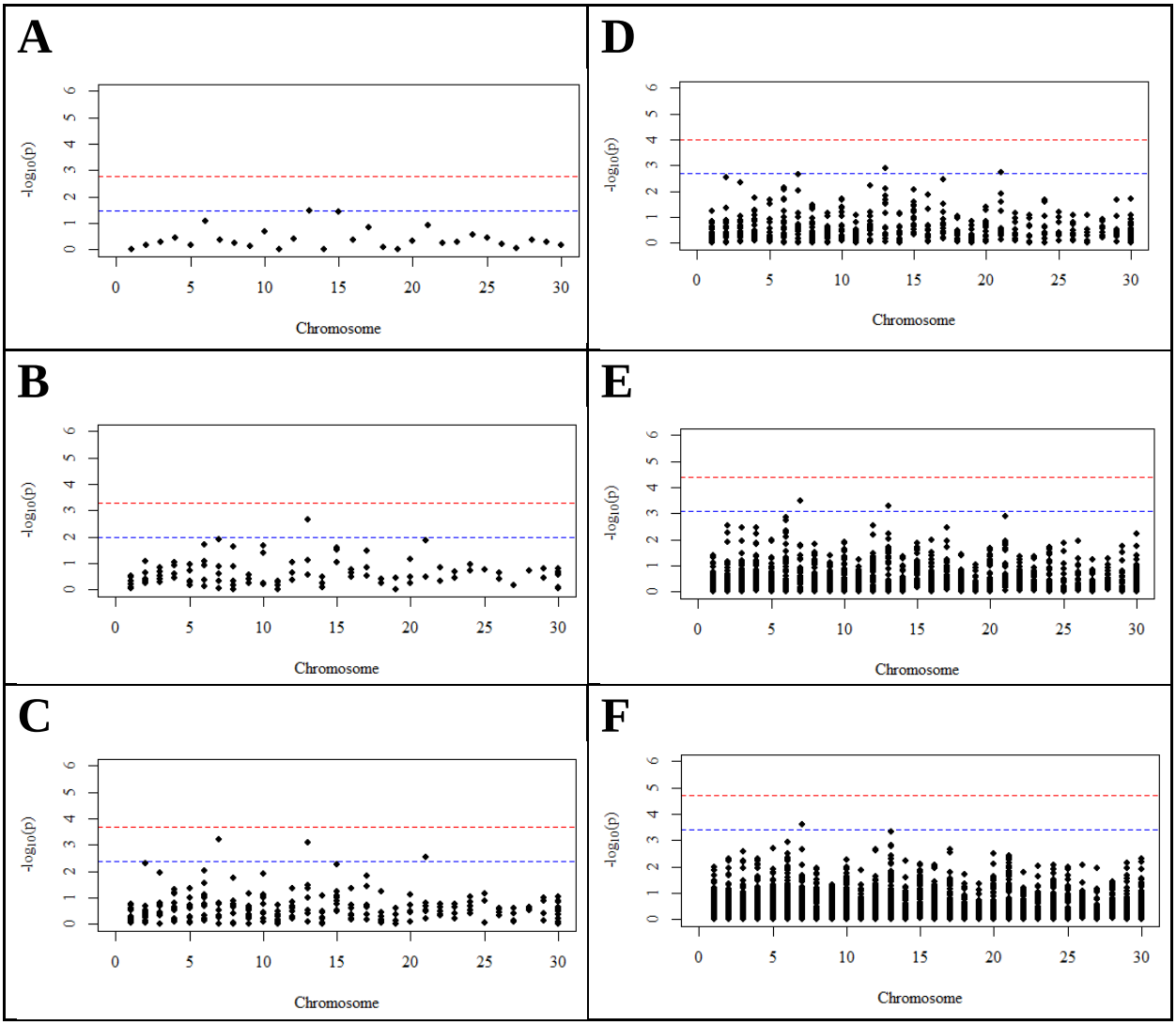

References

Chapter 1: Vertical Fiber Hide Defect Literature Review

Amakiri, S. F. 1975. The skin structure of some cattle breeds in Nigeria studied in relation to hide production. Nigerian Veterinary Medical Association 4(1):21-28.

Amos, G. L. 1958. Vertical fibre in relation to the properties of chrome side leather. Journal of the Society of Leather Trades' Chemists 42:79-90.

Blott, S. C., J. L. Williams, and C. S. Haley. 1998. Genetic variation within the Hereford breed of cattle. Animal Genetics 29:202-211.

Bitcover, E. H., A. L. Everett, W. E. Palm, W. Wind. 1974. Comparative physical properties of leather from young bull hides and steer hides. Journal of the American Leather Chemists Association 69:508-522.

Bureau of Labor Statistics. 2019. CPI Inflation Calculator. Retrieved from https://data.bls.gov/cgi-bin/cpicalc.pl

Cross, H. R., B. D. Schanbacher, and J. D. Crouse. 1985. Sex, age, and breed related changes in bovine testosterone and intramuscular collagen. Roman L. Hruska U.S. Meat Animal Research Center Beef Research Program Progress Report. 2:63-64.

Cundiff, L. V., P. R. Beuchler, M. V. Hannigan, A. L. Everett, & M. P. Dahms. 1987. Inheritance of Vertical-Fiber Hide Defect in Cattle. Journal of Heredity 78(1):24-28.

Cundiff, L. V., M. P. Dahms, M. V. Hannigan, A. L. Everett, & P. E. Buechler. 1988. Inheritance of Vertical Fiber Hide Defect. Roman L. Hruska U.S. Meat Animal Research Center 94:24-25.

Danielson, K. G., H. Baribault, D. F. Holmes, H. Graham, K. E. Kadler, and R. V. Iozzo. 1997. Targeted disruption of decorin leads to abnormal collagen fibril morphology and skin fragility. Journal of Cell Biology 136(3):729-743.

Dufty, J. H., D.E. Peters, & J. H. Bavinton. 1981. Reproductive performance of Hereford cattle affected with the vertical fiber hide defect. Journal of the American Leather Chemists Association 76(12):482-492.

Dufty, J. H., Peters, D. E., & Bavinton, J. H. 1983. Studies of the cause of the vertical fibre hide structure in Hereford cattle. Journal of the Society of Leather Technologists and Chemists 67:70-73.

Duivestein, J., W. Pitchford, & C. Bottema. 2000. Detection of vertical fiber hide defect (VFHD) in Hereford cattle hides by biopsy. Journal of the American Leather Chemists Association 95(3):92-101.

Everett, A. L., & M. V. Hannigan. 1978. The vertical fiber hide defect: transmission to progeny and relation to reproductive failures in crossbreeding test. Journal of the American Leather Chemists Association 73(10):458-469.

Everett, A. L., M. V. Hannigan, E. H. Bitcover, W. Windus, and J. Naghski. 1971. Hereditary influence on vertical fiber structure and strength variation in side upper leather. Journal of the American Leather Chemists Association 66:161-177.

Everett, A. L., H. J. Willard, and W. Windus. 1967. Microscopic study of leather defects: II. Inherent vertical fiber structure in side leather. Journal of the American Leather Chemists Association 62:25-44.

Grady, J. G., S. H. Elder, P. L. Ryan, C. E. Swiderski, and A. M. Rashmir-Raven. 2009. Biomechanical and molecular characteristics of hereditary equine regional dermal asthenia in Quarter Horses. Veterinary Dermatology 20:591-599.

Greiner, S. P. 2009. Beef Cattle Breeds and Biological Types. Virginia Cooperative Extension, publication 400-803.

Hannigan, M. V., A. L. Everett, and J. Naghski. 1973. The vertical fiber hide defect: biopsy study of twin cattle furnishes further proof of genetic origin, disproof of feeding influence. Journal of the American Leather Chemists Association 68:270-282.

Hannigan, M. V., A. L. Everett, M. P. Dahms, & P. R. Buechler. 1983. Vertical fiber hide defect: a biopsy study of Hereford and Angus cattle of known genealogy. Journal of the American Leather Chemists Association 78(7):178-187.

Hanset, R. and C. M. Lapiere. 1974. Inheritance of dermatosparaxis in the calf. Journal of Heredity 65:356-358.

Henrickson, R. L., M. D. Ranganayaki, & A. Asghar. 1984. Age, species, breed, sex, and nutrition effect on hide collagen. Critical Reviews in Food Science and Nutrition 20(3):159-172.

Holbrook, K. A., P. H. Byers, D. F. Counts, and G. A. Hegreberg. 1980. Dermatosparaxis in a Himalayan cat: II. Ultrastructural studies of dermal collagen. Journal of Investigative Dermatology 74:100-104.

Ishmael, W. 2020. Taking stock: Exploring U.S. cow herd composition. Retrieved from BEEF Magazine: Animal Health: https://www.beefmagazine.com/genetics/taking-stock-exploring-us-cow-herd-composition

Kronick, P. L. and P. R. Buechler. 1986. Fiber orientation in calfskin by laser light or x-ray diffraction and quantitative relation to mechanical properties. Journal of the American Leather Chemists Association 81(7):221-230.

Kronick, P. L., & M. S. Sacks. 1991. Quantification of vertical-fiber hide defect in cattle hide by small-angle light scattering. Journal of Connective Tissue Research 27(1):1-13.

Nusgens, B. V., Ch. Verellen-Dumoulin, T. Hermanns-Le, A. De Paepe, L. Nuytinck, G. E. Pierard, and Ch. M. Lapiere. 1992. Evidence for a relationship between Ehlers-Danlos type VII C in humans and bovine dermatosparaxis. Nature Genetics 1:214-217.

Ornes, C. L., J. J. Tancous, and W. T. Roddy. 1964. Inherent strength variations between and within hides. Journal of the American Leather Chemists Association 59:4-14.

Peters, D. E. and J. H. Bavinton. 1983. The characterization of vertical fiber and high weave structures of Hereford cattle hides. Journal of the Society of Leather Technologists and Chemists 67: 65-69.

Peters, D. E., & J. H. Dufty. 1985. The effectiveness of selective breeding for reducing the incidence of the vertical fibre hide. Journal of the American Leather Chemists Association 80(2):42-46.

Pirchner, F. 1969. Population Genetics in Animal Breeding. W. H. Freeman & Co., San Francisco.

Rutherford, B. U.S. Beef Herd Is Mostly Black But Changing Slightly. 2014 Retrieved from BEEF Magazine: Animal Health: https://www.beefmagazine.com/cattle-genetics/us-beef-herd-mostly-black-changing-slightly

Schied, R. J., E. H. Dolnick, and C. E. Terrill. 1970. A quick method for taking biopsy samples of the skin. Journal of Animal Science 30(5):771-773.

Simar, L. J. and E. H. Betz. 1971. Dermatosparaxis of the calf, a genetic defect of the connective tissue. 2. Ultrastructural study of the skin (abstr.). Hoppe-Seyler's Zeitschrift fur Physiologische Chemie 352:13.

Sizeland, K. H., M. M. Basil-Jones, R. L. Edmonds, S. M. Cooper, N. Kirby, A. Hawley, R. G. Haverkamp. 2013. Collagen orientation and leather strength for selected mammals. Journal of Agricultural and Food Chemistry 61:887-892.

Sizeland, K. H., R. L. Edmonds, M. M. Basil-Jones, N. Kirby, & A. Hawley. 2015. Changes to collagen structure during leather processing. Journal of Agricultural and Food Chemistry 63:2499-2505.

Smith, C. A. 1959. A note on the effects of method of ascertainment on segregation ratios. Annals of Human Genetics. 23:311-323.

Tancous, J. J. 1966. Occurrence and nature of pulpiness in side upper leather. Journal of the American Leather Chemists Association 61:4-15.

Tancous, J. J., W. T. Roddy, and F. O'Flaherty. 1969. Skin, Hide and Leather Defects. Book. Ch. 1: Defects due to natural characteristics of the skin or hide.

Tancous, J. J., W. Schmitt, and W. Windus. 1967a. The incidence and predictability of weakness and pulpiness in side upper leather. Journal of the American Leather Chemists Association 62:4-24.

Tancous, J. J., W. Schmitt, and W. Windus. 1967b. Pulpiness and weakness in side upper leather as related to fresh hides. Journal of the American Leather Chemists Association 62:781-807.

Thorstensen, T. C. 1969. Practical Leather Technology. Van Nostrand Reinhold Co., New York. p. 23.

Tryon, R. C., S. D. White, and D. L. Bannasch. 2007. Homozygosity mapping approach identifies a missense mutation in equine cyclophilin B (PPIB) associated with HERDA in the American Quarter Horse. Genomics 90:93-102.

United States Department of Agriculture and Animal and Plant Health Inspection Service (USDA-APHIS). 2009. Beef 2007-08. Part II: Reference of Beef Cow-Calf Management Practices in the United States, 2007-08. National Animal Health Monitoring System.

Yu, W. (1999, May). The mechanical properties of leather in relation to softness: a thesis submitted for the degree of Doctor of Philosophy. ProQuest LLC.

Zhou, H., J. G. H. Hickford, and Q. Fang. 2011. A premature stop codon in the ADAMTS2 gene is likely to be responsible for dermatosparaxis in Dorper sheep. Animal Genetics 43:471-473.

Chapter 2: Detection of vertical fiber hide defect in beef cattle

Amos, G. L. 1958. Vertical fibre in relation to the properties of chrome side leather. Journal of the Society of Leather Trades' Chemists 42:79-90.

Bitcover, E. H., A. L. Everett, W. E. Palm, W. Wind. 1974. Comparative physical properties of leather from young bull hides and steer hides. Journal of the American Leather Chemists Association 69:508-522.

Cundiff, L. V., P. R. Beuchler, M. V. Hannigan, A. L. Everett, & M. P. Dahms. 1987. Inheritance of Vertical-Fiber Hide Defect in Cattle. Journal of Heredity 78(1):24-28.

Cundiff, L. V., M. P. Dahms, M. V. Hannigan, A. L. Everett, & P. E. Buechler. 1988. Inheritance of Vertical Fiber Hide Defect. Roman L. Hruska U.S. Meat Animal Research Center 94:24-25.

Dufty, J. H., Peters, D. E., & Bavinton, J. H. 1983. Studies of the cause of the vertical fibre hide structure in Hereford cattle. Journal of the Society of Leather Technologists and Chemists 67:70-73.

Duivestein, J., W. Pitchford, & C. Bottema. 2000. Detection of vertical fiber hide defect (VFHD) in Hereford cattle hides by biopsy. Journal of the American Leather Chemists Association 95(3):92-101.

Everett, A. L., & M. V. Hannigan. 1978. The vertical fiber hide defect: transmission to progeny and relation to reproductive failures in crossbreeding test. Journal of the American Leather Chemists Association 73(10):458-469.

Everett, A. L., M. V. Hannigan, E. H. Bitcover, W. Windus, and J. Naghski. 1971. Hereditary influence on vertical fiber structure and strength variation in side upper leather. Journal of the American Leather Chemists Association 66:161-177.

Hannigan, M. V., A. L. Everett, and J. Naghski. 1973. The vertical fiber hide defect: biopsy study of twin cattle furnishes further proof of genetic origin, disproof of feeding influence. Journal of the American Leather Chemists Association 68:270-282.

Hannigan, M. V., A. L. Everett, M. P. Dahms, & P. R. Buechler. 1983. Vertical fiber hide defect: a biopsy study of Hereford and Angus cattle of known genealogy. Journal of the American Leather Chemists Association 78(7):178-187.

Naffa, R., C. Maidment, G. Holmes, and G. Norris. 2019. Insights into the molecular composition of the skins and hides used in leather manufacture. Journal of the American Leather Chemists Association 114:29-37.

Garbe, J. R. and Y. Da. 2008. Pedigraph: A Software Tool for the Graphing and Analysis of Large Complex Pedigree. User manual Version 2.4. Department of Animal Science, University of Minnesota.

Peters, D. E. and J. H. Bavinton. 1983. The characterization of vertical fiber and high weave structures of Hereford cattle hides. Journal of the Society of Leather Technologists and Chemists 67: 65-69.

Sizeland, K. H., M. M. Basil-Jones, R. L. Edmonds, S. M. Cooper, N. Kirby, A. Hawley, R. G. Haverkamp. 2013. Collagen orientation and leather strength for selected mammals. Journal of Agricultural and Food Chemistry 61:887-892.

Tancous, J. J. 1966. Occurrence and nature of pulpiness in side upper leather. Journal of the American Leather Chemists Association 61:4-15.

Tancous, J. J., W. Schmitt, and W. Windus. 1967a. The incidence and predictability of weakness and pulpiness in side upper leather. Journal of the American Leather Chemists Association 62:4-24.

Tancous, J. J., W. Schmitt, and W. Windus. 1967b. Pulpiness and weakness in side upper leather as related to fresh hides. Journal of the American Leather Chemists Association 62:781-807.

Chapter 3: Identification of quantitative trait loci associated with bovine ocular squamous cell carcinoma

Anastas, J. N., T. L. Biechele, M. Robitaille, J. Muster, K. H. Allison, S. Angers, and R. T. Moon. 2012. A protein complex of SCRIB, NOS1AP and VANGL1 regulates cell polarity and migration, and is associated with breast cancer progression. Oncogene. 31:3696–3708. doi:10.1038/onc.2011.528

Anderson, D. E. 1991. Genetic Study of Eye Cancer in Cattle. J. Hered. 82:21–26. doi:10.1093/jhered/82.1.21

Anderson, M. J. 2001. A new method for non-parametric multivariate analysis of variance. Austral Ecol. 26:32–46. doi:10.1111/j.1442-9993.2001.01070.pp.x

Anderson, M. J., and P. Legendre. 1999. An empirical comparison of permutation methods for tests of partial regression coefficients in a linear model. J. Stat. Comput. Sim. 62:271–303. doi:10.1080/00949659908811936

Blackwell, R. L., D. E. Anderson, and J. H. Knox. 1956. Age incidence and heritability of cancer eye in Hereford cattle. J. Anim. Sci. 15:943–951. doi:10.2527/jas1956.154943x

Braak, C. J. F. ter, M. P. Boer, L. R. Totir, C. R. Winkler, O. S. Smith, and M. C. A. M. Bink. 2010. Identity-by-Descent matrix decomposition using latent ancestral allele models. Genetics. 185:1045–1057. doi:10.1534/genetics.110.117390

Browning, S. R., and B. L. Browning. 2007. Rapid and accurate haplotype phasing and missing data inference for whole genome association studies by use of localized haplotype clustering. Am. J. Hum. Genet. 81:1084-1097. doi:10.1086/521987

Browning, S. R., and B. L. Browning. 2011. Haplotype phasing: existing methods and new developments. Nat. Rev. Genet. 12:703–714. doi:10.1038/nrg3054

Browning, S. R., and B. L. Browning. 2020. Probabilistic estimation of identity by descent segment endpoints and detection of recent selection. Am. J. Hum. Genet. 107:895–910. doi:10.1016/j.ajhg.2020.09.010

Candille, S. I., C. D. V. Raamsdonk, C. Chen, S. Kuijper, Y. Chen-Tsai, A. Russ, F. Meijlink, and G. S. Barsh. 2004. Dorsoventral patterning of the mouse coat by Tbx15. PLOS Biol. 2:e3. doi:10.1371/journal.pbio.0020003

Chen, J., and C.-M. Chuong. 2012. Patterning skin by planar cell polarity: the multi-talented hair designer. Exp. Dermatol. 21:81–85. doi:10.1111/j.1600-0625.2011.01425.x

Chiang, C. W. K., P. Ralph, and J. Novembre. 2016. Conflation of short identity-by-descent segments bias their inferred length distribution. G3 Genes Genom. Genet. 6:1287–1296. doi:10.1534/g3.116.027581

Cook, C. S., R. J. Peiffer, and P. E. Stine. 1984. Metastatic ocular squamous cell carcinoma in a cat. J. Am. Vet. Med. Assoc. 185:1547–1549.

De vries, A., T. G. M. F. Gorgels, R. J. W. Berg, G. H. Jansen, and H. Van steeg. 1998. Ultraviolet-B induced hyperplasia and squamous cell carcinomas in the cornea of XPA-deficient mice. Exp. Eye Res. 67:53–59. doi:10.1006/exer.1998.0485

Dill, M. T., L. Tornillo, T. Fritzius, L. Terracciano, D. Semela, B. Bettler, M. H. Heim, and J. S. Tchorz. 2013. Constitutive Notch2 signaling induces hepatic tumors in mice. Hepatology. 57:1607–1619. doi:10.1002/hep.26165.

Dugan, S. J., C. R. Curtis, S. M. Roberts, and G. A. Severin. 1991. Epidemiologic study of ocular/adnexal squamous cell carcinoma in horses. J. Am. Vet. Med. Assoc. 198:251–256.

Galili, T. 2015. dendextend: an R package for visualizing, adjusting, and comparing trees of hierarchical clustering. Bioinformatics. doi: 10.1093/bioinformatics/btv428

Gan, R., L. Lin, Dan-ping Zheng, Y. Zhao, L. Ding, Da-li Zheng, and Y. Lu. 2021. High expression of Notch2 drives tongue squamous cell carcinoma carcinogenesis. Exp. Cell Res. 399:112452. doi:10.1016/j.yexcr.2020.112452

Gardiner, M. R., J. L. Anderson, and D. E. Robertson. 1972. Cancer eye of cattle. J. Agr. West. Aust. 13:53-56.

Gaudet, P., M. S. Livstone, S. E. Lewis, and P. D. Thomas. 2011. Phylogenetic-based propagation of functional annotations within the Gene Ontology consortium. Brief. Bioinform. 12:449–462. doi:10.1093/bib/bbr042

Hamada, Y., A. Eguchi, K. Tanaka, M. Katsurahara, N. Horiki, M. Nakamura, M. Tenpaku, M. Iwasa, M. Ichishi, M. Watanabe, and Y. Takei. 2021. Plexin domain containing protein 2 is more expressed within the invasive area of human colorectal cancer tissues. Hum. Cell. doi:10.1007/s13577-021-00570-8

Hendrix, D. V. H. 2005. Equine ocular squamous cell carcinoma. Clin. Tech. Equine Pract. 4:87–94. doi:10.1053/j.ctep.2005.03.011

Hu, Z. L., C. A. Park, and J. M. Reecy. 2019. Building a livestock genetic and genomic information knowledgebase through integrative developments of Animal QTLdb and CorrDB. Nucleic Acids Res. 47:D701–D710. doi:10.1093/nar/gky1084

Hu, J., Z. Wang, Z. Chen, A. Li, J. Sun, M. Zheng, J. Wu, T. Shen, J. Qiao, L. Li, B. Li, D. Wu, and Q. Xiao. 2020a. DKK2 blockage-mediated immunotherapy enhances anti-angiogenic therapy of Kras mutated colorectal cancer. Biomed. Pharmacother. 127:110229. doi:10.1016/j.biopha.2020.110229

Hu, X., T. Han, Y. Bian, H. Tong, X. Wen, Y. Li, and X. Wan. 2020b. Knockdown of SLCO4C1 inhibits cell proliferation and metastasis in endometrial cancer through inactivating the PI3K/Akt signaling pathway. Oncol. Rep. 43:919–929. doi:10.3892/or.2020.7478

Ioannou, M. S., E. S. Bell, M. Girard, M. Chaineau, J. N. R. Hamlin, M. Daubaras, A. Monast, M. Park, L. Hodgson, and P. S. McPherson. 2015. DENND2B activates Rab13 at the leading edge of migrating cells and promotes metastatic behavior. J. Cell Biol. 208:629–648. doi:10.1083/jcb.201407068

Jakobsdottir, J., S. J. van der Lee, J. C. Bis, V. Chouraki, D. Li-Kroeger, S. Yamamoto, M. L. Grove, A. Naj, M. Vronskaya, J. L. Salazar, A. L. DeStefano, J. A. Brody, A. V. Smith, N. Amin, R. Sims, C. A. Ibrahim-Verbaas, S.-H. Choi, C. L. Satizabal, O. L. Lopez, A. Beiser, M. A. Ikram, M. E. Garcia, C. Hayward, T. V. Varga, S. Ripatti, P. W. Franks, G. Hallmans, O. Rolandsson, J.-H. Jansson, D. J. Porteous, V. Salomaa, G. Eiriksdottir, K. M. Rice, H. J. Bellen, D. Levy, A. G. Uitterlinden, V. Emilsson, J. I. Rotter, T. Aspelund, C. for H. and A. R. in G. E. Consortium, A. D. G. Consortium, G. and E. R. in A. D. Consortium, C. J. O'Donnell, A. L. Fitzpatrick, L. J. Launer, A. Hofman, L.-S. Wang, J. Williams, G. D. Schellenberg, E. Boerwinkle, B. M. Psaty, S. Seshadri, J. M. Shulman, V. Gudnason, and C. M. van Duijn. 2016. Rare Functional Variant in TM2D3 is Associated with Late-Onset Alzheimer's Disease. PLOS Genetics. 12:e1006327. doi:10.1371/journal.pgen.1006327

Kawakita, A., S. Yanamoto, S. Yamada, T. Naruse, H. Takahashi, G. Kawasaki, and M. Umeda. 2014. MicroRNA-21 promotes oral cancer invasion via the Wnt/β-Catenin Pathway by targeting DKK2. Pathol. Oncol. Res. 20:253–261. doi:10.1007/s12253-013-9689-y

Kong, A., G. Masson, M. L. Frigge, A. Gylfason, P. Zusmanovich, G. Thorleifsson, P. I. Olason, A. Ingason, S. Steinberg, T. Rafnar, P. Sulem, M. Mouy, F. Jonsson, U. Thorsteinsdottir, D. F. Gudbjartsson, H. Stefansson, and K. Stefansson. 2008. Detection of sharing by descent, long-range phasing and haplotype imputation. Nat. Genet. 40:1068–1075. doi:10.1038/ng.216

Kutuzov, M. A., N. Bennett, and A. V. Andreeva. 2010. Protein phosphatase with EF-hand domains 2 (PPEF2) is a potent negative regulator of apoptosis signal regulating kinase-1 (ASK1). Int. J. Biochem. Cell Biol. 42:1816–1822. doi:10.1016/j.biocel.2010.07.014

Lausch, E., P. Hermanns, H. F. Farin, Y. Alanay, S. Unger, S. Nikkel, C. Steinwender, G. Scherer, J. Spranger, B. Zabel, A. Kispert, and A. Superti-Furga. 2008. TBX15 mutations cause craniofacial dysmorphism, hypoplasia of scapula and pelvis, and short stature in cousin syndrome. Am. J. Hum. Genet. 83:649–655. doi:10.1016/j.ajhg.2008.10.011

Lee, J. H., S. R. Park, K.-O. Chay, Y.-W. Seo, H. Kook, K. Y. Ahn, Y. J. Kim, and K. K. Kim. 2004. KAI1 COOH-Terminal Interacting Tetraspanin (KITENIN), a member of the tetraspanin family, interacts with KAI1, a tumor metastasis suppressor, and enhances metastasis of cancer. Cancer Res. 64:4235–4243. doi:10.1158/0008-5472.CAN-04-0275

Lee, S., Y.-A. Song, Y.-L. Park, S.-B. Cho, W.-S. Lee, J.-H. Lee, I.-J. Chung, K.-K. Kim, J.-S. Rew, and Y.-E. Joo. 2011. Expression of KITENIN in human colorectal cancer and its relation to tumor behavior and progression. Pathol. Int. 61:210–220. doi:10.1111/j.1440-1827.2011.02646.x

Legendre, P., and M. J. Anderson. 1999. Distance-based redundancy analysis: testing multispecies responses in multifactorial ecological experiments. Ecol. Monogr. 69:1–24. doi:10.1890/0012-9615(1999)069[0001:DBRATM]2.0.CO;2

Legendre, P., and E. D. Gallagher. 2001. Ecologically meaningful transformations for ordination of species data. Oecologia. 129:271–280. doi:10.1007/s004420100716

Li, Y., J. Jing, W. Dang, Q. Han, X. Guo, K. Jia, Y. Cheng, K. Wang, E. Kebreab, and L. Lyu. 2021. Effects of Notch2 on proliferation, apoptosis and steroidogenesis in bovine luteinized granulosa cells. Theriogenology. 171:55–63. doi:10.1016/j.theriogenology.2021.05.009

Liu, W., M. Li, X. Chen, S. Zhu, H. Shi, D. Zhang, C. Cheng, and B. Li. 2018. MicroRNA-1 suppresses proliferation, migration and invasion by targeting Notch2 in esophageal squamous cell carcinoma. Sci. Rep. 8:5183. doi:10.1038/s41598-018-23421-3

Macgregor, S., P. M. Visscher, and G. Montgomery. 2006. Analysis of pooled DNA samples on high density arrays without prior knowledge of differential hybridization rates. Nucleic Acids Res. 34:e55–e55. doi:10.1093/nar/gkl136

Macgregor, S., Z. Z. Zhao, A. Henders, N. G. Martin, G. W. Montgomery, and P. M. Visscher. 2008. Highly cost-efficient genome-wide association studies using DNA pools and dense SNP arrays. Nucleic Acids Res. 36:e35–e35. doi:10.1093/nar/gkm1060

Maeda, S., and M. Karin. 2003. Oncogene at last—c-Jun promotes liver cancer in mice. Cancer Cell. 3:102–104. doi:10.1016/S1535-6108(03)00025-4

Marà, M., G. Di Guardo, A. Venuti, G. Marruchella, C. Palmieri, M. De Rugeriis, L. Petrizzi, P. Simeone, C. Rizzo, and L. Della Salda. 2005. Spontaneous ocular squamous cell carcinoma in twin goats: Pathological and biomolecular studies. J. Comp. Pathol. 132:96–100. doi:10.1016/j.jcpa.2004.06.007

McArdle, B. H., and M. J. Anderson. 2001. Fitting multivariate models to community data: A comment on distance-based redundancy analysis. Ecology. 82:290–297. doi:10.1890/0012-9658(2001)082[0290:FMMTCD]2.0.CO;2

McKay, S. D., R. D. Schnabel, B. M. Murdoch, L. K. Matukumalli, J. Aerts, W. Coppieters, D. Crews, E. D. Neto, C. A. Gill, C. Gao, H. Mannen, P. Stothard, Z. Wang, C. P. Van Tassell, J. L. Williams, J. F. Taylor, and S. S. Moore. 2007. Whole genome linkage disequilibrium maps in cattle. BMC Genetics. 8:74. doi:10.1186/1471-2156-8-74

Morine, Y., T. Utsunomiya, Y. Saito, S. Yamada, S. Imura, T. Ikemoto, A. Kitagawa, Y. Kobayashi, S. Takao, K. Kosai, K. Mimori, Y. Tanaka, and M. Shimada. 2020. Reduction of T-Box 15 gene expression in tumor tissue is a prognostic biomarker for patients with hepatocellular carcinoma. Oncotarget. 11:4803–4812. doi:10.18632/oncotarget.27852

Nateri, A. S., B. Spencer-Dene, and A. Behrens. 2005. Interaction of phosphorylated c-Jun with TCF4 regulates intestinal cancer development. Nature. 437:281–285. doi:10.1038/nature03914

Nguyen, D. X., A. C. Chiang, X. H.-F. Zhang, J. Y. Kim, M. G. Kris, M. Ladanyi, W. L. Gerald, and J. Massagué. 2009. WNT/TCF signaling through LEF1 and HOXB9 mediates lung adenocarcinoma metastasis. Cell. 138:51–62. doi:10.1016/j.cell.2009.04.030

Oksanen J., F. G. Blanchet, M. Friendly, R. Kindt, Pierre Legendre, D. McGlinn, P. R. Minchin, R. B. O'Hara, G. L. Simpson, P. Solymos, M. Henry, H. Stevens, E. Szoecs, and H. Wagner. 2020. vegan: Community Ecology Package. R package version 2.5-7. https://CRAN.R-project.org/package=vegan

Palamar, M., E. Kaya, S. Egrilmez, T. Akalin, and A. Yagci. 2014. Amniotic membrane transplantation in surgical management of ocular surface squamous neoplasias: long-term results. Eye. 28:1131–1135. doi:10.1038/eye.2014.148

Parrott, J. A., G. Kim, and M. K. Skinner. 2000. Expression and action of kit ligand/stem cell factor in normal human and bovine ovarian surface epithelium and ovarian cancer. Biol. Reprod. 62:1600–1609. doi:10.1095/biolreprod62.6.1600

Pausch, H., X. Wang, S. Jung, D. Krogmeier, C. Edel, R. Emmerling, K.-U. Götz, and R. Fries. 2012. Identification of QTL for UV-Protective eye area pigmentation in cattle by progeny phenotyping and genome-wide association analysis. PLOS ONE. 7:e36346. doi:10.1371/journal.pone.0036346

Peiffer, D. A., J. M. Le, F. J. Steemers, W. Chang, T. Jenniges, F. Garcia, K. Haden, J. Li, C. A. Shaw, J. Belmont, S. W. Cheung, R. M. Shen, D. L. Barker, and K. L. Gunderson. 2006. High-resolution genomic profiling of chromosomal aberrations using Infinium whole-genome genotyping. Genome Res. 16:1136–1148. doi:10.1101/gr.5402306

Peyravian, N., S. Nobili, Z. Pezeshkian, M. Olfatifar, A. Moradi, K. Baghaei, F. Anaraki, K. Nazari, H. Asadzadeh Aghdaei, M. R. Zali, E. Mini, and E. Nazemalhosseini Mojarad. 2021. Increased expression of VANGL1 is predictive of lymph node metastasis in colorectal cancer: results from a 20-Gene expression signature. J. Pers. Med. 11:126. doi:10.3390/jpm11020126

Purcell, S., B. Neale, K. Todd-Brown, L. Thomas, M. A. R. Ferreira, D. Bender, J. Maller, P. Sklar, P. I. W. de Bakker, M. J. Daly, and P. C. Sham. 2007. PLINK: A tool set for whole-genome association and population-based linkage analyses. Am. J. Hum. Genet. 81:559–575. doi:10.1086/519795

Qin, H.-D., X.-Y. Liao, Y.-B. Chen, S.-Y. Huang, W.-Q. Xue, F.-F. Li, X.-S. Ge, D.-Q. Liu, Q. Cai, J. Long, X.-Z. Li, Y.-Z. Hu, S.-D. Zhang, L.-J. Zhang, B. Lehrman, A. F. Scott, D. Lin, Y.-X. Zeng, Y. Y. Shugart, and W.-H. Jia. 2016. Genomic characterization of esophageal squamous cell carcinoma reveals critical genes underlying tumorigenesis and poor prognosis. Am. J. Hum. Genet. 98:709–727. doi:10.1016/j.ajhg.2016.02.021

Russell, W. C., J. S. Brinks, and R. A. Kainer. 1976. Incidence and heritability of ocular squamous cell tumors in Hereford cattle. J. Anim. Sci. 43:1156–1162. doi:10.2527/jas1976.4361156x

Russell, W. O., E. S. Wynne, G. S. Loquvam, and D. A. Mehl. 1956. Studies on bovine ocular squamous carcinoma (“cancer eye”). I. Pathological anatomy and historical review. Cancer. 9:1–52. doi:10.1002/1097-0142(195601/02)9:1<1::AID-CNCR2820090102>3.0.CO;2-Z

Shah, Y. M., and G. R. van den Brink. 2015. c-Kit as a novel potential therapeutic target in colorectal cancer. Gastroenterology. 149:534–537. doi:10.1053/j.gastro.2015.07.027

Sironi, G., P. Riccaboni, L. Mertel, G. Cammarata, and D. E. Brooks. 1999. p53 protein expression in conjunctival squamous cell carcinomas of domestic animals. Vet. Ophthalmol. 2:227–231. doi:10.1046/j.1463-5224.1999.00086.x

Staaf, J., J. Vallon-Christersson, D. Lindgren, G. Juliusson, R. Rosenquist, M. Höglund, Å. Borg, and M. Ringnér. 2008. Normalization of Illumina Infinium whole-genome SNP data improves copy number estimates and allelic intensity ratios. BMC Bioinformatics. 9:409. doi:10.1186/1471-2105-9-409

Turner, S. D. 2018. qqman: an R package for visualizing GWAS results using Q-Q and manhattan plots. J. Open Source Software. 3:731. doi:10.21105/joss.00731

Wang, J.-F., L. She, B.-H. Su, L.-C. Ding, F.-F. Zheng, D.-L. Zheng, and Y.-G. Lu. 2011. CDH12 promotes the invasion of salivary adenoid cystic carcinoma. Oncol. Rep. 26:101–108. doi:10.3892/or.2011.1286

Wright, S. 1931. Evolution in Mendelian Populations. Genetics. 16:97–159.

Yoon, T. M., S.-A. Kim, J. K. Lee, Y.-L. Park, G. Y. Kim, Y.-E. Joo, J. H. Lee, K. K. Kim, and S. C. Lim. 2013. Expression of KITENIN and its association with tumor progression in oral squamous cell carcinoma. Auris Nasus Larynx. 40:222–226. doi:10.1016/j.anl.2012.07.006

Zhang, Y., X. Pu, M. Shi, L. Chen, Y. Song, L. Qian, G. Yuan, H. Zhang, M. Yu, M. Hu, B. Shen, and N. Guo. 2007. Critical role of c-Jun overexpression in liver metastasis of human breast cancer xenograft model. BMC Cancer. 7:145. doi:10.1186/1471-2407-7-145

Zhou, C., X. He, Q. Zeng, P. Zhang, and C. Wang. 2020. CCDC7 Activates interleukin-6 and vascular endothelial growth factor to promote proliferation via the JAK-STAT3 pathway in cervical cancer cells. Oncotargets Ther. 13:6229–6244. doi:10.2147/OTT.S244663

Zhou, Y., B. L. Browning, and S. R. Browning. 2020. Population-specific recombination maps from segments of identity by descent. Am. J. Hum. Genet. 107:137–148. doi:10.1016/j.ajhg.2020.05.016